

January 2012

# Synthesis Of Novel Ionic Liquid Tagged Porphyrin Media Designed For The Oxidation Of Lignin

Joseph Hugh Franklin Baker  
*Eastern Kentucky University*

Follow this and additional works at: <https://encompass.eku.edu/etd>

 Part of the [Chemistry Commons](#)

---

## Recommended Citation

Baker, Joseph Hugh Franklin, "Synthesis Of Novel Ionic Liquid Tagged Porphyrin Media Designed For The Oxidation Of Lignin" (2012). *Online Theses and Dissertations*. 120.  
<https://encompass.eku.edu/etd/120>

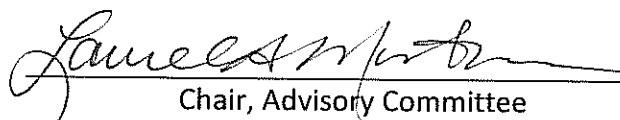
This Open Access Thesis is brought to you for free and open access by the Student Scholarship at Encompass. It has been accepted for inclusion in Online Theses and Dissertations by an authorized administrator of Encompass. For more information, please contact [Linda.Sizemore@eku.edu](mailto:Linda.Sizemore@eku.edu).

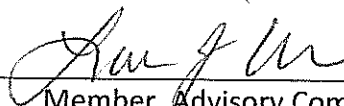
SYNTHESIS OF NOVEL IONIC LIQUID TAGGED PORPHYRIN MEDIA DESIGNED FOR THE  
OXIDATION OF LIGNIN


By


Joseph Baker

Thesis Approved:

  
Chair, Advisory Committee

  
Member, Advisory Committee

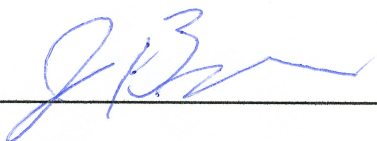
  
Member, Advisory Committee

  
Member, Advisory Committee

  
Dean, Graduate School

STATEMENT OF PERMISSION TO USE

In presenting this thesis in partial fulfillment of the requirements for a Master of Science Degree at Eastern Kentucky University, I agree that the Library shall make it available to borrowers under rules of the Library. Brief quotations from this thesis are allowable without special permission, provided that accurate acknowledgment of the source is made. Permission for extensive quotation from or reproduction of this thesis may be granted by my major professor, or in [his/her] absence, by the Head of Interlibrary Services when, in the opinion of either, the proposed use of the material is for scholarly purposes. Any copying or use of the material in this thesis for financial gain shall not be allowed without my written permission.

Signature 

Date 11/30/12

SYNTHESIS OF NOVEL IONIC LIQUID TAGGED PORPHYRIN MEDIA DESIGNED FOR THE  
OXIDATION OF LIGNIN

By

Joseph Baker

Bachelor of Science  
Missouri State University  
Springfield, Missouri  
2010

Submitted to the Faculty of the Graduate School of  
Eastern Kentucky University  
in partial fulfillment of the requirements  
for the degree of  
MASTER OF SCIENCE  
December, 2012

Copyright © Joseph Baker, 2012  
All rights reserved

## DEDICATION

This thesis is dedicated to my parents Richard and Julie Baker as well as my two sisters and close friends. The pursuit of Masters' Degree at Eastern Kentucky University has involved many ups and downs and at times a near separation from those mentioned above. I feel that their support regardless of the sacrifices made to complete this thesis have been vital to my success.

## ACKNOWLEDGMENTS

I would like to thank my advisor Dr. Morton and committee members Dr. Shi, Dr. Wilson, and Dr. Otieno for their knowledge and advisement as well as their compassion and interest in myself and my success at Eastern Kentucky University. I would also like to acknowledge Dr. Bruce Pratt and the Center for Renewable and Alternative Fuel Technologies for their financial support and for allowing me to be a representative for them at conferences. Special thanks go to Dr. Samuel Morton for the catalytic data as well as the opportunity to do research at the Center for Applied Energy Research when it was beneficial. Along with that goes thanks to Justin Mobley and Robby Pace for help with the HPLC standards and method development. Another individual that needs recognition is Dr. Baltisberger, who actually gave me a couple of vials of clean deuterated NMR solvent when it was desperately needed and allowed me to use his NMR at Berea College anytime it was available. Last but certainly not least is acknowledgement of Gage Wallace for his friendship along with help and support in the lab.

## Abstract

The ever growing need for a viable renewable fuel source has led to this thesis project; the biomimetic lignin degradation by means of a homogeneous oxidative catalyst in corresponding ionic liquids. Lignin comprises nearly a third of lignocellulosic biomass and is cross-linked to both cellulose and hemicellulose. Current utilization methods of lignin do not generate the full value of the polymer, because they do not yield many of the valuable feed stock chemicals it is comprised of. To improve the value of the biomass as a whole and create a viable economy for the US's transition to biofuels, better utilization methods need to be developed. To this end, we have developed ionic liquid tagged metalloporphyrin catalysts and coupled them in ionic liquids that are known to dissolve lignin in an attempt to more efficiently isolate the feedstock chemicals contained within lignin. Synthesis of four ionic liquid tagged metalloporphyrin catalysts has been completed with moderate yields. The array of catalysts has been synthesized, as the functionalization of the metalloporphyrin is known to have a great effect on its catalytic abilities. Recently groups have shown a significant increase in the reusability of the ionic catalysts when coupled with ionic liquids, helping a major hurdle in the biomimetic process. We have performed initial catalytic studies with two of our novel ionic metalloporphyrins and compared their activity with a non-ionic metalloporphyrin. Under similar conditions in 1-allyl-3-methylimidazolium xylenesulphonate our novel catalysts outperformed the comparative non-ionic porphyrin catalyst significantly.



## TABLE OF CONTENTS

CHAPTER	PAGE
I. INTRODUCTION .....	1
1.1 LIGNOCELLULOSIC BIOMASS .....	2
1.1.1 Cellulose .....	3
1.1.2 Hemicellulose .....	3
1.1.3 Lignin .....	4
1.1.3.1 Lignin Linkages.....	6
1.1.3.2 Pretreatment Methods .....	7
1.1.3.2.1 Mechanical Comminution .....	8
1.1.3.2.2 Ionic Liquid Dissolution .....	8
1.1.3.2.3 Kraft Pulping Process .....	9
1.1.3.2.4 Steam Explosion .....	10
1.1.3.2.5 Acid Hydrolysis .....	11
1.2 WHITE ROT FUNGI (NATURE'S SOLUTION) .....	11
1.2.1 Phanerochaete Chrysosporium .....	14
1.3 IONIC LIQUIDS .....	14
1.3.1 Synthetic Routes .....	15
1.3.1.1 Ion Exchange (Secondary Ionic Liquids).....	16
1.3.2 Ionic Liquid Applications .....	17
1.4 LIGNIN AND LIGNIN MODEL COMPOUNDS IN IONIC LIQUIDS .....	18
1.5 PORPHYRINS .....	21

1.5.1 Synthetic Routes .....	22
1.5.1.1 Adler and Lindsey Methods .....	22
1.5.1.2 Dipyrrromethane Porphyrin Synthesis .....	23
1.5.2 Porphyrin Catalytic Studies .....	24
1.5.2.1 Porphyrin Epoxidation .....	25
1.5.2.2 Porphyrin as Heck Catalyst .....	29
1.5.2.3 Porphyrin Oxidations of Lignin Model Compounds .....	29
II. METHODS AND RESULTS .....	32
2.1 SYNTHESIS OF BENZYL IONIC LIQUID TAGGED PORPHYRINS .....	32
2.1.1 $\alpha$ -bromotolualdehyde (Cp1) .....	33
2.1.2 5, 10, 15, 20-tetrakis(p-tolylbromide)porphyrin (Cp2) .....	33
2.1.3 5, 10, 15, 20-tetrakis(p-tolyl 1-methylimidazolium)porphyrin bromide (Cp3) .....	34
2.1.4 5, 10, 15, 20-tetrakis(p-tolyl triphenylphosphonium)porphyrin bromide (Cp4) .....	34
2.1.5 Iron(5, 10, 15, 20-tetrakis(p-tolyl 1-methylimidazolium)porphyrin bromide) chloride (Cp5) .....	35
2.1.6 Iron(5, 10, 15, 20-tetrakis(p-tolyl triphenylphosphine)porphyrin bromide) chloride (Cp6) .....	36
2.2 SYNTHESIS OF PYRIDINIUM IONIC LIQUID TAGGED PORPHYRINS .....	36
2.2.1 5, 10, 15, 20-tetrakis(p-pyridyl)porphyrin (Cp7) .....	36

2.2.2	5, 10, 15, 20-tetrakis(N-3-bromopropylpyridinium-4-yl)porphyrin bromide (Cp8) .....	37
2.2.3	5, 10, 15, 20-tetrakis(N-allylpyridinium-4-yl)porphyrin bromide (Cp9) .....	37
2.2.4	5, 10, 15, 20-tetrakis(N-butylpyridinium-4-yl)porphyrin bromide (Cp10) .....	38
2.2.5	Iron(5, 10, 15, 20-tetrakis(N-allylpyridinium-4-yl)porphyrin bromide) chloride (Cp11) .....	38
2.2.6	Iron(5, 10, 15, 20-tetrakis(N-butylpyridinium-4-yl)porphyrin bromide) chloride (Cp12) .....	39
2.3	SYNTHESIS OF PROPOXY IONIC LIQUID TAGGED PORPHYRINS .....	40
2.3.1	5, 10, 15, 20-tetrakis(p-3-bromopropoxyphenyl)porphyrin (Cp13) .....	40
2.4	CATALYTIC STUDIES .....	40
III.	EXPERIMENTAL DISCUSSION .....	43
3.1	SYNTHESIS OF BENZYL IONIC LIQUID TAGGED PORPHYRINS .....	44
3.1.1	Synthesis of Cp1 .....	46
3.1.2	Synthesis of Cp2 .....	47
3.1.3	Synthesis of Cp3 and Cp4 .....	49
3.1.4	Synthesis of Cp5 and Cp6 .....	52
3.2	SYNTHESIS OF PYRIDINIUM IONIC LIQUID TAGGED PORPHYRINS .....	53
3.2.1	Synthesis of Cp7 .....	55

3.2.2 Attempted Synthesis of Cp8 .....	56
3.2.3 Synthesis of Cp9 .....	57
3.2.4 Synthesis of Cp10 .....	59
3.2.5 Synthesis of Cp11 .....	60
3.2.6 Synthesis of Cp12 .....	60
3.3 SYNTHESIS OF PROPOXY IONIC LIQUID TAGGED PORPHYRINS .....	61
3.3.1 Synthesis of Cp13 .....	61
3.4 CATALYTIC RESULTS AND DISCUSSION .....	62
IV. CONCLUSIONS AND FUTURE WORK .....	68
REFERENCES .....	70
APPENDIX .....	78

## LIST OF FIGURES

FIGURE	PAGE
1.1 Cellulose Illustration .....	3
1.2 Hemicellulose Illustration .....	4
1.3 Coniferyl alcohol, p-Coumaryl alcohol, and Sinapyl alcohol.....	5
1.4 Determined Lignin Structure from Beech .....	6
1.5 Examples of $\beta$ -O-4 and 4-O-5 Linkages .....	7
1.6 Chemical Structures of Heme and Laccase .....	13
1.7 List of Common Ionic Liquid Cations .....	15
1.8 Formation of Hibbert's Ketones Through Acidolysis .....	20
1.9 Porphine, Heme, and Porphyrin .....	22
1.10 Common Co-Oxidants mCPBA, PhIO, Hydrogen Peroxide .....	25
1.11 Iron Porphyrin Epoxidation Mechanism with Hydrogen Peroxide .....	27
1.12 Heck Reaction Catalyzed by a Pd Porphyrin Analogue .....	29
1.13 Structures of Model Compounds Studied by Cui and Dolphin .....	31
2.1 The Molecular Structure of FeT1239.....	42
3.1 Synthesis of Benzyl Ionic Liquid Tagged Porphyrins .....	45
3.2 $^1\text{H-NMR}$ Spectrum of Cp1 .....	47
3.3 $^1\text{H-NMR}$ Spectrum of Cp2 .....	48
3.4 $^1\text{H-NMR}$ Spectrum of Cp4 .....	52
3.5 Synthesis of Ionic Liquid Tagged Pyridinium Porphyrins .....	54
3.6 $^1\text{H-NMR}$ Spectrum of Cp7 .....	56

3.7 Structure and $^1\text{H-NMR}$ Spectrum of Cp13 .....	62
3.8 Porphyrin Reusability System Comparison .....	63
3.9 The Catalytic Oxidation Scheme .....	64
3.10 The Conversion of Veratryl Alcohol .....	65
3.11 Chromatogram from the Oxidation of Veratryl Alcohol .....	67
A.1 $^1\text{H-NMR}$ of Cp3 in $\text{Methanol}_{d4}$ .....	81
A.2 $^1\text{H-NMR}$ of Cp4 in $\text{DMSO}_{d6}$ .....	82
A.3 $^1\text{H-NMR}$ of Cp9 in $\text{DMSO}_{d6}$ .....	83
A.4 $^1\text{H-NMR}$ of Cp10 in $\text{Methanol}_{d4}$ .....	84
A.5 IR of Cp3 .....	86
A.6 IR of Cp5 .....	87
A.7 IR of Cp6 .....	88
A.8 IR of Cp9 .....	89
A.9 IR of Cp11 .....	90
A.10 IR of Cp10 .....	91
A.11 IR of Cp12 .....	92
A.12 Synthesized Chemical Structures .....	95

## LIST OF TABLES

TABLE	PAGE
2.1 Averaged Molar Amounts of Each Species for Catalytic Trials .....	41
A.1 <sup>1</sup> H-NMR Data.....	79
A.2 IR Data.....	85
A.3 UV-VIS Data.....	93
A.4 Average Mass of Veratryl Alcohol in AMIMXS Based on HPLC.....	94
A.5 Average Mass of Veratraldehyde in AMIMXS Based on HPLC. ....	94

## LIST OF ABBREVIATIONS

AMIMXS .....	1-allyl-3-methylimidazolium xylenesulfonate
AMIMCl .....	1-allyl-3-methylimidazolium chloride
BF <sub>3</sub> .....	boron trifluoride
BF <sub>4</sub> <sup>-</sup> .....	tetrafluoroborate
BMIMCl .....	1-butyl-3-methylimidazolium chloride
BMIMXS .....	1-butyl-3-methylimidazolium xylenesulfonate
CHCl <sub>3</sub> .....	chloroform
DDQ .....	2,3-dichloro-5,6-dicyanobenzoquinone
DMF .....	dimethylformamide
DMSO .....	dimethylsulfoxide
GG .....	guiacylglycerol-β-guiacyl ether
LiP .....	Lignin Peroxidase
mCPBA .....	meta-chloroperoxybenzoic acid
MnP .....	Manganese Peroxidase
PhIO .....	iodosobenzene
PPh <sub>3</sub> .....	triphenylphosphine
TCBQ .....	2,3,5,6-tetrachlorobenzoquinone
TLC .....	Thin Layer Chromatography
TMS .....	tetramethylsilane



## CHAPTER I

### INTRODUCTION

With rising gas prices, the demand for renewable fuel sources has never been greater. Lignocellulosic biomass is one of the primary targets for a renewable fuel source. Goals have been set to increase the percentage of derived organic chemicals to 25% and increase the percentage of transportation fuels from biomass to 30% by 2025.<sup>1</sup> Bioethanol is commonly used as an additive to gasoline at 10-20%, currently produced from corn and sugars, however its production is in competition with food sources causing a huge ethical issue. Cellulosic ethanol could be a solution to this ethical dilemma as it can be produced from natural resources such as plants and grasses. However, current production technology does not allow for competitive pricing.<sup>2</sup> To drive this price down to be competitive it must be processed and utilized much more efficiently. Lignocellulosic biomass is composed of three main polymers: lignin, cellulose, and hemicellulose. Hemicellulose and cellulose are relatively less complex in structure compared to lignin. In large part due to their lack of complexity, their utilization is much more optimized and a much higher percentage of mass is already converted to usable bio-derived feedstock. Lignin is between 15-35% of the whole biomass and is comprised of many potentially valuable aromatic chemicals. Isolation of these valuable chemicals has been estimated to quadruple the current value of the whole biomass.<sup>3</sup> To meet the goals above, it is vital to learn to produce a

high percentage of these aromatics from lignin and incorporate them into the value of the biomass as a whole. Our potential process for the degradation of this polymer is to couple ionic liquids and oxidative ionic liquid tagged metalloporphyrin catalysts; each having previous successful implications in its own right. Coupling the two will not only do away with common solubility issues of porphyrins but should also increase the stability of the porphyrin catalysts themselves. Increasing the value of biomass would be a huge step towards the goals stated above by adding a renewable feedstock for valuable organic chemicals and fossil fuels.

### **1.1 LIGNOCELLULOSIC BIOMASS**

Lignocellulosic biomass encompasses the cell walls of grasses, trees, plants, and many other natural renewable species. Now that gas prices have risen dramatically, the search for sustainable renewable energy is at a premium. In 2011, biomass only accounted for about 4.5% of the United States total energy usage.<sup>3</sup> For that number to increase the utilization of the natural resource must be maximized. Lignocellulosic biomass is very complex causing the efficiency to be problematic. It is comprised of three structurally different polymers; lignin, cellulose, and hemicellulose. These three polymers are covalently bound to each other, making separation of the polymers alone very difficult and costly. Lignocellulosic biomass is usually segregated into hardwoods and softwoods. Each of which has its own chemical variations that often add more complications in separations and utilization. Even when separated from cellulose and hemicellulose, lignin is still vastly under valued and usually just burned as a low grade

energy source.<sup>4</sup> This is a large part of the deficiency in the utilization of lignocellulosic biomass and a major problem associated with its conversion to a fuel.

### 1.1.1 Cellulose

Cellulose is a glucose linear straight chain polymer (**Figure 1.1**) that comprises between 23 and 53% of a lignocellulosic plant. It is a  $\beta(1-4)$  linked spiralling polymer. It has the highest degree of polymerization, being between 7000-15000 units. It can be isolated in a relatively pure form by common delignification techniques followed by alkali extractions.<sup>5</sup>

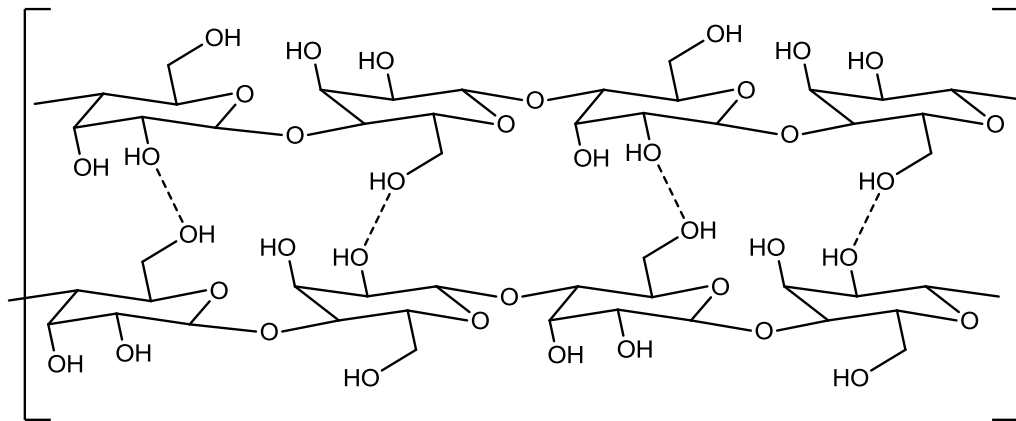


**Figure 1.1:** Cellulose Illustration.<sup>5</sup>

### 1.1.2 Hemicellulose

Hemicelluloses are irregular polymers composed of glucose, xylose, galactose, mannose, fucose, arabinose, glucuronic acid and galacturonic acid (**Figure 1.2, p. 4**).

Currently hemicelluloses are utilized as a source of sugar, fuel, and feedstock for

various chemicals. They have also found applications as additives in papermaking, gels, surfactants, and drug carriers.<sup>6</sup> In the cell wall they are hydrogen bonded to cellulose and covalently bound to lignin. Separation can be done any of the common delignification methods and washing with an ethanol water solution.<sup>7</sup>

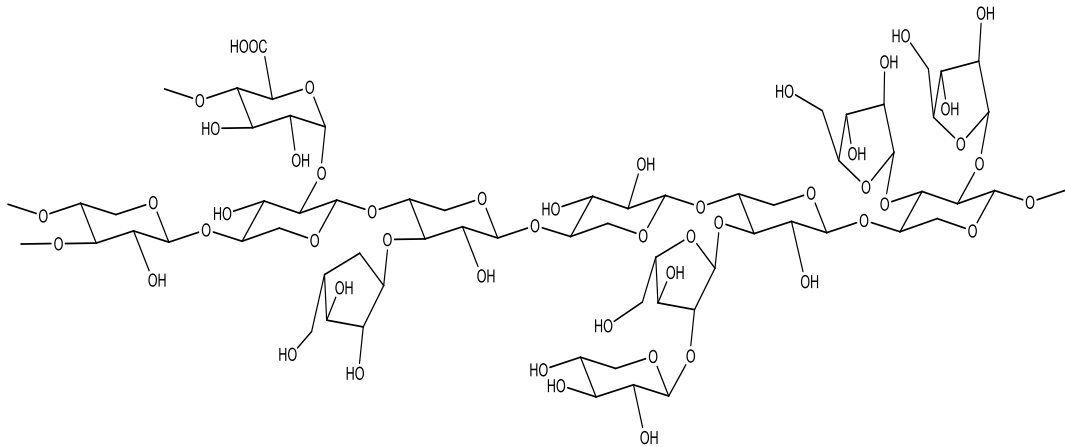


**Figure 1.2:** Hemicellulose Illustration.<sup>7</sup>

### 1.1.3 Lignin

Lignin is the second most abundant polymer on Earth<sup>8</sup>. It was first identified by Anselm Payen in 1838.<sup>9</sup> Cellulose and hemicellulose are held together by lignin which gives the biomass source its physical toughness. Lignin forms covalent crosslinking bonds between the cellulose and hemicellulose successfully preventing easy separation. As a cross linking reagent it also has potential value in resins, epoxides, and adhesives.<sup>10</sup> Major known issues with the above class of materials is that the lignin itself must be in a very pure form and the processes are very dependant on the type of lignin being used.

Lignin is a rigid amorphous polymer made up of three main monomers

(Figure 1.3) ; coniferyl alcohol (A), synapyl alcohol (B), and p-coumaryl alcohol (C).

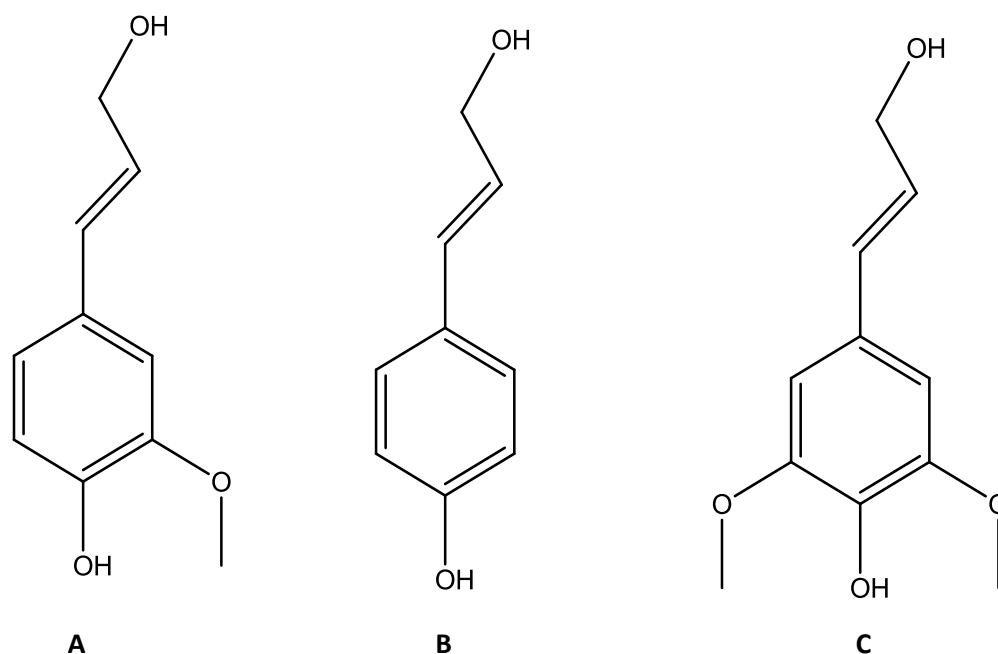


**Figure 1.3:** Coniferyl alcohol, p-Coumaryl alcohol, and Sinapyl alcohol.<sup>11</sup>

Radical polymerization of these three building blocks form many variations of phenyl propanoid units contributing to its amorphous structure (Figure 1.4, p. 6).<sup>12</sup> The monomers themselves comprise different percentages of the lignin when coming from different sources or even from the same source. Generally, the more synapyl alcohol the harder and stronger the source will be (trees and nuts) while the more coumaryl alcohol the softer the source will be (plants and grasses).<sup>11</sup> Lignin varies in the percentage of the whole biomass, 15-35% depending on the source.<sup>1</sup> The overall consequences of lignins variability and strength are costly removal and little value due to its complexity.

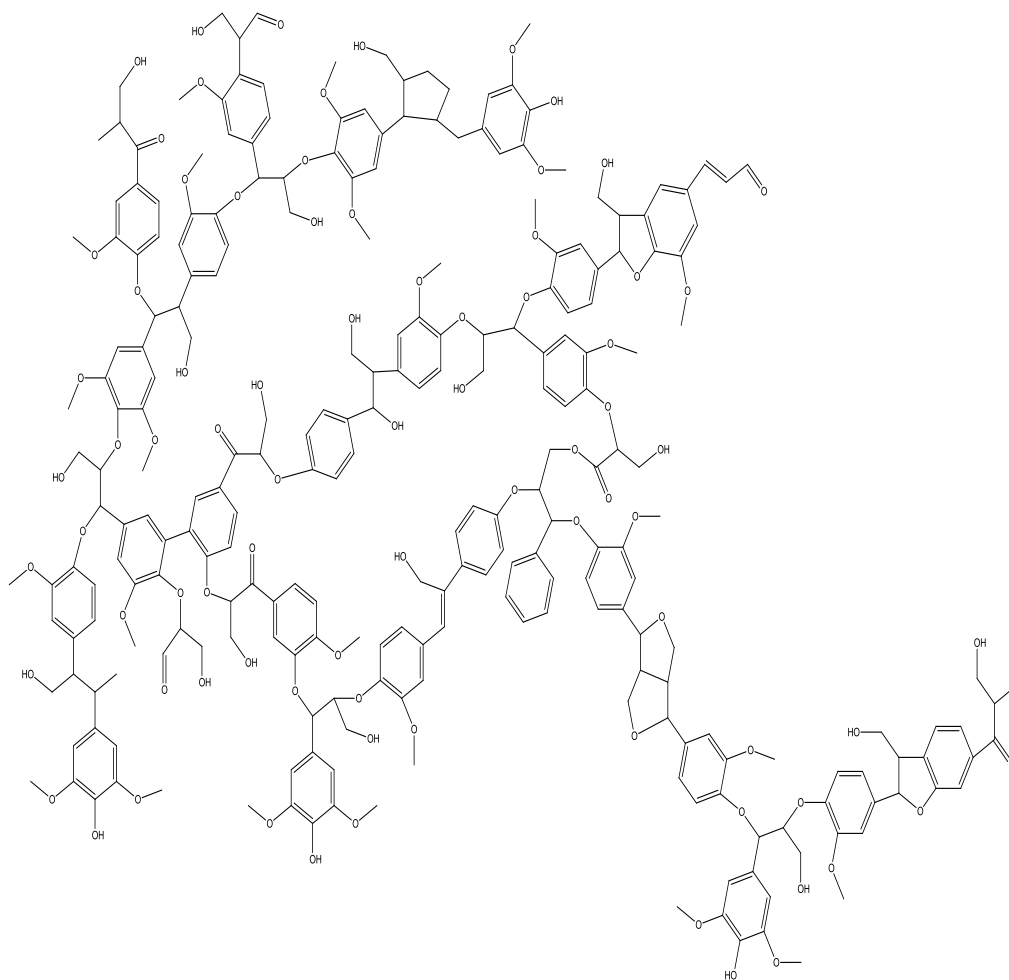


**Figure 1.4:** Determined Lignin Structure from Beech.<sup>13</sup>

### 1.1.3.1 Lignin Linkages

Over 50% of the covalent linkages in lignin are comprised of the  $\beta$ -O-4 type bonds (**Figure 1.5, p.7**). As a result many catalytic degradation studies involve model compounds containing a  $\beta$ -O-4 bond. The second most common bond is a 5-5 bond which is a direct bond of the aromatic rings and can be up to 27% of the total lignin

linkages. Other known less common linkages are the  $\beta$ -5, 4-O-5,  $\beta$ -1,  $\alpha$ -O-4, and the  $\beta$ - $\beta$  bond.<sup>11</sup>

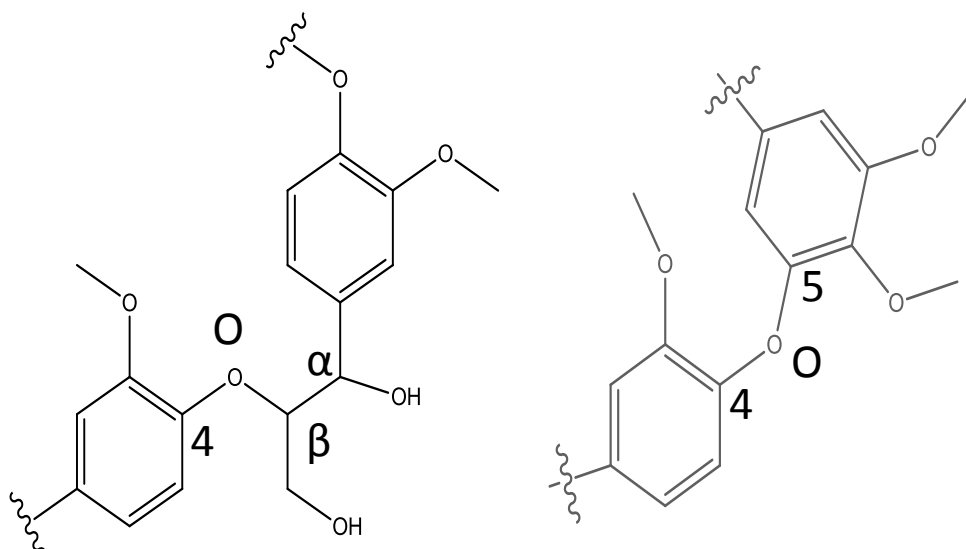


**Figure 1.5:** Examples of  $\beta$ -O-4 and 4-O-5 Linkages.<sup>11</sup>

### 1.1.3.2 Pretreatment Methods

Pretreatment is the breaking of the covalent bonds of the three lignocellulosic polymers. It is very cost intensive and a major problem for all lignocellulose usage. The ideal pretreatment method would include features such as high yields for all feedstocks, highly digestible pretreated solid, zero sugar degradation, minimal toxicity in reagents, ability to utilize large particles, low cost reactors, zero solid-waste, functionality with moisture, minimum energy costs, and lignin recovery.<sup>14</sup> Some of the currently utilized and studied lignin removal methods include mechanical

comminution, ionic liquid dissolution, the Kraft method, acid hydrolysis, steam explosion, and many others.

#### **1.1.3.2.1 Mechanical Comminution**

Mechanical processes have been developed but are very energy intensive usually involving mechanical milling, grinding, or chipping. Generally the smaller particles obtained from the process the more cost involved in the process.<sup>2</sup> The energy needed to breakdown the biomass is heavily dependant on source. A knife mill takes about 120 kWh/ton for an average particle size of 1.6mm with hardwood lignocellulosic source versus 7.5 kWh/ton when straw is the source.<sup>15</sup> The decrease in particle size is directly related to the accessibility of the cellulose for cellulase hydrolysis.

#### **1.1.3.2.2 Ionic Liquid Dissolution**

Ionic liquids are being looked at as an alternative solution to delignification for multiple reasons; mainly their non-volatile nature and reusability. Ionic liquids are considered green solvents because of their low vapor pressure and non-flammability. Certain ionic liquids have shown the ability to selectively dissolve lignin from cellulose and hemicellulose. Besides being green solvents, possibly the most important feature of ionic liquids towards their pretreatment applicability is their aptitude to dissolve lignin in a state that it can be further worked on. Many of the previous extraction processes involve harsh chemicals and high temperatures that are detrimental to the lignin. As a result most of lignin's potential value is lost upon removal and is just burned



as a low grade fuel source. Ionic liquids have also been examined with the additions of strong acids themselves and produced strong delignification results.<sup>8</sup> The current drawbacks are the difficulty to scale up and the effect they could potentially have on enzymatic processes.<sup>14</sup>

#### **1.1.3.2.3 Kraft Pulping Process**

The Kraft process is the most utilized pretreatment method worldwide.<sup>16</sup> With their core being a paper industry, extracting lignin is vital as it is directly related to the decoloration of the paper. The method involves a mixture of sodium hydroxide and sodium sulfide kept at about 170 °C. The sodium hydroxide in effect raises the pH high enough that it deprotonates the aryl phenolic groups. The ionization of the polymer allows the digestion into solution. This is important as it is this feature of lignin that allows it to be easily separated from both cellulose and hemicelluloses, as well as many of the smaller depolymerization products, sugars, and inorganic molecules.<sup>4</sup> The cellulose, hemicellulose, smaller depolymerization products, sugars, and inorganic molecules are soluble in neutral and acidic media, so lowering the pH of the solution causes only the lignin polymers to precipitate. Depolymerization is known to primarily occur at the aryl hydroxy and ether bonds on the  $\alpha$  and  $\beta$  carbons of the propanoid units conjoining the aromatic subunits. Kraft method studies, as well as most other studies on model compounds, show a strong selectivity for the phenolic groups over the methoxy with depolymerization.<sup>17</sup> In the Kraft delignification it has been shown that depolymerization occurs at the phenolic groups first and then methoxy groups

after the latter is completely finished. Similar results have been found with  $\beta$ -O-4 linked model compounds. Evtuguin and others have shown that under similar conditions with an oxidative catalyst,  $[\text{PMo}_7\text{V}_5\text{O}_{40}]^{8-}$ , and a reaction time of 20 minutes, the phenol 1-(3-Methoxy-4-hydroxyphenyl)-2-(2-methoxyphenoxy)ethanol was converted at 100% versus the methoxylated 1-(3,4-dimethoxyphenyl)-2-(2-methoxyphenoxy)ethanol conversion of only 20%.<sup>17</sup>

The kraft lignin precipitated product is usually just burned but can be methyl-sulfonated and used in higher valued applications, such as dye dispersants, agrochemical dispersants, and dopants in conductive polymers.<sup>4</sup> This is done by reacting the kraft lignin with formaldehyde and then followed by the addition of sodium sulfite. The nonsulfonated lignin is usually at a relatively high level of purity with a small percentage of common impurities such as carbohydrate moieties and some sulfur content from the pulping. Unmodified kraft lignin has a smaller percentage of it used in applications such as an anti-oxidant, adsorbent, and UV screens for active compounds in some crop protection chemicals.<sup>4</sup>

#### **1.1.3.2.4 Steam Explosion**

Another highly used pretreatment method is steam explosion. The chipped biomass is exposed to high-pressure steam and then it is quickly removed causing the biomass to undergo an explosive decompression. Temperatures range from 160-260 °C and pressures from 0.69-4.83 MPa. It is exposed from a few seconds to minutes at these conditions before returning back to atmospheric pressure. It does degrade

hemicellulose and alters the lignin allowing the cellulose to be hydrolyzed. Efficiency of the hydrolysis of cellulose has been reported up to 90% in a 24 hour period.<sup>14</sup>

Its advantages are zero recycling and zero environmental costs. Steam explosion is recognized as being much more cost effective on hardwoods than softwoods. However, it is energy intensive, yields are not always that good, and much of the hemicellulose is destroyed.

#### **1.1.3.2.5 Acid Hydrolysis**

Acid Hydrolysis is very effective in hydrolyzing cellulose, however it is more expensive than most pretreatment processes. Reactors must be resistant to corrosion making them very costly. Temperatures and acid concentrations have been shown to vary the results of the pretreatment significantly. Lower temperatures with dilute acids have been shown to be highly effective by Esteghlalian and others with xylose yields nearing 90% at only 1.1% acid concentration w/w.<sup>18</sup> In fact, higher temperatures have been shown to decrease yields due to sugar decomposition.<sup>19</sup>

### **1.2 WHITE ROT FUNGI (NATURE'S SOLUTION)**

It has been established since the 1930's that White Rot Fungi are what decompose lignin from decaying lignocellulosic biomass. White Rot Fungi are capable of degrading both cellulose and hemicellulose along with lignin. In hardwoods it is known to decompose each component simultaneously, however this is almost never

seen in softwoods.<sup>20</sup> It was not until the 1980's that the actual enzymes involved in the degradation started to become evident. The three main enzymes involved were all discovered between 1983 to 1987 and include Lignin Peroxidase (LiP), Manganese Peroxidase (MnP), and Laccase.<sup>21</sup> The first two active sites are hemes (**Figure 1.6 (A), p.13**), both with ferric centers. Heme's are most noted for their role in hemoglobin as an oxygen transferring agent in blood. However, they have many other functionalities and are located in many different proteins. As hemes are parts of much larger proteins, they tend to have very different sterically hindering environments and ligated ligands. The environment of the heme has a significant effect on the oxidation potential of the iron center and a corresponding effect on the activity in the body.<sup>22</sup> For example, in hemoglobin the heme is ligated by a histidine imidazole and acts as an oxygen transporting agent, while cytochrome P-450's heme is ligated by a cysteine sulfur atom and acts as an oxygenase. (There are also two sets of electron transferring heme active proteins termed catalases and peroxidases. Both react with hydrogen peroxide but differently. Catalases perform a disproportionation reaction with hydrogen peroxide, expected to be used in the body to prevent build up of the potentially dangerous oxidant. Peroxidases are more synthetically applicable as they use hydrogen peroxide as a sacrificial oxidant to catalyze a variety of oxidation of both organic and inorganic species.<sup>22</sup> Laccase's active site is a tetra copper, three and one system (**Figure 1.6 (B), p. 13**). It also has a great oxidation capability causing depolymerization as well as polymerization with lignin.

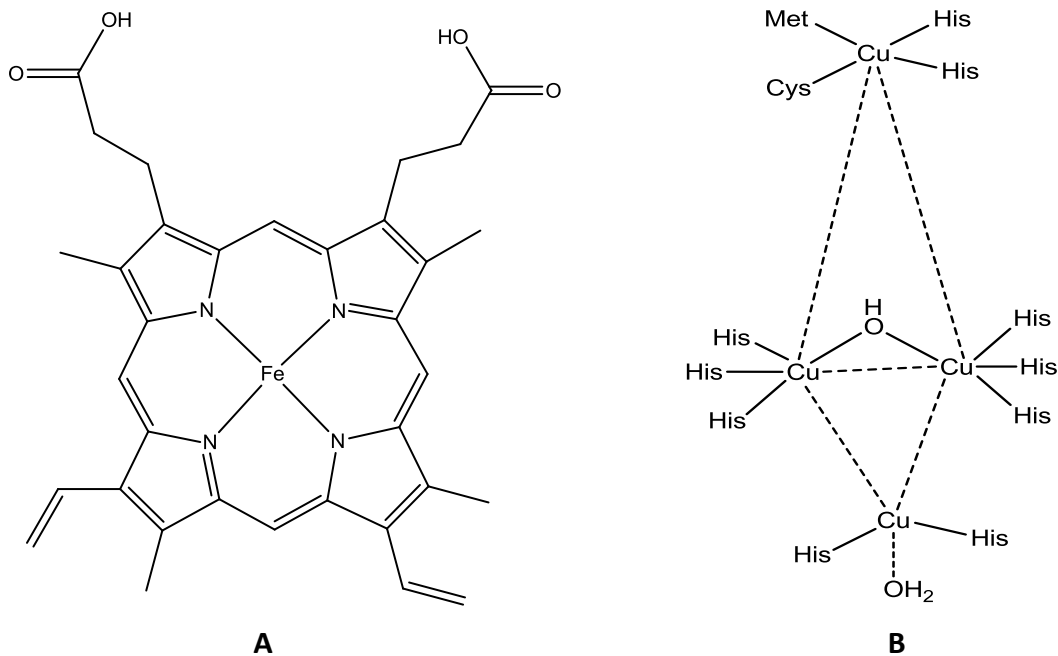


**Figure 1.6:** Chemical Structures of Heme and Laccase.<sup>23</sup>

LiP, MnP, and Laccase are a subset of many other lignin oxidases; phanochaete chrysosporium alone contains 16 different lignin oxidases. Kinetic studies of these enzymes with oxygen binding do show that they bind oxygen much stronger than other enzymes with heme active sites such as myoglobin or horseradish peroxidase.<sup>24</sup> Another class of lignin degrading enzymes are termed lignin-degrading auxiliary enzymes. The separation between classes are based on direct and indirect action with lignin degradation, lignin oxidases are involved directly while lignin-degrading auxiliary enzymes are hydrogen peroxide producers.

### **1.2.1 Phanerochaete Chrysosporium**

Phanerochaete chrysosporium is the most studied and most potent of the many different White Rot Fungi; each of which is classified as White Rot Fungi for its lignin degradation capabilities. The phanerochaete chrysosporium was first identified by Tien and Kirk in 1983.<sup>25</sup> It is about 42,000 daltons and has a physiological pH value of 4.5.<sup>26</sup> Lignin Peroxidase (LiP) and Manganese Peroxidase (MnP) actually comprise only 1% of all secreted proteins from the organism, while the 16 oxidases as a whole are nearly 11% of the secreted proteins. Chrysosporium is the only known white rot fungi that does not produce laccases. LiP is the key component known to be oxidized by hydrogen peroxide and then cause degradation of the lignin polymer by both partial polymerization and depolymerization.<sup>27</sup>

### **1.3 IONIC LIQUIDS**

Ionic liquids are generally defined as salts with melting point temperatures below 100 °C. They are relatively novel and feature many uncommon beneficial characteristics making them a hot topic of research. These liquid organic salts have shown many industrial and catalytic applications in the fields of organic and inorganic chemistry acting as both co-catalysts and solvents. As salts, ionic liquids are made up of a cation and anion; altering either of which can drastically change the salts physical and solvation characteristics.<sup>28</sup>

### 1.3.1 Synthetic Routes

The most common route to an ionic liquid is an alkylation reaction of an alkyl halide and an amine. The alkylated amine then becomes the cation with the halide as the coordinating anion. Common cations (**Figure 1.7**) include imidazolium (**A**), pyrrolidinium (**B**), pyridinium (**C**), ammonium (**D**), piperidinium (**E**), phosphonium (**F**), and sulfonium (**G**). The synthesis scheme does not involve any catalysts and most of the time, is solvent free as well. These two features make the synthesis of an ionic liquid a very green process and relatively straight forward. Depending on the alkyl halide in the reaction, syntheses times can be significant if just heating and stirring are applied, thus much research has been done on utilizing microwave and power ultrasound to speed the process up dramatically.<sup>28</sup>

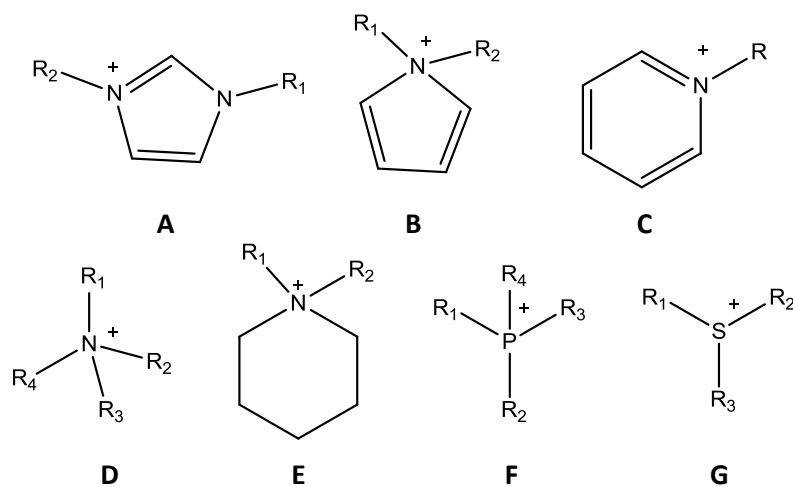


**Figure 1.7:** List of Common Ionic Liquid Cations.<sup>29</sup>

The microwave and ultrasound processes have also been coupled together and can increase reaction rates from multiple days to a couple hours. Reaction rates for the alkyl halide follow general substitution rules, so iodides are faster than bromides and bromides are faster than chlorides. The size of the alkyl halide also has a significant role on the reaction time; longer chains slow down the rate of the reaction significantly.

#### **1.3.1.1 Ion Exchange (Secondary Ionic Liquids)**

Following the formation of the ionic liquid, anion exchange is often done to adjust the solvent's characteristics. This type of ionic liquid is generally termed as a secondary ionic liquid. Common anions include the halides  $\text{Cl}^-$ ,  $\text{Br}^-$ , and  $\text{I}^-$ , but also exchange anions including  $\text{Al}_2\text{Cl}_7^-$ ,  $\text{Al}_3\text{Cl}_{10}^-$ ,  $\text{Sb}_2\text{F}_{11}^-$ ,  $\text{FeCl}_4^-$ ,  $\text{ZnCl}_5^-$ ,  $\text{Zn}_3\text{Cl}_7^-$ ,  $\text{CuCl}_2^-$ ,  $\text{SnCl}_2^-$ ,  $\text{NO}_3^-$ ,  $\text{PO}_4^-$ ,  $\text{HSO}_4^-$ ,  $\text{SO}_4^{2-}$ ,  $\text{CF}_3\text{SO}_3^-$ ,  $\text{ROSO}_3^-$ ,  $\text{CF}_3\text{CO}_2^-$ ,  $\text{C}_6\text{H}_5\text{SO}_3^-$ ,  $\text{PF}_6^-$ ,  $\text{SbF}_6^-$ ,  $\text{BF}_4^-$ ,  $(\text{CF}_3\text{SO}_2)_2\text{N}^-$ ,  $\text{N}(\text{CN})_2^-$ ,  $\text{BR}_4^-$ , and  $\text{RCB}_{11}\text{H}_{11}^-$ .<sup>30</sup> Exchanging anions can dramatically change the solvent's features, including polarity and density. Changing the polarity of an ionic liquid solvent can eliminate the hydration that occurs when exposed to air. This could be important in large batches such as in industrial applications. Anion exchange can be done by metathesis or with an ion exchange column. The process used usually depends on the characteristics of the products versus the starting material, and purity level needed for the application of use. The major issue with the metathesis method is that the products are both salts. When the resulting ionic liquid is still hydrophilic, it can be nearly impossible to purify the ionic liquid to a spectroscopic level. In cases where higher purity levels are necessary an ion exchange column is often used.



One major problem with ionic liquid research is obtaining very pure samples. As stated above the synthetic route to an ionic liquid is very straightforward and usually resulting in high yields, however purification is not always easy. In many cases impurities can be washed away with other solvents or distilled utilizing the ionic liquids low vapor pressure, however this usually does not leave the ionic liquid “pure”. Halides and imidazoles are difficult to get rid of by either of the above two methods, thus simple methods have been developed to analytically determine the purity levels of these solvents. Halides can easily be measured with an ion selective electrode or by cyclic voltammetry. Residual 1-methylimidazole will show up in an  $^1\text{H-NMR}$  analysis or much quicker with a colorimetric test with  $\text{CuCl}_2 \cdot 2\text{H}_2\text{O}$  that was developed in 2000 by Holbrey and others.<sup>31</sup> The addition of the  $\text{CuCl}_2 \cdot 2\text{H}_2\text{O}$  will turn the ionic liquid blue with as little as 8 mmol/L of methylimidazole in solution.

### **1.3.2 Ionic Liquid Applications**

One of the most intriguing features of ionic liquids is their catalytic and co-catalytic abilities. Often catalytic reactions will take different routes than in traditional organic solvents. There are numerous examples in the literature of ionic liquids changing the synthetic route, activity, and even selectivity of the synthesis. The overall effect of using an ionic liquid in synthesis is still hard to predict and often are chosen more at random than task specific. Task Specific Ionic Liquids are a more specific class of ionic liquids that are not only used as the solvent but co-catalysts in an experiment.

Alkylation of benzene has been done at 50 °C with high yields in an alkyl pyridinium ionic liquid and ferrous chloride as the catalyst. Product formation occurred without the catalyst but not enough to be an efficient synthetic route with yields between 15 and 20% at most. Still the combination allows for significantly lower thermal conditions and easy separation compared to an organic solvent. The ionic liquid anions compared were the tetrafluoroborate and trifluoroacetate, the latter produced higher yields in every experimental run.<sup>32</sup> There is really no explanation given as to why this is, but it is a great example of the tunability of ionic liquids that should be more predictable in the near future. Being ionic in nature, ionic liquids can be predicted to stabilize the transition states of ionic intermediates often causing energy barriers to be lower and reaction times and yields to be improved.

Ionic liquids are electrochemically conductive just as inorganic salts are. Electrochemical applications include uses in mechanical actuator devices, electrolyte mediator solutions in photovoltaic cells, electrolytes in electrochemical super capacitors, lithium batteries, and treatment of nuclear waste.<sup>29</sup>

#### **1.4 LIGNIN AND LIGNIN MODEL COMPOUNDS IN IONIC LIQUIDS**

Lignin oxidation studies have been done with many inorganic co-catalysts in an attempt to maximize the output while minimizing energy usage. Some of these studies have been in variant pH aqueous solutions and some more recently have been completed in neat ionic liquids.<sup>33</sup> Possibly the most important aspect of lignin

dissolution studies with ionic liquid oxidation strategies is the ability to recycle and reuse the ionic liquid itself. Ionic liquids are considered green solvents but their disposal is not, and their cost is still very high relative to other common organic solvents and a major problem associated to industrial scale up. Ideally the post oxidative lignin would be broken down into clean, valuable, and functional chemicals, with further separation very easy. However, current oxidations generally only degrade lignin to levels of about 10 degrees of polymerization.<sup>6</sup> At molecular weights this high distillation is still not a feasible option. Therefore non-polar organic extractions of the oxidized lignin products are usually done for ionic liquid recycling. Another viable method is to decompose the lignin byproducts into humin. With proper conditions, a 100% delignification can be achieved with  $\text{CrCl}_3 \cdot 6\text{H}_2\text{O}$ . It is worth noting that even in an ionic liquid aqueous ethanol solution 7:3 the chromium hydrate had a significantly greater activity than the nonhydrate. In fact at a 170 °C, yields of the humin were in the 89-100% range with the hydrate and 46-51% without.<sup>9</sup> The humin products were simply filtered out after each use.

There have been many oxidation studies of lignin model compounds in ionic liquids with other metal chlorides. The  $\beta$ -O-4 bond is the most common linkage in lignin and therefore a common bond type for model compound studies. Guaiacylglycerol- $\beta$ -guaiacyl ether (GG) (**Figure 1.8, p. 20**) and veratrylglycol- $\beta$ -guaiacyl ether (VG) are very common for these studies.

In a comparison study of the different metal chlorides with GG in BMIMCl, AlCl<sub>3</sub>, FeCl<sub>3</sub>, and CuCl<sub>2</sub> all had conversion percentages at 90% and higher.<sup>33</sup> The main products were guaiacol, hibbert's ketones, the enol ether, and varying percentages of dimers of each. Hibbert's ketones are well known to occur when treating β-O-4 linkages with acids in organic solvents.<sup>34</sup>

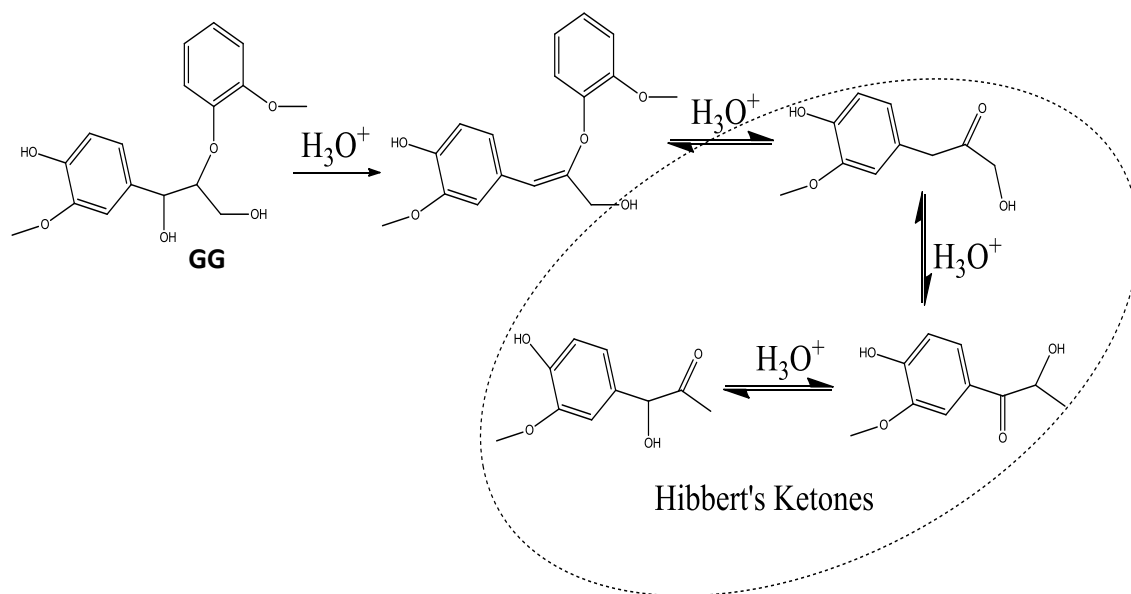


**Figure 1.8:** Formation of Hibbert's Ketones Through Acidolysis.<sup>35</sup>

There have also been numerous studies with strong protic acids showing signs of increased activity with lignin model compounds in ionic liquids. In fact, the above studies show similar results and thus it is suspected that an in situ HCl species is actually what is catalyzing the reaction.<sup>29</sup> Further evidence of HCl catalyzing the reaction was accomplished by demonstrating the amount of guaiacol formed relied heavily on the water content in the ionic liquid. Up to a 32:1 ratio of water to GG showed an increase in the amount of guaiacol formed. Diederick demonstrated that

[BMIM]MeSO<sub>4</sub> in a 1:10 ratio with sulfuric acid can selectively rid xylan and lignin components.<sup>8</sup> Xylan has been identified as a chemical that assists lignin recalcitrance, and the removal is the reason given for the tremendous delignification from the solvent mixture. Main products were furfural and hydroxymethylfurfural. These were further oxidized with higher concentrations of acid in solution to levulinic acid and acetic acid.

### 1.5 PORPHYRINS

The first isolated porphyrin was accomplished in 1840 by Berzelius, a medicinal chemist. It was isolated by a sulfuric acid treatment of blood, removing the heme from hemoglobin. The sharp strong near UV absorbance band was first discovered by Sorret in 1883 and the band is still termed the Sorret band today.<sup>36</sup> Porphyrins are heme like 26 electron aromatic compounds with powerful oxidizing power in the presence of sacrificial co-oxidants. Porphyrins (**Figure 1.9 (C), p.22**) are functionalized porphines (**A**), analogues of nature's extremely active heme (**B**). Porphyrins have been synthesized with many d-block metals including Fe, Mn, Cu, Zn, Co, V, Ti, Zr, Hf, Nb, Ta, Cr, Mo, Pd, and W.<sup>37</sup> Crystal structures have shown that the position of the metal varies with the type of metal as well as the substituents on the porphyrin itself. Porphyrins are very attractive biomimetic catalysts due to their tunability, activity over a wide pH range, and oxidizing power.

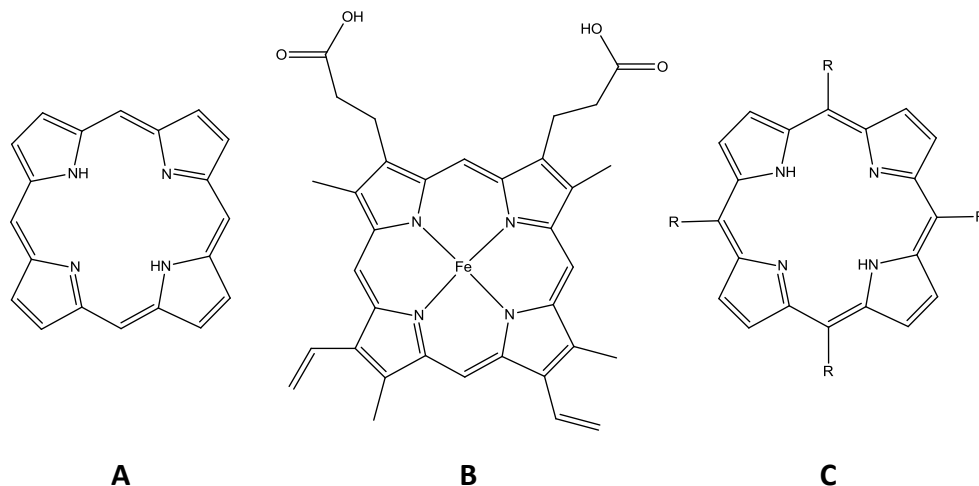


**Figure 1.9:** Porphine, Heme, and Porphyrin.

### 1.5.1 Synthetic Routes

The two most currently used methods to synthesizing a porphyrin were developed by Adler and Longo, and Lindsey.<sup>38</sup> The first known successful synthetic attempt at synthesizing hemin was done by Fischer in 1929, and he soon won the Nobel Prize in 1930.<sup>36</sup> Rothmund was able to synthesize porphine (**Figure 1.9, (A)**) by mixing benzaldehyde and an equivalent amount of pyrrole in pyridine with a very high pressure system at 150 °C for 24 hours in 1936.<sup>39</sup>

#### 1.5.1.1 Adler and Lindsey Methods

In 1967 Adler and Longo developed the more traditional method for large scale porphyrin synthesis. They found that the reaction proceeded faster with much higher yields if the reaction was open to air and an organic acid was used as the solvent instead of pyridine.<sup>40</sup>

Lindsey developed his own synthetic method in 1986. He utilized the idea that the reaction was in equilibrium between the porphyrinogen and polypyrrylmethanes and found that the equilibrium can be altered favorably by lowering the concentrations of the aldehyde and pyrrole. At higher concentrations the equilibrium will favor the formation of the long chained polypyrrylmethanes, however at lower concentrations the equilibrium will favor the porphyrinogen. At lower concentrations with much milder conditions a much higher yield can be produced, about twice that of Adler's method.<sup>38</sup> The method does require its own oxidizing agent, usually 2,3,5,6-tetrachlorobenzoquinone (TCBQ) or 2,3-dichloro-5,6-dicyanobenzoquinone (DDQ); either agent will take the porphyrinogen to the porphyrin product. The new method uses a non-polar aprotic organic solvent and a Lewis acid catalyst versus the refluxing organic acid. The less strenuous conditions allow for more variation in the substituents of the porphyrin. In the past, substituents such as alcohols, dioxanes, and others could not be completed as the reaction conditions were too extreme causing degradation.<sup>38</sup> For all the great additions Lindsey's method provides, it does come with the limitations of difficulty in scaling up, additional time, additional solvent use, environmentally harmful lewis acids like Borontrifluoride etherate ( $\text{Et}_2\text{O}\cdot\text{BF}_3$ ), and cost.

#### **1.5.1.2 Dipyrromethane Porphyrin Synthesis**

One of the few common methods to synthesize a porphyrin involves the condensation reaction of two dipyrromethane molecules with an aldehyde. Synthesis in this method has some advantages. These include, overall yields which are usually on

par with Lindsey's method at about 30%, and asymmetric porphyrin synthesis can be more predictable and the products be more easily separated. The traditional method to synthesizing dipyrromethane compounds involves the condensation of an aldehyde with pyrrole catalyzed by a strong Lewis acid such as trifluoroacetic acid in refluxing toluene. Recently a research group from Azad College in India, developed a quick organic solvent free, high yielding method, with  $\text{SnCl}_2$  as the catalyst. With over fourteen compounds they were able to synthesize the dipyrromethane in over 80% yields and in many cases above 95%.<sup>41</sup>

### 1.5.2 Porphyrin Catalytic Studies

Following biological advancements in determination of the active sites in the lignin degrading enzymes, began porphyrin oxidation studies with lignin and lignin model compounds.<sup>42</sup> Research has progressed in the area of axial ligand effects, solvent effects, and aryl substituent effects on the catalytic capabilities of metalloporphyrins over the past 30 years. Many different catalytic oxidation reactions have been studied such as epoxidations and other single electron radical reactions. Porphyrin oxidation is known to go by a couple of different routes. One way involves a single electron oxidizing radical and the second route is a two electron oxo-transfer oxidation.<sup>43</sup> Porphyrin oxidations need a sacrificial oxidant, the most commonly studied co-oxidant is likely hydrogen peroxide (**Figure 1.10 (C), p.25**); others include *m*-chloroperoxybenzoic acid (mCPBA) (**A**) and iodosobenzene (PhIO) (**B**) and derivatives.



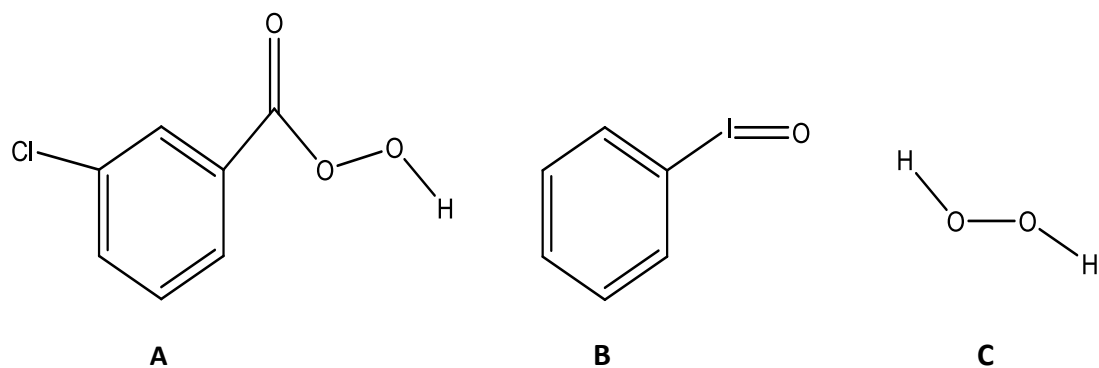


**Figure 1.10:** Common Co-Oxidants mCPBA, PhIO, Hydrogen Peroxide.

### 1.5.2.1 Porphyrin Epoxidation

Experimental studies have shown that the various oxidants will produce different active or inactive porphyrin species. For example, molecular oxygen can be used as the oxidizing species in many applications, however it is ineffective in epoxidation reactions because the active oxene species (**Figure 1.11, p. 27**) does not form with molecular oxygen. Its active species is the neutral FeIV oxo species.<sup>44</sup> Epoxidations have also been shown to not produce any product even with hydrogen peroxide as the oxidant. Hydrogen peroxide does produce the active oxene complex at lower concentrations, however it also reacts with the oxene complex and destroys it, forming water and oxygen at higher concentrations.<sup>45</sup> Oxygen can then further react with the iron(III) porphyrin to form the oxo complex but that complex is not active in epoxidations. Studies by Traylor and others demonstrated a very important piece of information with hydrogen peroxide as the oxidant; increasing electron withdrawing substituents has a strong effect on the selectivity of the oxene complex. A near linear

relationship was shown with electron withdrawing groups and yields of multiple epoxidation products with hydrogen peroxide as the oxidant.<sup>46</sup> In further studies he was also able to show that this was only applicable to peroxides and inverse kinetics applied to electron withdrawing substituents when PhIO was used as the co-oxidant. This has to do with a proton transfer at the transition state at which the release of the active oxene complex occurs.<sup>47</sup> Groves and others found that the active species with styrene was favored in polar solvents only. In a similar study with benzene as the solvent, Groves expected the mechanism followed a more direct route with an attack of the FeIV-oxo on the alkene bond.<sup>48</sup> Traylor and others have heavily repeated that this is not an active species and have significant evidence of this based on stereo selectivity of the epoxidations. The oxene complex produces a high stereo excess of the exo product whereas the oxo intermediate has no activity and therefore stereoselectivity. According to Traylor the formation of the epoxides is not from the reaction of the porphyrin oxo complex but with the reaction of peroxy radicals formed from *in situ* reactions which are known epoxidizing agents with little to no stereo selectivity. Stephenson came back to the epoxidation mechanism and determined that the active species was the radical cation however it was significantly activated by a substitution of the chloride ligand with a methoxy, providing Groves explanation that the active species only occurs in polar solvents.<sup>49</sup> Stephenson then went a step further and proved that the actual intermediate was a coordinated methoxy group to a porphyrin cation and that this mechanism functions with other non-sterically hindered alcohols.<sup>50</sup> Two different peaks appeared in a <sup>1</sup>H-NMR spectra at 82 and 65 ppm from

the pyrrole protons in the ring, one corresponding the ligated chloride and one to the solvated cation.<sup>51</sup>

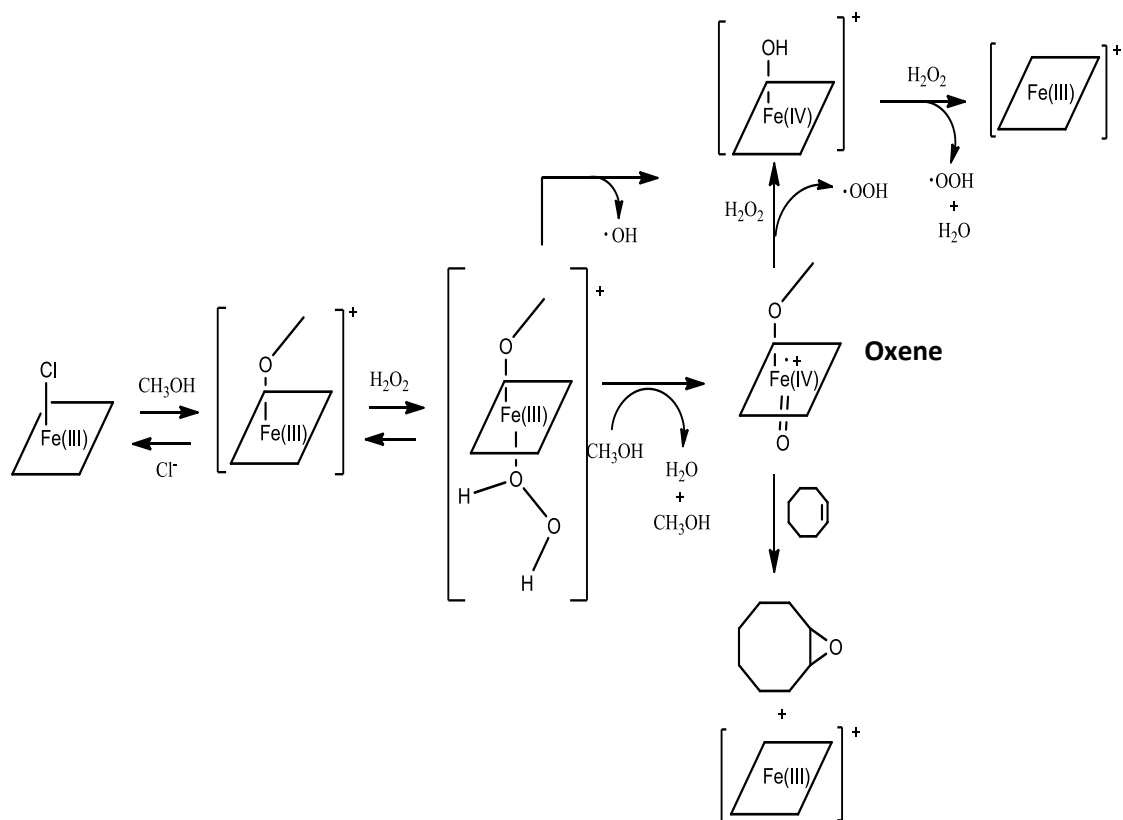


**Figure 1.11:** Iron Porphyrin Epoxidation Mechanism with Hydrogen Peroxide.<sup>51</sup>

Oxidation potentials for porphyrins have been reported to be partially dependent on the electron-withdrawing ability of the aryl substituents as mentioned above. More electron-withdrawing substituents mean more oxidizing potential. However, this does not always translate to kinetics studies.<sup>43</sup> Inverse kinetics has been established in the oxidation of a series of benzyl alcohols and unsaturated carbon compounds in acetonitrile with mCPBA as the oxidant. An FeIV radical cation oxene complex following an *in situ* disproportionation reaction from the small amount of

water has been confirmed to assist forming the active oxidizing species. This was determined by UV-Vis spectroscopy and kinetic studies. The reaction rate clearly decreased in each experiment after increasing the concentration of the inactive FeIII disproportionation product.<sup>43</sup>

The oxidation of naphthalene to naphthol continued to show that the selectivity as well as activity can significantly change when altering the solvent, even in reactions differing from epoxidations.<sup>52</sup> In the study, the most electron deficient porphyrin had the highest turnover number in each run, however variations in solvent, as well as the oxidative co-catalyst had dramatic effects on yields, selectivity, and turnover number. Metalloporphyrins confirmation and oxidizing potential have been shown to change according to the electron density of the metal center, thus the effect seen is probably due to the metal being more exposed versus interactions of the ligands. Another interesting aspect to the research, was the addition of weak bases such as imidazole and pyridine. They had substantial effects on selectivity and activity, with imidazole making a larger contribution than pyridine. The effects of the imidazole were relatively equal with the three different porphyrins, however pyridine only had a significant contribution with the most electron deficient porphyrin and not any with either of the more electron rich porphyrins. The reactions were performed in methanol, and the results indicate that it can be inferred from the increase in reaction rates with the addition of imidazole, that the imidazole did exchange with the methanol and

coordinated to the porphyrin even in the presence of an alcohol that has proven to help create the active oxene complex already.

### 1.5.2.2 Porphyrin as Heck Catalyst

An ionic pyridinium porphyrin with a palladium metal center was synthesized by Wan and Liu and comparatively tested with PdCl<sub>2</sub> as a Heck Reaction catalyst in an ionic liquid.<sup>53</sup> The porphyrin was found to be highly recyclable and more active than the traditional PdCl<sub>2</sub> catalyst at the same concentration. At a 0.005% (mol) relative to the ester, the porphyrin catalyst yielded 98% of the corresponding product (**Figure 1.2**), while PdCl<sub>2</sub> only managed 54%.

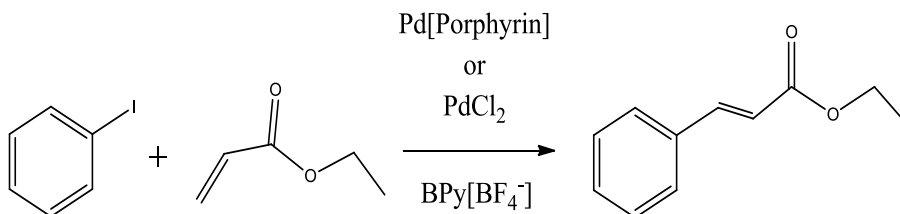


**Figure 1.12:** Heck Reaction Catalyzed by a Pd Porphyrin Analogue.

The paper also noted the difference in yields based on the solvent used. The BPy[BF<sub>4</sub><sup>-</sup>] was the highest with quantitative yields, BMIM[BF<sub>4</sub><sup>-</sup>] only produced a 76% yield. In fact with DMF as the solvent they were able to produce a 94% yield.

### 1.5.2.3 Porphyrin Oxidations of Lignin Model Compounds

With lignins amorphous complex structure, model compounds are beneficial to study as data can be much more predictable and reproducible than that obtained from

lignin studies themselves. Monomeric and dimeric model compounds have been extensively studied with many of the common delignification methods as well as many fungal cultures and biomimetic porphyrin catalysts. Cui and Dolphin studied a series of model compounds with a very polar sterically hindering iron tetrasulfonato porphyrin. Many studies have demonstrated that porphyrins with these characteristics behave more like peroxidases do in nature. Dimers with  $\beta$ -O-4,  $\beta$ -5, and  $\beta$ -1 linkages were all studied with t-BuOOH as the co-oxidant.<sup>54</sup> The  $\beta$ -O-4 model compound was 4-Ethoxy-3-methoxyphenylglycerol- $\beta$ -guaiacyl ether (**Figure 1.13 (EG), 31**). The dimer was cleaved at the  $C_{\alpha}$ - $C_{\beta}$  position leaving the major products as the veratraldehyde derivative 4-ethoxy-3-methoxybenzaldehyde and guaiacol. The  $\beta$ -1 dimer studied was 1-(4-ethoxy-3-methoxyphenyl)-2-(4-methoxyphenyl)-1,3-propanediol (**Figure 1.13 (PG), 31**). Again the  $C_{\alpha}$ - $C_{\beta}$  bond was cleaved separating the two aromatic ring structures into monomers, however varying levels of oxidation were completed forming at least 6 different products. Ethyl-dehydrodiisoeugenol (**Figure 1.13 (EHG), p. 31**) was studied as a  $\beta$ -5 dimer. The oxidation yielded at least 8 different compounds, however most were dimers with varying degrees of oxidation at the aromatic rings. In fact aromatic ring cleavage was observed for this reaction yielding the corresponding diester compounds.

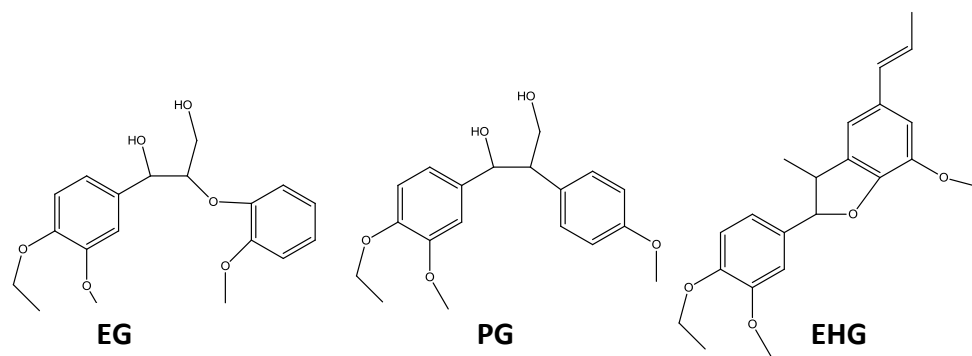


**Figure 1.13:** Structures of Model Compounds Studied by Cui and Dolphin.<sup>54</sup>

## CHAPTER II

### METHODS AND RESULTS

Reactions were carried out in an open atmosphere unless noted. Pyrrole was freshly distilled and used within a week. All solvent drying was done in a rotatory evaporator equipped with both a high vacuum pump and house vacuum. Solvents and reagents were bought from either Fisher Scientific or Sigma Aldrich. All reagents were used as bought unless otherwise noted. Silica gel thin layer chromatography (TLC) plates and 70-200 mesh silica gel for column chromatography. Yields for the ionic porphyrins were calculated based on the maximum number of moles and mass weighed subtracting any water that could be identified in the  $^1\text{H}$ -NMR spectrum.  $^1\text{H}$ -NMR spectra reported were collected on a 300 MHz JEOL at Berea College. Chemical shifts are reported based on a tetra-methyl silane (TMS) standard that was added or came with each deuterated solvent. Infrared Spectroscopy spectra were obtained on an Attenuated Total Reflection Infrared (ATR-IR) Spectrometer. UV-Vis data were recorded on a Varian Spectrometer. All the data presented for each compound is tabulated in the Appendix.

#### 2.1 SYNTHESIS OF BENZYL IONIC LIQUID TAGGED PORPHYRINS

Compounds from section 2.1 are displayed in the appendix (**Figure A.12, p. 95**).



### 2.1.1 $\alpha$ -bromotolualdehyde (Cp1)

This procedure was taken from Win, Li, and Schlenoff, and utilized as previously published.<sup>55</sup> In a 3-neck round bottom flask, 3.00 g of  $\alpha$ -bromotolunitrile (15.3 mmol, 1 equiv) was dissolved in 30 mL of toluene under N<sub>2</sub> at 0 °C. To the flask, 20 mL of 1.08 M DIBAL-H (43.2 mmol) in hexanes was added drop wise over several minutes and stirred for 75 minutes. Chloroform (40 mL) and 10% (w/w) HCl (100 mL) were added and the reaction was allowed to stir for an additional hour at room temperature. The mixture was separated and the organic layer dried with magnesium sulfate, concentrated *in vacuo*, and washed with hexanes. Yield 2.62 g (86%). <sup>1</sup>H-NMR (CDCl<sub>3</sub>) 9.93 (s, 1H, alde), 7.79 (d, 2H, CH phenyl), 7.49 (d, 2H, CH phenyl), 4.43 (s, 2H, CH<sub>2</sub> methyl) ppm, melting point 98.6 – 100.0 °C.

### 2.1.2 5, 10, 15, 20-tetrakis(p-tolylbromide)porphyrin (Cp2)

A 1 L round bottom flask was charged with 1.00 g  $\alpha$ -bromotolualdehyde (5 mmol, 1 equiv), 500 mL of chloroform (to a concentration of 0.01 M aldehyde), and 0.34 g of pyrrole (5 mmol, 1 equiv). The reaction mixture was stirred for 25 minutes under N<sub>2</sub> and 0.035 g of boron trifluoride-etherate (0.25 mmol) was added drop wise and stirred for an additional 75 minutes. Triethylamine (0.25 g, 0.25 mmol) and 1.29 g of TCBQ (5 mmol, 1 equiv) were added to the reaction mixture with stirring. The resulting mixture was stirred in a preheated sand bath and refluxed for an additional hour. The mixture was concentrated to approximately 20 mL and crystallized out with methanol and placed in a freezer at -10 °C for 30 minutes. The solid product was

filtered and washed with methanol again until the filtrate was clear. Yield 0.608g (52%).  
 $^1\text{H-NMR}$  ( $\text{CDCl}_3$ ) 8.91 (s, 8H, CH pyr), 8.24 (d, 8H, CH phenyl), 7.74 (d, 8H, CH phenyl), 4.92 (s, 8H, CH methyl), -2.91 (s, 2H, NH ring) ppm. 3326 and 3307 (m, N-H), 3028 (m, C-H), 1608, 1555, and 1502 (m, C=C), 1259 (s,  $\text{CH}_2\text{Br}$ )  $\text{cm}^{-1}$ . UV-Vis ( $\text{CHCl}_3$ ) 420max, 517, 551, 589, 646 nm.

### **2.1.3 5, 10, 15, 20-tetrakis(p-tolyl 1-methylimidazolium)porphyrin bromide (Cp3)**

To a 25 mL round bottom flask 0.300 g of **Cp2** (0.304 mmol, 1 equiv) was added and dissolved in 6.00 mL of 1-methylimidazole. The mixture was heated and stirred 4 days at 110 °C in a  $\text{N}_2$  environment. The crude mixture was initially crystallized out with ether and then redissolved in methanol and again crystallized out with a 9:1 isopropanol ether solution. The mixture was placed in a -10 °C freezer for 3 hours and filtered and washed with isopropanol until the filtrate was clear. Yield 0.252 g (44%).  
 $^1\text{H-NMR}$  ( $\text{DMSO}_{d6}$ ) 9.54 (s, 4H, CH imid), 8.79 (s, 8H, CH pyr), 8.26 (d, 8H, CH phenyl), 8.08 (d, 4H, CH imid), 7.88 (d, 8H, CH phenyl) 7.85 (d, 4H, CH imid), 5.81 (s, 8H,  $\text{CH}_2$  alpha), 3.97 (s, 12H,  $\text{CH}_3$  imid), -2.97 (s, 2H, NH ring) ppm. IR 3142 and 3106 (m, C-H), 1611, 1571, and 1559 (m, C=C), 1157 (s, C-N)  $\text{cm}^{-1}$ . UV-Vis ( $\text{H}_2\text{O}$ ) 420max, 431 nm.

### **2.1.4 5, 10, 15, 20-tetrakis(p-tolyl triphenylphosphine)porphyrin bromide(Cp4)**

To a 25 mL round bottom flask was added 4.00 mL of DMF 0.200 g of **Cp2** (0.203 mmol, 1 equiv), and 0.250 g of triphenylphosphine (0.953 mmol, 4.7 equiv) then the flask was heated to a 100 °C under  $\text{N}_2$ . The reaction was stopped after 45 hours and

concentrated to dryness with a rotary evaporator. The crude product was redissolved in 5 mL of methanol and precipitated out with 2 mL of ether added dropwise and filtered. The product was then washed heavily with ether until the filtrate was nearly clear. Yield 0.274 g (58%).  $^1\text{H-NMR}$  8.79 (s, 8H, CH pyr), 8.05 (d, 24H, CH phos), 8.018 (d, 8H, CH phenyl), 7.99 (m, 24H, CH phos), 7.96 (m, 12H, CH phos), 7.48 (d, 8H, CH phenyl), 5.66 (d, 8H,  $\text{CH}_2$  methyl) ppm.

#### **2.1.5 Iron (5, 10, 15, 20-tetrakis(p-tolyl 1-methylimidazolium)porphyrin bromide) chloride (Cp5)**

A 0.100 g amount of **Cp3** (0.076 mmol, 1 equiv) was added to a 25 mL round bottom flask followed by the addition of 2.00 mL of water. After stirring the mixture 0.075 g (0.377 mmol, 5 equiv) of  $\text{FeCl}_2 \cdot 4\text{H}_2\text{O}$  were added to the mixture and then refluxed for 24 hours<sup>56</sup>. The solvent was dried on a rotary evaporator and the remaining crude product was redissolved in a minimal amount of methanol (~2 mL). The product was then crystallized with the addition of isopropanol and filtered. The product was washed heavily with isopropanol to insure that all of the excess  $\text{FeCl}_2$  was removed. Yield 0.096 g (90%). IR 3141 and 3105 (m, C-H), 1613, 1572, and 1560 (m, C=C), 1158 (s, C-N), 998 (s, N-Fe)  $\text{cm}^{-1}$ . UV-Vis ( $\text{H}_2\text{O}$ ) 415max, 516, 558 nm.

### **2.1.6 Iron (5, 10, 15, 20-tetrakis(p-tolyl triphenylphosphine)porphyrin bromide) chloride (Cp6)**

A 0.100 g of **Cp4** (0.0479 mmol, 1 equiv) was added to a 25 mL round bottom flask. An addition of 4.00 mL of water and stirring was done before the addition of 0.029 g of  $\text{FeCl}_2 \cdot 4\text{H}_2\text{O}$  (0.227 mmol, 4.74 equiv)<sup>56</sup>. The mixture was then refluxed for 25 hours. After removing the solvent the crude compound was redissolved in 2 mL of methanol and crystallized with a minimal amount of ether. The product was washed thoroughly and filtered. Yield 0.0801 g (77%). IR 3056 (m, C-H), 1615, 1586, and 1553 (m, C=C), 1436 and 1110 (s, C-P), 996 (s, N-Fe)  $\text{cm}^{-1}$ . UV-Vis 419max, 520 nm.

## **2.2 SYNTHESIS OF PYRIDINIUM IONIC LIQUID TAGGED PORPHYRINS**

Compounds from section 2.2 are displayed in the appendix (**Figure A.12, p. 95**).

### **2.2.1 5, 10, 15, 20-tetrakis(4-pyridyl)porphyrin (Cp7)**

A three neck 1 L round bottom flask was charged with 200 mL of propionic acid heated to 120 °C and then 5.112 g of 4-pyridinecarboxaldehyde (47.8 mmol, 1 equiv) and 3.29 g (49.0 mmol, slight excess) of pyrrole were added. The reaction mixture temperature was raised to refluxing and continued to stir for 75 minutes. Then the mixture was allowed to cool to near room temperature and concentrated to about 10 mL with a rotary evaporator. The product was crystallized out after adding 100 mL of methanol and put in the freezer for 30 minutes at -10 °C. The mixture was then filtered and rinsed with a small amount of additional methanol. Yield 1.162 g (16%). <sup>1</sup>H-NMR

(CdCl<sub>3</sub>) 9.00 (d, 8H, CH phenyl), 8.80 (s, 8H, CH pyr), 8.10 (d, 8H, CH phenyl), -2.99 (s, 2H, NH ring) ppm. IR 3312 (m, NH), 3089 (m, CH phenyl), 1594 (s, CC phenyl) cm<sup>-1</sup>. UV-Vis (CHCl<sub>3</sub>) 419max, 513, 543, 587, 643 nm.

### 2.2.2 5, 10, 15, 20-tetrakis(N-3-bromopropylpyridinium-4-yl)porphyrin bromide (Cp8)

In a 250 mL round bottom flask, 10.44 g of 1,3-dibromopropane (12x excess) were added to 0.200 g of **Cp7** (0.324 mmol, 1 equiv) in 25 mL of DMF and allowed to stir at 40 °C for 96 hours. The crude product was concentrated to about 5 mL of DMF and crystallized with 40 mL of a 1:1 mixture of ethyl acetate and chloroform. The mixture was cooled at -10 °C for 5 hours and filtered. The product was further purified by dissolving in a small amount of methanol and filtering. The filtrate was dried by the rotary evaporator and weighed. Crude Yield 0.172 g (37%). <sup>1</sup>H-NMR (DMSO<sub>d6</sub>) 9.50 (d, 8H, CH phenyl), 9.21 (d, 8H, CH pyr), 8.98 (d, 8H, CH phenyl), 5.06 (t, 8H, CH ), 2.85 (m, 8H, CH allyl), 2.51 (t, 4H, CH<sub>2</sub> alkyl), -3.13 (s, 2H, NH) ppm.

### 2.2.3 5, 10, 15, 20-tetrakis(N-allylpyridinium-4-yl)porphyrin bromide (Cp9)

A 50 mL round bottom flask was charged with 3.25 mL of DMF before adding 0.200 g of **Cp7** (0.324 mmol, 1 equiv) and put in a N<sub>2</sub> environment. After stirring 0.196 g of allyl bromide (1.62 mmol, 5 equiv) was added and the mixture was brought to 80 °C and stirred for 24 hours. After cooling to room temperature, ether was added drop wise to the flask and the product was filtered and washed with ether until the filtrate was clear. Yield 0.271 g (61%). <sup>1</sup>H-NMR (Methanol<sub>d4</sub>) 9.57 (d, 8H, CH phenyl), 9.28 (d,

8H, CH pyr), 9.08 (d, 8H, CH phenyl), 6.51 (m, 4H, CH allyl), 5.87 (d, 4H, CH allyl), 5.66 (s, 4H, CH allyl), 5.63 (d, 8H, CH<sub>2</sub> alkyl) ppm. IR 3088 and 3030 (m, C-H), 1630 and 1592 (s, C-N), 1559 1507 (m, C=C), 1159 (s, C-C) cm<sup>-1</sup>. UV-Vis (H<sub>2</sub>O) 423max, 519, 585 nm.

#### **2.2.4 5, 10, 15, 20-tetrakis(N-butylpyridinium-4-yl)porphyrin bromide (Cp10)**

A 50 mL round bottom flask was charged with 8.20 mL of DMF before adding 0.500 g of **Cp7** (0.810 mmol, 1 equiv) and put in a N<sub>2</sub> environment. After stirring 0.532 g of 1-bromobutane (3.89 mmol, 4.8 equiv) was added and the mixture was brought to 125 °C and continued to stir for 45 hours. After cooling to room temperature 2 mL of ether was added to the flask and the product was filtered. The product was then washed with ether until the filtrate was clear. Yield 0.623 g (55%). <sup>1</sup>H-NMR (CdCl<sub>3</sub>) 9.52 (d, 8H, CH phenyl), 9.378 (s, 8H, CH pyr), 9.01 (d, 8H, CH phenyl), 5.04 (t, 8H, CH<sub>2</sub> alkyl), 2.39 (m, 8H, CH<sub>2</sub> alkyl), 1.72 (m, 8H, CH<sub>2</sub> alkyl), 1.19 (t, 12H, CH<sub>3</sub> alkyl) ppm. IR 3092, 3058, and 3022 (m, C-H), 1592 (s, C-N), 1542 and 1467 (m, C=C), 1401 (s, CH<sub>2</sub>), 1350 (s, CH<sub>3</sub>) cm<sup>-1</sup>. UV-Vis (H<sub>2</sub>O) 422max, 529, 565, 598 nm.

#### **2.2.5 Iron (5, 10, 15, 20-tetrakis(N-allylpyridinium-4-yl)porphyrin bromide) chloride (Cp11)**

A 0.100 g amount of **Cp9** (0.0907 mmol, 1 equiv) were added to a 25 mL round bottom flask followed by the addition of 3.00 mL of water. After stirring the mixture 0.095 g (0.478 mmol, 5.27 equiv) of FeCl<sub>2</sub>·4H<sub>2</sub>O was added to the mixture and then refluxed for 24 hours.<sup>56</sup> The solvent was dried on a rotary evaporator and the

remaining crude product was redissolved in a minimal amount of methanol (~2mL). The product was then crystallized with the addition of isopropanol and filtered. Still crude, the product was recrystallized in methanol and precipitated out with a 1:4 ethanol/isopropanol mixture. The product was washed heavily with isopropanol to insure that all of the excess FeCl<sub>2</sub> was removed. Yield 0.087 g (80%). IR 3112, 3085, and 3051 (m C-H), 1631 (s, C-N), 1610 and 1596 (m, C=C), 1000 (s, N-Fe) cm<sup>-1</sup>. UV-Vis (H<sub>2</sub>O) 402max, 414, 523 nm.

#### **2.2.6 Iron (5, 10, 15, 20-tetrakis(N-butylpyridinium-4-yl)porphyrin bromide) chloride (Cp12)**

A 0.150 g of **Cp10** (0.129 mmol, 1 equiv) were added to a 25 mL round bottom flask followed by the addition of 3.00 mL of water. After stirring the mixture 0.127 g (0.639 mmol, 5 equivalents) of FeCl<sub>2</sub>·4H<sub>2</sub>O was added to the mixture and then refluxed for 24 hours.<sup>56</sup> The solvent was removed on a rotary evaporator and the remaining crude product was redissolved in a minimal amount of methanol. The product was then crystallized with the addition of an 8:1 isopropanol/ether mixture and filtered. The product was washed heavily with the same isopropanol/ether mixture to insure that all of the excess FeCl<sub>2</sub> was removed. Yield 0.155 g (96%). IR 3122, 3083, and 3054 (m, C-H), 1596 (s C-N), 1538 and 1494 (m, C=C), 1411 (s CH<sub>2</sub>), 1350 (s, CH<sub>3</sub>) cm<sup>-1</sup>. UV-Vis (H<sub>2</sub>O) 418, 452max, 544 nm.

## 2.3 SYNTHESIS OF PROPOXY IONIC LIQUID TAGGED PORPHYRINS

### 2.3.1 5, 10, 15, 20-tetrakis(p-3-bromopropoxyphenyl)porphyrin (Cp13)

This procedure was taken from Wang and others, and utilized as previously published.<sup>57</sup> A 250 mL round bottom flask was charged with 55 mL of DMF followed by an addition of 0.250 g of 5, 10, 15, 20-tetrakis(p-hydroxy)porphyrin (0.368 mmol, 1 equiv). The mixture was then basified with the addition of 0.305 g of potassium carbonate and put under N<sub>2</sub>. An excess 3.59 g of 1,3-dibromopropane (17.8 mmol, 48 equivalents) was then added to the mixture and stirred at room temperature for 23 hours. The solvent was removed by a rotary evaporator and the resulting crude solid was redissolved in dichloromethane and washed with water. A silica gel column, with dichloromethane as the solvent was used to further purify the product. The elution was monitored with TLC. Once the clean product was isolated it was again dried with the rotary evaporator and weighed. Yield 0.105 g (25%). <sup>1</sup>H-NMR (CdCl<sub>3</sub>) 8.86 (d, 8H, CH pyr), 8.14 (d, 8H, CH phenyl), 7.30 (d, 8H, CH phenyl), 4.40 (t, 8H, OCH<sub>2</sub> propyl), 3.79 (t, 8H, CH<sub>2</sub>Br propyl), 2.95 (m, 8H, CH<sub>2</sub> propyl) ppm. UV-Vis (CHCl<sub>3</sub>) 420max, 518, 555, 593, 650 nm.

## 2.4 CATALYTIC STUDIES

Both **Cp5** and **Cp11** were catalytic tested with veratryl alcohol in 1-allyl-3-methylimidazolium xylenesulfonate (AMIMXS) and 30% w/w concentrated hydrogen



peroxide as the sacrificial oxidant. Experiments (**Table 2.1**) were mixed in a larger batch and ran as triplicates to ensure precise results.

**Table 2.1:** Averaged Molar Amounts of Each Species for Catalytic Trials.

Catalyst	mmol of alcohol	mmol of peroxides	mmol of catalyst
<b>Cp5</b>	0.1498	0.221	0.0039
<b>Cp11</b>	0.1625	0.221	0.0046
<b>FeT1239</b>	0.1486	0.221	0.0046

Studies were completed in a reactor accompanied by a HPLC. Samples were preheated to 50 °C before injection. The HPLC autosampler took samples every hour beginning with a blank sample with no peroxide present ensuring that no oxidation was occurring without the co-oxidant. The solvent system used was a water/methanol gradient. The elution of the alcohol came off at 6.758 minutes and the aldehyde at 10.563 minutes. The two wavelengths monitored with the diode array detector were 280 nm and 320 nm. The oxidation was allowed to go well after completion for convenience and to ensure the peroxide was completely decomposed. Calibrations were ran for veratryl alcohol and veratraldehyde with standard samples in 1-allyl-3-methylimidazolium chloride (AMIMCl). Slopes of the calibrations of veratryl alcohol and veratraldehyde used were 5043.6 ( $R^2 = 0.9998$ ) and 22015 ( $R^2 = 0.9938$ ) respectively. Thus the actual mass of sample calculated was the eluting peak size over the slope. An auto injection system was attached to HPLC eliminating the need for an internal standard. Comparison studies were completed with Iron(III) 5, 10, 15, 20-tetrakis(4-

sulfonato phenyl)porphyrin chloride (**FeT1239**) that was purchased and used as is  
(**Figure 2.1**).

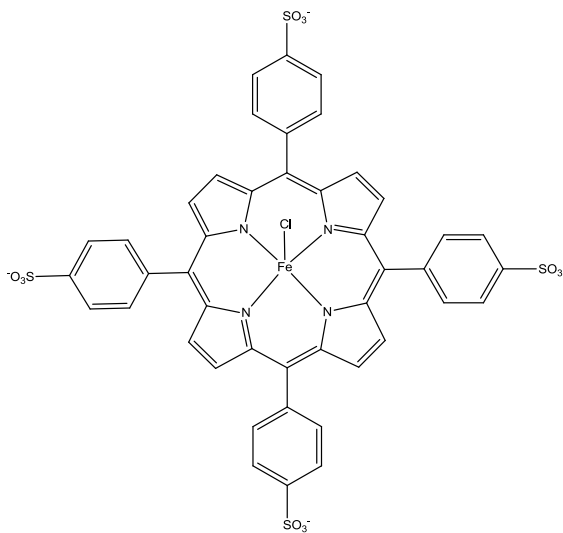


**Figure 2.1:** The Molecular Structure of **FeT1239**.

## CHAPTER III

### EXPERIMENTAL DISCUSSION

The goal of our experimental studies was to couple the solvating power of an ionic liquid with the oxidizing power of a metalloporphyrin. A common problem associated with inorganic catalysts including porphyrins is solubility in aqueous or even very polar solvents, such as an ionic liquid. To resolve this issue and to amplify the oxidizing power of the porphyrin, the catalysts developed were tagged with an ionic liquid substituent. This allows for a purely homogeneous reaction in an ionic liquid.

Many previous oxidation studies have been done with an array of porphyrins and there are a couple trends that can be seen from different substituents in the meso positions. Heavier and more electron withdrawing tends to increase the activity of the porphyrin in solution. Computational measurements have been done demonstrating that both of these properties aid in displacing the metal further from the center of molecule.<sup>58</sup> Displacing the metal means it is more likely to come into contact with other species and therefore be more active. It would seem that a tetracationic porphyrin would be very electron withdrawing and thus very active in solution. The synthesis of **Cp12** was done with size in mind as it is over 2000 mass units. It is about 700 mass units heavier than any other synthesized in the project. Theoretically there are many routes to producing an ionic liquid tagged porphyrin, however the main considerations were costs, novelty, activity, and simplicity of synthesis. Iron was chosen as the primary

metal for the oxidation studies due to previous unpublished results from past comparison studies between nonionic and ionic iron and manganese porphyrins done at the Center for Applied Energy Research (CAER).

### **3.1 SYNTHESIS OF BENZYL IONIC LIQUID TAGGED PORPHYRINS**

Two different ionic liquid tagged metalloporphyrin systems were developed. The first system has the alkyl halide on the starting porphyrin (**Figure 3.1, p.45**); this creates an ionic liquid functional group when attacked by a nucleophilic amine or phosphine. **Cp2** was synthesized by the Lindsey method at a very high yield of 52%. The addition of the stronger nucleophilic triphenylphosphine drastically reduced the reaction time and was found to increase yields significantly compared to 1-methyl imidazole. The second system is functionalized with a pyridine which forms an ionic liquid tag when attacked by an alkyl halide (**Figure 3.5, p.54**).



### 3.1.1 Synthesis of Cp1

The synthesis of benzyl ionic liquid tagged porphyrins began with an oxidation of a cyanide group to the aldehyde seen as the starting material (**Figure 3.1**). The procedure was taken by Wen and Schlenoff and performed as written<sup>55</sup>. As stated in the experimental, DIBAL-H was added slowly; the reaction mixture will turn yellow if added too quickly. The yellow impurity was found to be removed with lots of cold hexanes or by chromatography, but it is much easier to just add it slowly. The yellow impurity in the product does show up in a <sup>1</sup>H-NMR spectrum in the hydrocarbon region. It takes a very small amount of impurity to turn the bright white flakey crystal to a more powdery yellowish solid. When the product was in question, it was examined by a melting point apparatus first.

The <sup>1</sup>H-NMR data (**Figure 3.2, p. 47**) does show confirmation of a complete transformation, with the formation of a singlet at 9.93 ppm and proper integration values. The peak at 9.93 ppm is near the 10 ppm that is predicted for an aldehyde's proton. Melting point measurements were also a near match to literature value at 98.6-100.0 °C for a pure sample.

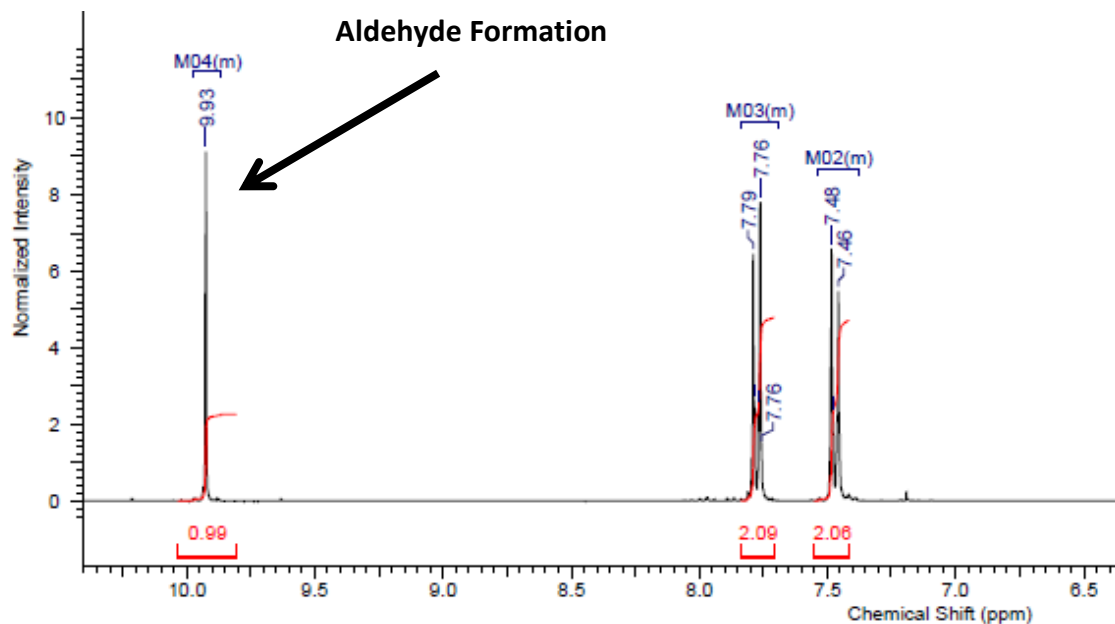


**Figure 3.2:** <sup>1</sup>H-NMR Spectrum of Cp1.

### 3.1.2 Synthesis of Cp2

Once the starting material was formed, the following step to the scheme is a Lindsey porphyrin synthesis. The experiment itself is very sensitive to a lot of different variables and relative yields varied greatly from experiment to experiment. Important steps to watch are the dryness of the CHCl<sub>3</sub>, the purity of the pyrrole, the initial stir time, the stir time after adding the BF<sub>3</sub>, and the length of time to oxidize and clean up the product. After mixing in the TCBQ it is very important to work quickly as it is a known porphyrin degrader. Purification can be done with a column and dichloromethane, however it is more time consuming and the resulting product still must be washed extensively with methanol after. It is a waste of solvent and time to go that route. Crystallization from concentrated cold CHCl<sub>3</sub> is important to getting a pure compound.

The  $^1\text{H-NMR}$  data for **Cp2 (Figure 3.3)** shows the doublet of doublets of the protons on the phenyl ring at 8.11 and 7.72 ppm as well as the singlet more upfield at 4.79 ppm accounting for the methylbromide hydrogens. One interesting aspect to the  $^1\text{H-NMR}$  data obtained for all of the analyzed porphyrins were the internal CH protons on the pyrrole rings. The CH protons at 8.77 ppm actually show up as a wide singlet on the JEOL 300 MHz NMR used. Integration was always a near match, but the resolution was not high enough to observe the splitting from these protons. The internal ring protons also have a severe peak broadening to the point that they are near undetectable, but they are there and the area integrates out properly. UV-Vis data are a match with literature data with the sorret band 420 nm followed by Q bands at 517, 551, 589, and 646 nm. The IR did have a couple small variations however the NH peak is at  $3327\text{ cm}^{-1}$ , also there is a peak at  $3026\text{ cm}^{-1}$  corresponding to  $\text{sp}^3$  methyl carbons, and a strong peak at  $1221\text{ cm}^{-1}$  corresponding to the carbon bromide bond.

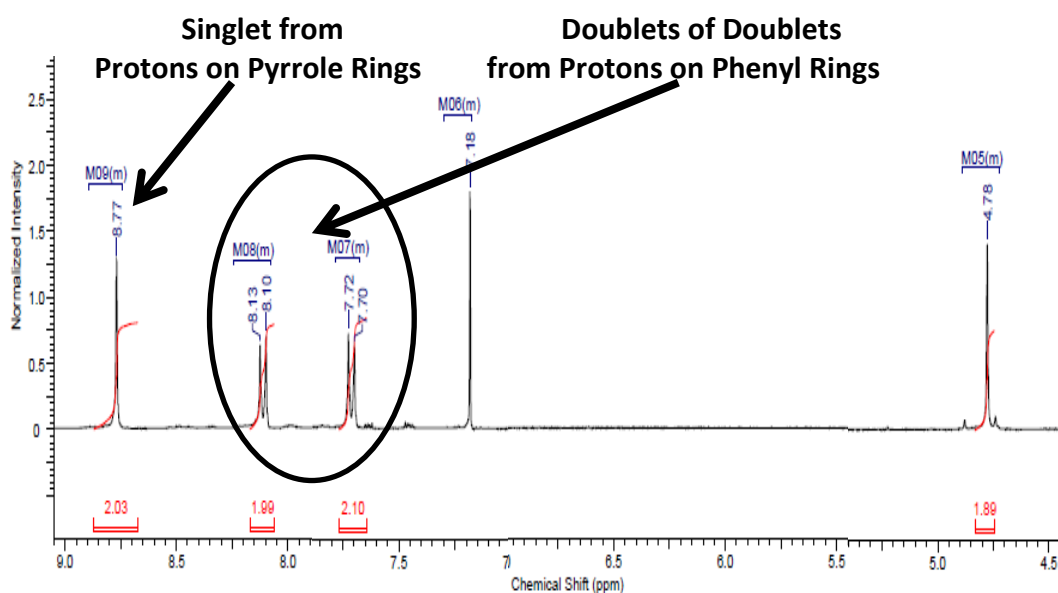


**Figure 3.3:**  $^1\text{H-NMR}$  Spectrum of Cp2.



### 3.1.3 Synthesis of Cp3 and Cp4

The following reactions are  $\text{SN}^2$  substitutions resulting in the ionic liquid substituent. Methylimidazole is not as strong of a nucleophile as  $\text{PPh}_3$  and the corresponding synthetic scheme proved to be much more difficult. The synthesis of **Cp3** was accomplished but with low yields. Optimization was attempted and needs to be further done to mass produce the catalyst, but temperatures above  $110\text{ }^\circ\text{C}$  actually decreased yields of the ionic product. Reactions were attempted at temperatures as high as  $160\text{ }^\circ\text{C}$  to try and force the reaction to completion but none of the ionic porphyrin was isolated, actually a small amount of an unidentified non polar solvent soluble purple solid was formed. Longer reaction times did seem to help, and if the reaction were to be further optimized even longer would be attempted. The isolated products that were analyzed continually had impurities that appeared to be methylimidazole as well as remaining unreacted methylbromide on the starting porphyrin **Cp2**. At one point it was thought that prep liquid chromatography was going to be the only way to obtain a pure product. Cephadex is actually a common non-polar purification gel, with similar applicability as silica gel, that would have also worked if necessary. It is a long hydrocarbon based packing material that can be used in column chromatography similar to a reverse phase HPLC column packing material. The ionic nature of the porphyrins cause them to stick to silica gel, making silica gel TLC and column chromatography less useful. TLC was done throughout the experimental trials to determine when the starting material was gone, however it could not separate any

of the ionic products due to sticking. Failures in purification methods in the two solvent crystallization methods attempted were from the polarity of the precipitating solvent. Solvent systems that were less polar than the 9:1 isopropanol/ether were unable to separate the fully substituted porphyrin from the incomplete substituted products, confirmed by  $^1\text{H-NMR}$ . Yields were likely lower than the actual amount of formed product in the reaction mixture as some could have easily not precipitated out in the crystallization. Without a non-polar TLC plate, this cannot be easily determined from the filtrate. The  $\text{PPh}_3$  reaction was much simpler as it is more nucleophilic and the sheer size of the phenyl substituents cause the product to be much less polar; it is actually insoluble in water at room temperature. By having the product less polar it can be easily precipitated from methanol with just ether. A higher temperature of  $140\text{ }^\circ\text{C}$  was attempted but resulted in slightly lower yields.

The **Cp3**  $^1\text{H-NMR}$  spectrum (**Figure A.1, p. 81**) has all of the expected peaks with near ideal integration values. The singlet at 9.31 ppm is expected for the CH bond on the imidazole between nitrogen atoms. The spectrum displayed in the appendix was done in deuterated methanol; the solvent seemed to have a strong solvating effect on the internal pyrrole protons, even stronger than that of DMSO. This observation is made based on the complete disappearance of the internal NH protons in the spectrum as well as the abnormal peak shapes of the CH protons on the pyrrole rings. Other  $^1\text{H-NMR}$  analysis was done in deuterated  $\text{DMSO-d}_6$  which did display the NH peak and the CH peak proving that they are there. Since those peaks do appear normal in the

deuterated DMSO solvent, it is fair to say that it is the methanol interaction causing the distortion. Methanol was used as displayed in the appendix because it is much less hygroscopic, and as water is already a dominant peak from the possible hydrates being formed, it was important not to add any additional water from the solvent. DMSO is very hygroscopic, and a major issue when water content is an issue, and almost impossible to purify after hydration. A major indication of the success of the experiment is the near 1 ppm peak shift of the methylbromide proton peak to the ammonium salt methylproton peak. **Cp2** shows this peak at 4.79 ppm (**Figure 3.3, p. 48**) versus the 5.81 ppm in **Cp3 (Figure A.1, p. 81)**; there are also no mixed signals showing isolation of the completely converted product. The IR spectrum of **Cp3 (Figure A.5, p. 86)** shows the strong water peak where the weak N-H peaks were before the alkylation. Many other papers have referenced their ionic porphyrins as hydrates in the past. Also important to the IR spectrum is the absence of the CH<sub>2</sub>Br peak at 1221 cm<sup>-1</sup> in the starting material.

The <sup>1</sup>H-NMR data for **Cp4 (Figure 3.4, p.52)** has many of the proton peaks overlapping but that is expected for the compound. The large cluster of peaks should account for four different signals and 68 protons per molecule. The doublet from the phenyl ring slightly upfield at 7.48 ppm integrates to 3.68, a little less than half of the whole porphyrin relative to internal pyrrole protons. The integration value of the whole cluster is 31.14, very close to ideal as again a small percentage away from half the whole porphyrin as is the doublet upfield. The confirmation of the product is again in

the change of the methylbromide peak. The new doublet at 5.65 ppm (**Figure 3.4**) is from the methyl phosphorus bond formation. In this case binding to the phosphorus atom causes a splitting of the singlet into a doublet because  $^{31}\text{P}$  is a spin  $\frac{1}{2}$  nuclei and a 100% abundant. Again water is in the spectrum showing the formation of an expected hydrate.

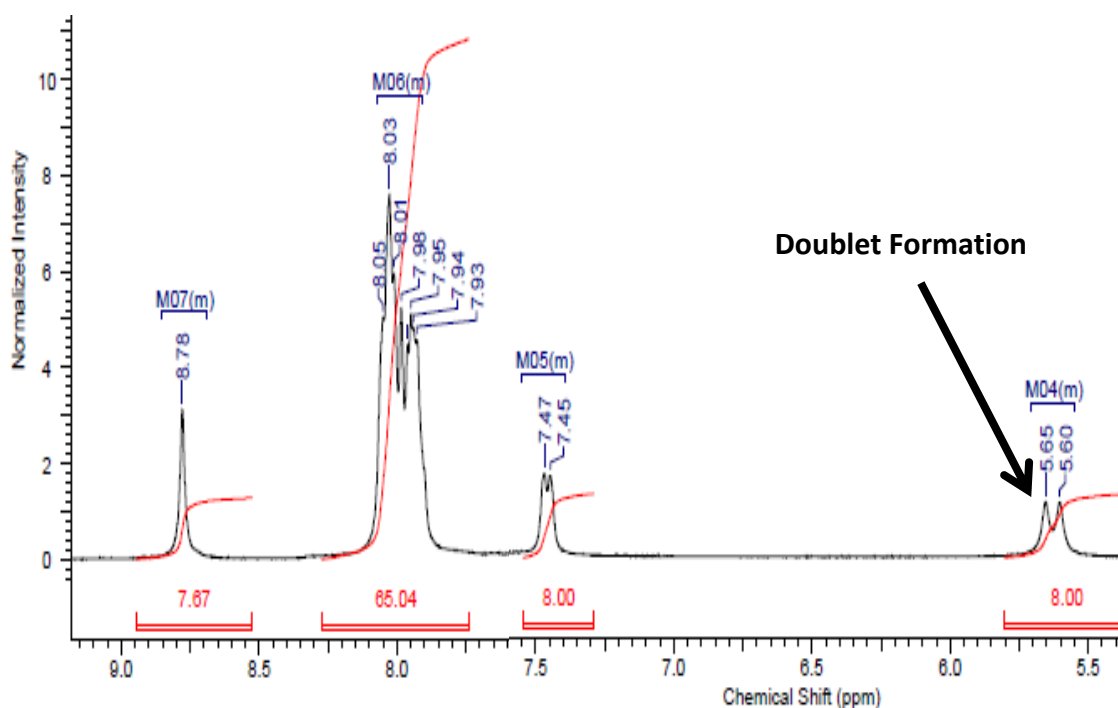


**Figure 3.4:**  $^1\text{H}$ -NMR Spectrum of Cp4.

### 3.1.4 Syntheses of Cp5 and Cp6

The final step of the synthetic route was metallation. Using water as a solvent was ideal as it tends to promote ionization very well, it is cheap, and it has a relatively high boiling point. For this reaction to occur, the labile hydrogen atoms off the internal pyrrole molecules must leave. The reaction was attempted with the addition of sodium

carbonate, but surprisingly it inhibited the reaction verified by UV-Vis spectroscopy. Polarities of the metallated products did increase noticeably which allowed for any non-metallated porphyrin to be separated again by a two solvent crystallization method. The challenge was determining the purity of the metallated compound.  $^1\text{H-NMR}$  of **Cp5** was attempted however due to the paramagnetic nature of the ferrous porphyrin failed. At least it did show that the species is an iron(III) compound with relative certainty. It is possible to be high spin iron(II) but highly unlikely as any iron metallation with an iron halide results in the halide being positioned axially to the iron in the corresponding porphyrin, making it iron(III). The IR data shows clear metallation for both **Cp5** (**Figure A.6, p. 87**) and **Cp6** (**Figure A.7, p. 88**). Each spectrum has a new strong peak representing the N-Fe bond; it is at  $998\text{ cm}^{-1}$  for **Cp5** and at  $996\text{ cm}^{-1}$  for **Cp6**. Yields for the metallation procedure were both very high at 90 and 77% accordingly.

### 3.2 SYNTHESIS OF PYRIDINIUM IONIC LIQUID TAGGED PORPHYRINS

The second system has the nucleophile on the starting porphyrin by a pyridine meso substituent (**Figure 3.5, p. 54**). This allows for the formation of the ionic liquid functional group with attack of an alkyl halide. The strength of the leaving group has a strong effect on the reaction rate and conditions necessary for the reaction to proceed. This can be seen by comparing the conditions of the synthesis of **Cp9** and **Cp10**. The former has a stabilizing double bond making the bromide more readily to leave and allows for the milder conditions.

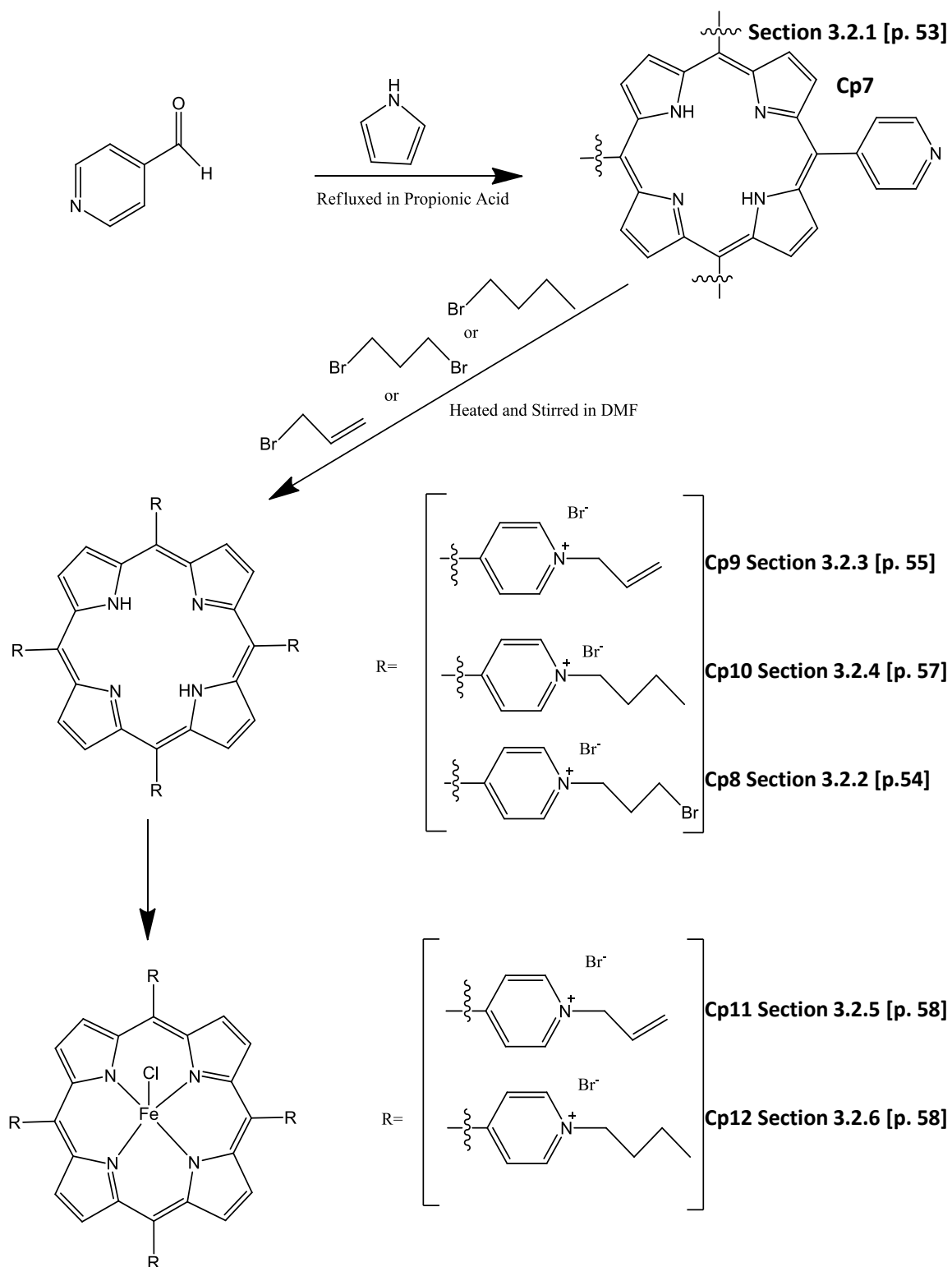


**Figure 3.5:** Synthesis of Ionic Liquid Tagged Pyridinium Porphyrins.

### 3.2.1 Synthesis of Cp7

**Cp7** was synthesized by the Adler Longo method. Reactions were carried out at scales between 2.55 g and 10.2 g of the aldehyde. The workup procedure involved a preheated propionic acid solvent mixture followed by the addition of pyrrole and the aldehyde nearly simultaneously but always pyrrole then aldehyde. Cleanup started a lengthy column using a 4:1 propionic acid/methanol as the eluent solvent mixture, but this was very time consuming and the resulting product was still not clean, so other purification routes were tested. This turned out to be very beneficial as crystallization with methanol saves hours of time per reaction, yields were higher, and it saves a lot of solvent per reaction. This porphyrin has been synthesized previously by other groups with higher yields (up to 33%), but this was not as easy to scale up and the amount of solvent used was significantly greater.<sup>59</sup>

The <sup>1</sup>H-NMR (**Figure 3.6, p. 56**) is very nice and relatively clean, small amounts of left over methanol and water are there. Again the internal pyrrole peaks are present as a singlet but not surprising after the spectra from **Cp2** with the same solvent and instrument. There is a much wider gap in the doublets of doublets in **Cp7** as expected due to the signals coming from the pyridine rings versus the phenyl of **Cp2**. Yields were actually very high for the method chosen. The 16% is about the expected maximum for this synthetic strategy.<sup>38</sup> IR data again has the key peaks expected for the product, medium N-H peak at 3312, aromatic C-H peak at 3089, and a strong C=C aromatic peak from the phenyl group at 1594 cm<sup>-1</sup>. UV-Vis data had a strong sorret band at 419 nm with Q bands at 513, 543, 587, and 643 nm.

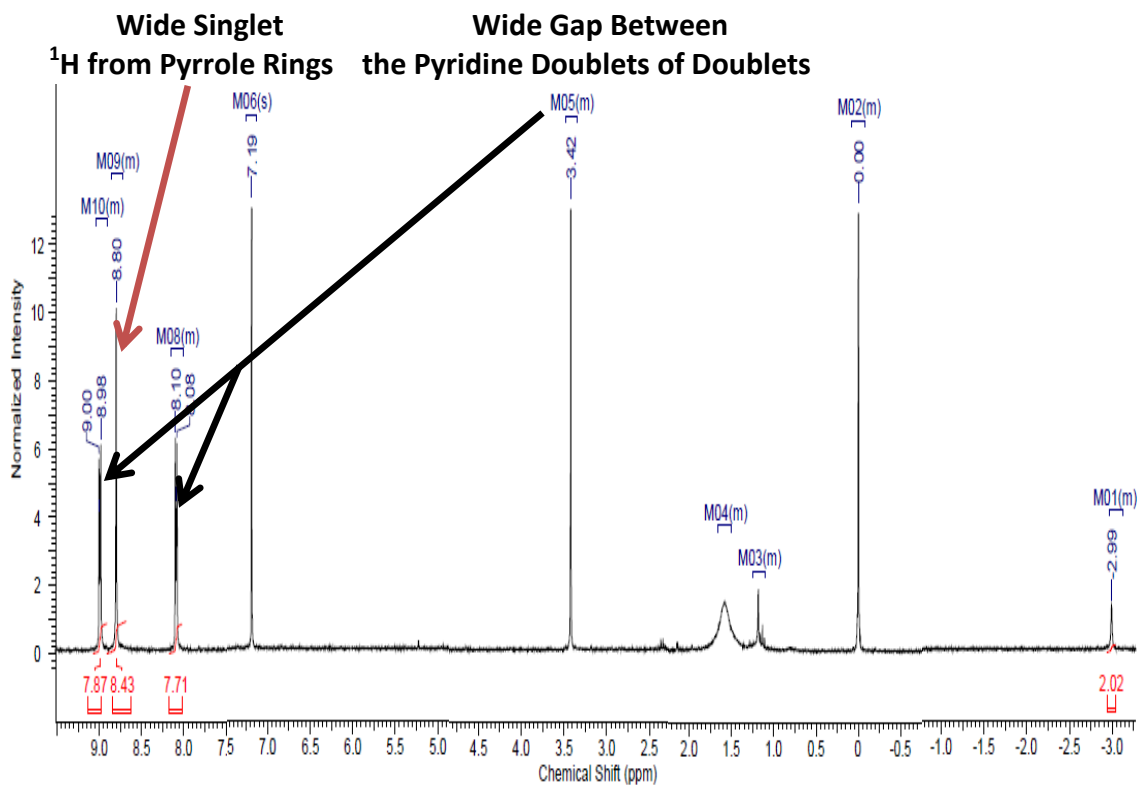


**Figure 3.6:**  $^1\text{H-NMR}$  Spectrum of Cp7.

### 3.2.2 Attempted Synthesis of Cp8

The reaction for the formation of Cp8 is of an  $\text{S}_{\text{N}}2$ , but very temperamental with lots of potential side products. Obtaining a clean sample was extremely difficult and in fact it is still undeterminable if it was successful. A telling  $^1\text{H-NMR}$  spectrum was taken, however due to the combination of a hydrated compound and a hydrated old  $\text{DMSO-d}_6$  solvent the representative peaks were barely over the baseline. However, the peaks do match with what would be expected for the compound, except the integration on the expected  $\text{CH}_2\text{Br}$  triplet is half of the value it should be. The triplet at 5.06 ppm is the first of the hydrocarbon peaks shifted very far down field due to the nitrogen cation as



well as the strong aromatic presence from the porphyrin. There is a quintet at 2.85 ppm corresponding to the CH<sub>2</sub> in the middle of the propyl chain. As all of the other ionic porphyrin species, there is a huge water peak covering any other possible peaks between 3.95 ppm and 3.60 ppm. There is a final triplet at 2.51 ppm, but the integration is half of what it should be relative to the rest of the peaks. It is worth noting that an attempt was made to further make the species octacationic by functionalizing with PPh<sub>3</sub>. The reaction is nearly identical to the **Cp4** route, but this did not appear to react confirmed by the near identical IR obtained before and after the reactions were completed. This again supports the <sup>1</sup>H-NMR data that something happened to the CH<sub>2</sub>Br of the propyl group. The <sup>1</sup>H-NMR was not able to be reproduced once new solvents were purchased and the product measured had already appeared to decompose as the bright metallic purple solid became a dark green color. Due to the difficulty of the reaction and quick alteration of the product, this synthetic route stopped here.

### 3.2.3 Synthesis of Cp9

This reaction is an SN<sup>2</sup> reaction involving the allyl bromide attacking the aryl pyridyl nitrogen, resulting in an alkylation. From ionic liquid synthesis attempts it was known that this reagent would react faster than any of the alkyl bromides. The expected reason is the stabilization of the allylic cation formed in the transition state. Part of the reason for choosing this ligand was because of that very reason as yields

from compounds synthesized up to this time had been relatively poor. The main reasons of the low yields were known to be from incomplete reactions, regardless of the amount of time allowed or temperature used. To combat this, stronger nucleophiles and electrophiles such as the  $\text{PPh}_3$  and this allyl bromide were used. As expected, synthesis was far simpler and better results were obtained in a fraction of the time. A 58% yield is not incredible but effective and accomplished with a tenth or less of the amount of work put into a few of the previous reactions with a greater yield. DMF was chosen as the solvent as it has been used in the literature in the few cases of other ionic porphyrins formed. Also, it is one of a few common solvents that can solubilize both the products and reactants in this synthesis. One common literature solution worth noting is to choose a solvent which the ionic species precipitates out at completion of the reaction driving any equilibrium towards completion and making the cleanup very easy, however the porphyrin synthetic routes chosen require it to be functionalized at all four positions causing this to be very difficult to predict.

The  $^1\text{H-NMR}$  data (**Figure A.3, p. 83**) corresponds very well to the expected product. As before, there is a large water peak at 3.64 ppm and also a small amount of DMF left in the sample. Many of the allyl peaks are not well separated but do integrate correctly and in the correct region when accounting for the shift from the electron withdrawing porphyrin. There are 0.55 ppm and 0.9 ppm peak shifts on the **Cp7** pyridine protons with the formation of pyridinium ionic bond on **Cp9**. IR data again has a very broad water peak, but it also has new sharp C=C peaks at 1630 and 1593  $\text{cm}^{-1}$ .

### 3.2.4 Synthesis of Cp10

Synthesis of **Cp10** followed similarly to **Cp9**, a  $\text{SN}^2$  reaction developed in heated DMF. The products  $^1\text{H-NMR}$  spectrum (**Figure A.4, p. 84**) matches very well with the expected splitting patterns and peak shifts. The protons on the pyridinium rings do show up as doublets and integrate to near equivalent values in the spectrum. They are also significantly shifted ( $\sim 0.5$  and  $0.9$  ppm) downfield like **Cp9** as expected from the neighboring ammonium cation formed in the product. The pyrrole C-H peak is again very broad and comparable to that of the  $^1\text{H-NMR}$  of **Cp3** also done in deuterated methanol. The butyl proton peaks have a nice trend of peak shifts downfield, with the closest to aromatic system having the greatest peak shift. The peaks are very well separated and properly integrate. The water amount integrates out to about a 13:1  $\text{H}_2\text{O}$ /porphyrin molecule. Relatively low amount compared to the others as could be expected due to the more hydrophobic butyl substituents. The IR spectrum (**Figure A.10, p. 91**) for the compound is hard to compare to the other ionic porphyrins in this thesis. It is obvious that the water peak is not nearly as prevalent and broad as in all of the other ionic porphyrin molecules but plenty of water did show up in the  $^1\text{H-NMR}$  spectrum. The ideal peak shifts of the phenyl protons in the  $^1\text{H-NMR}$  spectrum does prove the cation formation. Yields at 61% are sufficient but could possibly be higher with longer reaction time.

### 3.2.5 Synthesis of Cp11

The metallation of **Cp9** was completed and examined by both IR and UV-Vis. The IR spectrum of **Cp11** (**Figure A.9, p. 90**) confirms metallation with a strong peak at  $1000\text{ cm}^{-1}$  representing the Fe-N bond at the center of **Cp11**. The UV-Vis data shows a blue shift in the porphyrin, as the sorret band at 423 nm in **Cp9** shifted to 402 nm after the metallation in **Cp11**. The product was isolated in good yields at 80%.

### 3.2.6 Synthesis of Cp12

**Cp10** was metallated and analyzed by both IR and UV-Vis. As expected the IR spectrum (**Figure A.11, p. 92**) does show the strong Fe-N peak at  $991\text{ cm}^{-1}$ . The UV-Vis spectrum actually did show a red shift in the sorret band. The sorret band red shifted from 418 nm in **Cp10** to 452 nm in **Cp12**. The red shift indicates the metallation caused the porphyrin core to become less planar.<sup>60</sup> The variation from the other three compounds is likely associated with the absence of  $\pi$  donation from the butyl group whereas the other three all are donors. DFT calculations have shown that this donation from substituents on the phenyl rings in the meso positions of a porphyrin actually decrease the HOMO-LUMO gap by destabilizing the HOMO.<sup>61</sup> This phenomenon is also known to be enhanced by distortions in the center of porphyrin molecule.<sup>62</sup>

### 3.3 SYNTHESIS OF PROPOXY IONIC LIQUID TAGGED PORPHYRINS

#### 3.3.1 Synthesis of Cp13

The synthesis of **Cp13 (Figure 3.7, p. 62)** was completed, as a porphyrin with the ionic tag further from the porphyrin center was thought to potentially be a more recyclable catalyst. The longer arms of the catalyst would likely allow for more of a  $\pi$  interaction with the ionic linkages and the metal center. This should protect the porphyrin as well as make incoming ligands more labile and active. Synthesis of the product was completed and successful, however with much lower yields than that of the publication taken from. A yield of 80% was reported, much higher than the experimentally obtained 25%. The expected variation in yields came from the addition of 1,3-dibromopropane. It is a reaction that can easily form porphyrin dimers or even oligomers. It was noted that much of the residual solid that was left after removing the DMF solvent did not dissolve in the dichloromethane as expected. This caused difficulty in the wash step as much of the insoluble solid was just floating in between layers making them near indistinguishable.

Isolation of the product was successful as can be seen from the sharp UV-Vis sorret band at 420 nm and  $^1\text{H-NMR}$  data. The literature only had  $^1\text{H-NMR}$  data and elemental analysis to compare to. The  $^1\text{H-NMR}$  data (**Figure 3.7, p. 62**) does matchup well with a few discrepancies in some peak signals upfield. The major literature discrepancies are in the alkyl groups located upfield at 3.79 and 2.52 ppm. The

literature for these two peak shifts are at 3.57 and 2.3 ppm.<sup>57</sup> Considering the largest discrepancy is 0.05 ppm outside of these two numbers and the integration and peak splittings fit the structure, it can be concluded that the isolation of the product was successful.

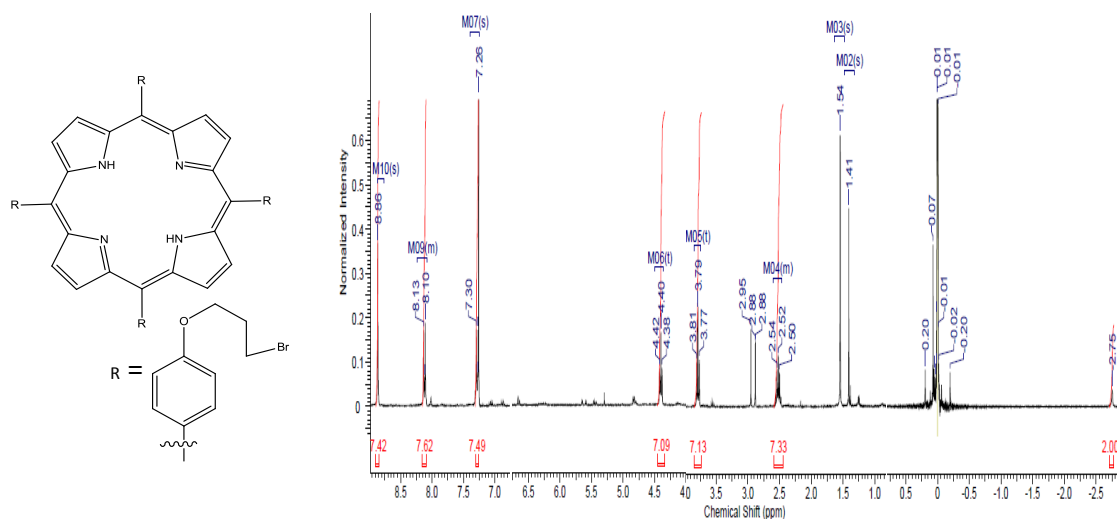


**Figure 3.7:** Structure and <sup>1</sup>H-NMR Spectrum of Cp13.

### 3.4 CATALYTIC RESULTS AND DISCUSSION

Porphyrins do degrade and unravel over time and reusability is a major problem due to their synthetic costs. Studies by Liu and others have demonstrated that coupling a pyridinium tagged porphyrin in a similar ionic liquid actually extends the life of the porphyrin when compared to a non-ionic porphyrin in an organic solvent.<sup>59</sup> The reusability of the catalyst was examined with both types of systems until the level of conversion of styrene fell off below 65% for the ionic system and 10% for the non-ionic system (**Figure 3.8, p. 63**). The non-ionic System was Mn(II)Cp7 in acetonitrile and the

ionic system was Mn(5, 10, 15, 20 (N-methylpyridinium 4-yl)porphyrin) BF<sub>4</sub><sup>-</sup> in N-methylpyridinium BF<sub>4</sub><sup>-</sup>.

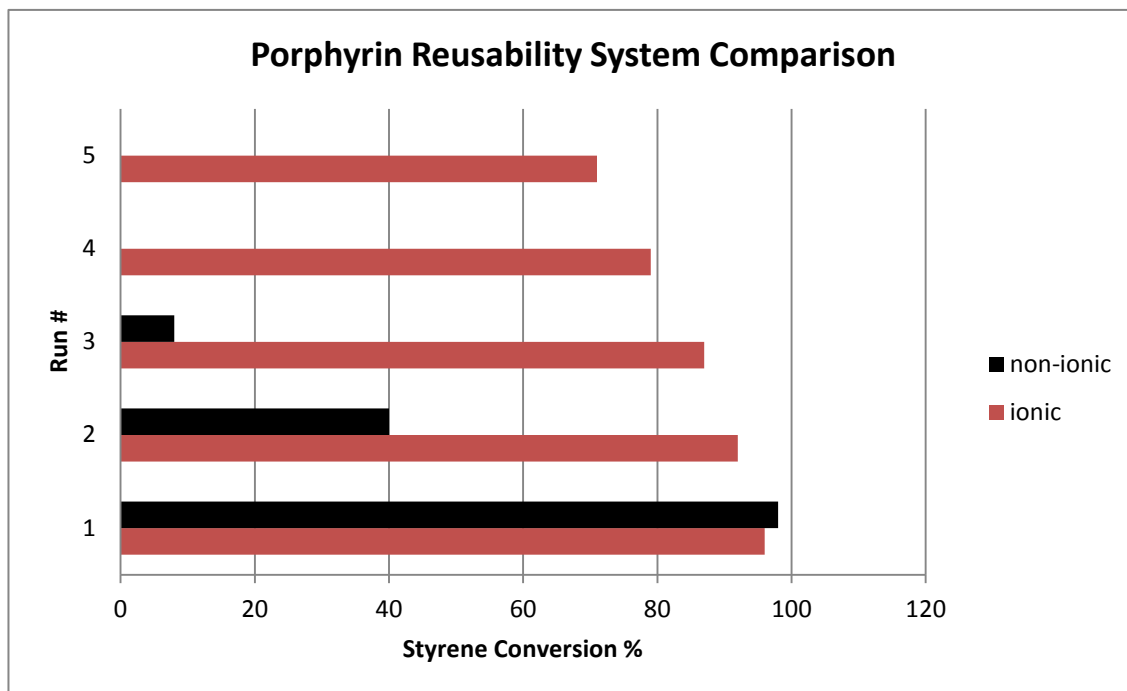


**Figure 3.8:** Porphyrin Reusability System Comparison.<sup>59</sup> Source : Liu, Y.; Zhang, H.-J.; Lu, Y.; Cai, Y.-Q.; Liu, X.-L., Mild oxidation of styrene and its derivatives catalyzed by ionic manganese porphyrin embedded in a similar structured ionic liquid. *Green Chemistry* 2007, 9 (10), 1114-1119.

The group used a slightly different ionic porphyrin and similar reusability results were obtained.<sup>63</sup> Possibly even more interesting than their first study was the finding that the ionic porphyrin had a very similar degradation pattern to the nonionic porphyrin in the acetonitrile solution. Also, a very important finding was the enhancement of the turnover rate with the optimized water concentration in the ionic liquid. The reaction rate went from 4% conversion in 5 minutes to 93% conversion in 5 minutes with a 5

mmol addition of water. This enhancement was not seen for the same catalyst in acetonitrile.<sup>63</sup>

The catalytic data obtained was done in accordance with studies from Anil and others (**Figure 3.9**).<sup>64</sup>

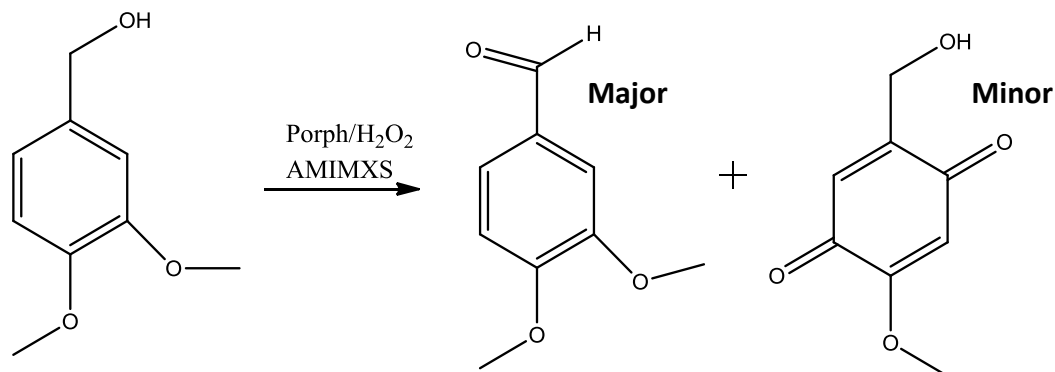


**Figure 3.9:** The Catalytic Oxidation Scheme.

Veratryl alcohol contains two methoxy groups as well as a benzyl alcohol substituent, common structures seen in lignin itself. It is a known mediator in white rot fungi delignification.<sup>65</sup> It has been shown that *Phanerochaete Chrysosporium* fungi is not able to degrade polymeric lignin without the presence veratryl alcohol.<sup>66</sup> It is expected that it transfers a one electron oxidizing species to the large polymer from the heme active sites in LiP. Mechanistic proposals for the formation of veratraldehyde and the quinone have been developed based on the radical cation mediator and its known decomposition with increasing OH<sup>-</sup> concentration.<sup>67</sup>



Comparison studies (**Figure 3.10**) were done with **Cp5** and **Cp11** and another common polar porphyrin analogue that was also used by Anil **FeT1239** (**Figure 2.1, p.42**).

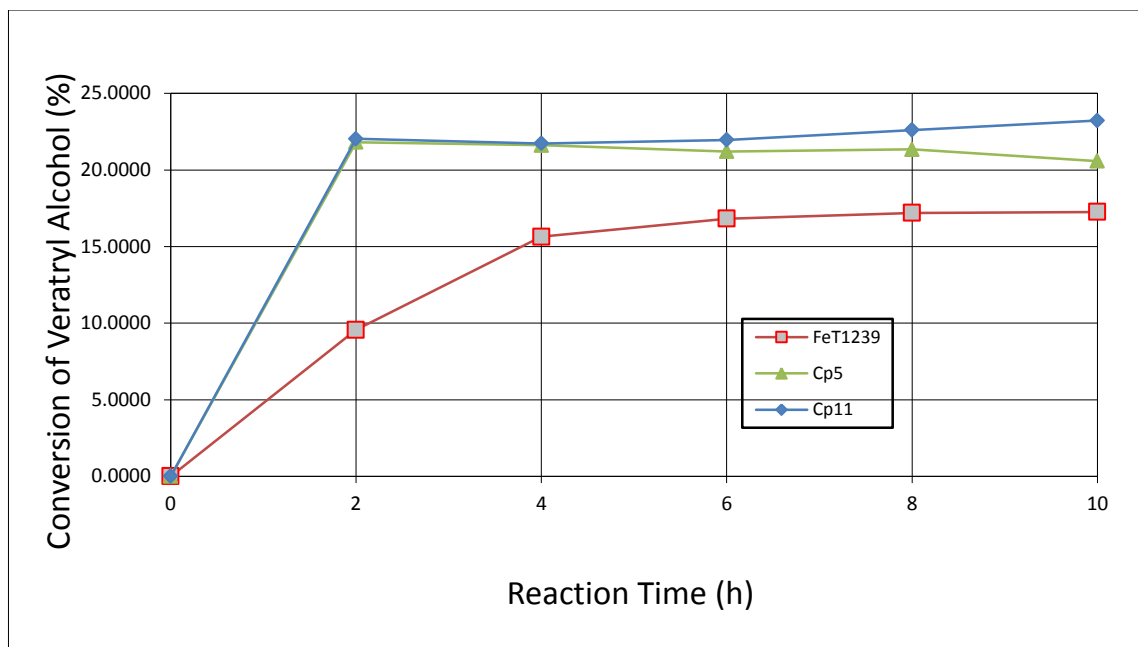


**Figure 3.10:** The Conversion of Veratryl Alcohol.

From our preliminary results in the comparison study it is clear that there is significantly higher activity with our ionic porphyrin catalysts. This was really just a trial run and there are far more optimizations to be studied. The catalytic studies were stopped mainly due to injection issues with the autosampler found shortly after the data taken here. However, the ionic liquid tagged porphyrins were much more active with the hydrogen peroxide and produced a higher overall conversion% with a slightly lower amount of catalyst. From the literature,<sup>59, 63-64</sup> the ionic liquid tagged catalysts

also could be expected to degrade at a slower rate compared to the nonionic counterparts if tests were permitted. All of the porphyrins had low yields relative to Anil's results, even with the same catalyst **FeT1239**. After 6 hours in BMIMPF<sub>6</sub><sup>-</sup> with a 1% (mol) of **FeT1239** catalyst, he obtained a 27% aldehyde yield based on the alcohol content. The higher yields are most likely a solvent effect due to the very weakly coordinating strength of the hexafluorophosphate anion in the ionic liquid. It can also be explained by the possible oxidation of the ionic liquid used AMIMXS. The peroxy radicals formed as side products in the reaction of the peroxide and the porphyrin could be oxidizing the allyl substituent on the ionic liquid. The decrease in yields would be expected as some of the radicals will recombine to reform the peroxide and be used again by the porphyrin.<sup>49</sup> The chromatograms obtained from the oxidation do show increasing small amounts of very polar unidentified products coming off around the dead time (**Figure 3.11, p. 67**) ; these peaks could also be signals from small amounts of quinones formed. It is more likely to be a derivative of the ionic liquid as the quinones would be expected to stick to the non-polar column more than AMIMXS. It is not the porphyrin as there were no corresponding signals before the addition of the peroxides. Further evidence of this affecting the resulting yields is that the peak size of this unknown product stopped increasing after the two hour mark, same time as the conversion of the veratryl alcohol.

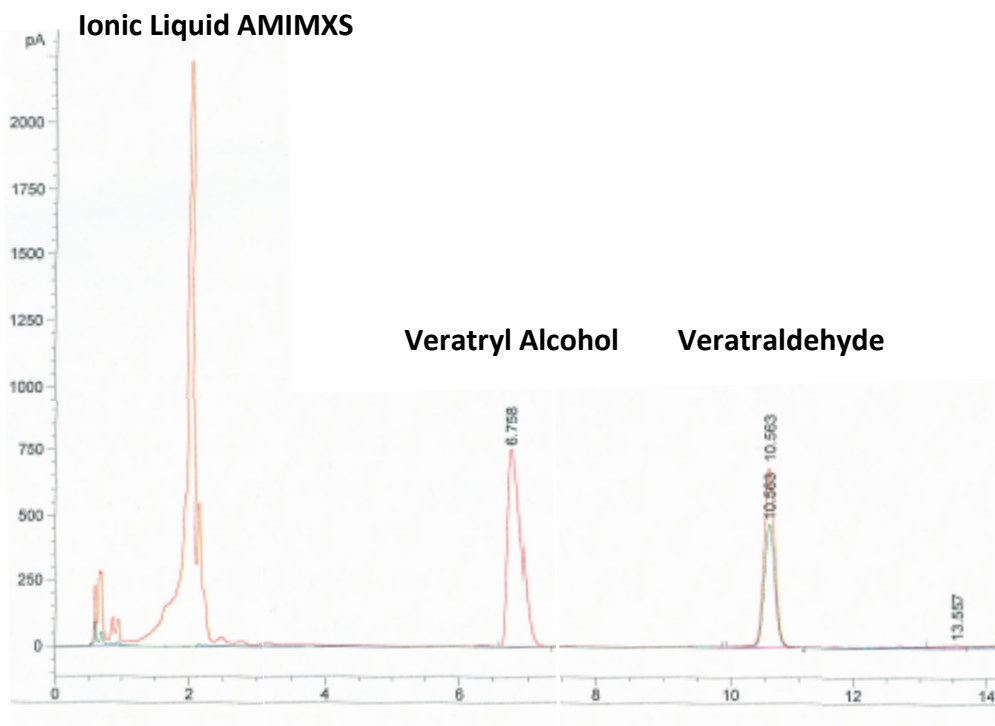


**Figure 3.11:** Chromatogram from the Oxidation of Veratryl Alcohol.

## CHAPTER IV

### CONCLUSIONS AND FUTURE WORK

Two different synthetic paths to ionic liquid tagged metalloporphyrins have been exploited. After mastering the synthesis both schemes can be accomplished in about a week with moderate yields. Both the Adler and Lindsey methods were utilized successfully for the initial formation of the porphyrin. The reaction conditions necessary for the tagging of the ionic liquid to the porphyrin were found to be heavily dependent on the strength of the nucleophile or electrophile depending on the system. The ionic liquid tagged porphyrins all have a large water impurity that is apparent in the  $^1\text{H-NMR}$  spectra, leading to the speculation of hydrates. The metallation of each ionic liquid tagged porphyrin with  $\text{FeCl}_2 \cdot 4\text{H}_2\text{O}$  in water was shown to be successful by the formation of a strong sharp peak between  $991$  and  $1000\text{ cm}^{-1}$  corresponding to the Fe-N bond formation. The most intriguing part to the research was the significantly increased activity of the catalysts tested in the oxidation of veratryl alcohol. There are numerous possibilities for the higher activity including increased mobility in the solvent caused from the increased polarity of the ionic liquid tags. Also increased electron deficiency because of the cationic meso substituents causing for metal displacement and better selectivity as has been seen in the literature before with electron deficient porphyrin catalysts.<sup>46, 52</sup>

There are lots of optimizations that need to be continued both synthetically and especially catalytically. Our initial studies are very exciting, however these were simply comparison studies of the nonionic versus ionic porphyrins without either being properly optimized. Some synthetic optimization has been done, but it can be improved with more experimental trials. Along with synthetic optimization is finding a method to grow crystals for absolute verification of the structures and further detail into the confirmations. There are many aryl functionalities to experiment with, including continuation of the longer alkyl ligand synthesis. More simple adjustments are with the axial ligands of the metal center and the metal center itself, only an iron chloride has been tested here but there are many others known to exist including perchlorates and triflates that are likely to be more active. Possibly the most important would be analysis with other lignin model compounds, including one with a  $\beta$ -O-4 linkage. There was only one ionic liquid tested, as there are hundreds of thousands of possibilities, it would be useful to obtain a library of sorts as to the effect they have on the porphyrin oxidation studies. Along with solvent effects, are pH studies of the ionic liquids. It is common in the literature to see drastic differences in catalytic results at different pH levels. Although the nonionic manganese porphyrins did not perform well in the veratryl alcohol system relative to the iron porphyrins, manganese ionic porphyrins should be looked at as they are more active in many cases in the literature. Finally, for catalytic studies reusability of the porphyrin catalysts should be looked at. In the literature, different systems have shown to produce drastic effects on the number of catalytic cycles before the porphyrins are degraded and inactive.<sup>64</sup>

## REFERENCES

1. Morton S. A.; Morton, L. A., Ionic Liquids for the Utilization of Lignocellulosics. In *Thermochemical Conversion of Biomass to Liquid Fuels and Chemicals*, Crocker, M., Ed. Royal Society of Chemistry: 2010; Vol. 1, pp 305-341.
2. Ricardo Soccol, C.; Faraco, V.; Karp, S.; Vandenberghe, L. P. S.; Thomaz-Soccol, V.; Woiciechowski, A.; Pandey, A., Chapter 5 - Lignocellulosic Bioethanol: Current Status and Future Perspectives. In *Biofuels*, Ashok, P.; Christian, L.; Steven, C. R.; Claude-Gilles, D.; Pandey, A.; Edgard, G., Eds. Academic Press: Amsterdam, 2011; pp 101-122.
3. Zhang, Y. H., Reviving the carbohydrate economy via multi-product lignocellulose biorefineries. *Journal of Industrial Microbiology & Biotechnology* **2008**, *35* (5), 367-375.
4. Lora, J., Chapter 10 - Industrial Commercial Lignins: Sources, Properties and Applications. In *Monomers, Polymers and Composites from Renewable Resources*, Mohamed Naceur, B.; Alessandro, G., Eds. Elsevier: Amsterdam, 2008; pp 225-241.
5. Liu, C.-F.; Sun, R.-C., Chapter 5 - Cellulose. In *Cereal Straw as a Resource for Sustainable Biomaterials and Biofuels*, Elsevier: Amsterdam, 2010; pp 131-167.
6. Barbat, A.; Gloaguen, V.; Sol, V.; Krausz, P., Aqueous extraction of glucuronoxylans from chestnut wood: New strategy for lignin oxidation using phthalocyanine or porphyrin/H<sub>2</sub>O<sub>2</sub> system. *Bioresource Technology* **2010**, *101* (16), 6538-6544.
7. Ren, J.-L.; Sun, R.-C., Chapter 4 - Hemicelluloses. In *Cereal Straw as a Resource for Sustainable Biomaterials and Biofuels*, Elsevier: Amsterdam, 2010; pp 73-130.
8. Diedericks, D.; Rensburg, E. v.; del Prado García-Aparicio, M.; Görgens, J. F., Enhancing the enzymatic digestibility of sugarcane bagasse through the application of an ionic liquid in combination with an acid catalyst. *Biotechnology Progress* **2012**, *28* (1), 76-84.

9. Yu, H.; Hu, J.; Fan, J.; Chang, J., One-Pot Conversion of Sugars and Lignin in Ionic Liquid and Recycling of Ionic Liquid. *Industrial & Engineering Chemistry Research* **2012**, *51* (8), 3452-3457.
10. Stewart, D., Lignin as a base material for materials applications: Chemistry, application and economics. *Industrial Crops and Products* **2008**, *27* (2), 202-207.
11. Zakzeski, J.; Bruijninx, P. C. A.; Jongerius, A. L.; Weckhuysen, B. M., The Catalytic Valorization of Lignin for the Production of Renewable Chemicals. *Chemical Reviews* **2010**, *110* (6), 3552-3599.
12. Pińkowska, H.; Wolak, P.; Złocińska, A., Hydrothermal decomposition of alkali lignin in sub- and supercritical water. *Chemical Engineering Journal* **2012**, *187* (0), 410-414.
13. Collinson, S. R.; Thielemans, W., The catalytic oxidation of biomass to new materials focusing on starch, cellulose and lignin. *Coordination Chemistry Reviews* **2010**, *254* (15–16), 1854-1870.
14. Alvira, P.; Tomás-Pejó, E.; Ballesteros, M.; Negro, M. J., Pretreatment technologies for an efficient bioethanol production process based on enzymatic hydrolysis: A review. *Bioresource Technology* **2010**, *101* (13), 4851-4861.
15. Joseph, L. M.; Aminul, I., Lignin Chemistry, Technology, and Utilization: A Brief History. In *Lignin: Historical, Biological, and Materials Perspectives*, American Chemical Society: 1999; Vol. 742, pp 2-99.
16. Institute for Renewable Energy Research. Renewable Energy. <http://www.instituteforenergyresearch.org/energy-overview/renewable-energy/> (accessed August,12, 2012).
17. Evtuguin, D. V.; Daniel, A. I. D.; Silvestre, A. J. D.; Amado, F. M. L.; Neto, C. P., Lignin aerobic oxidation promoted by molybdovanadophosphate polyanion [PMo7V5O40]8-. Study on the oxidative cleavage of  $\beta$ -O-4 aryl ether structures using model compounds. *Journal of Molecular Catalysis A: Chemical* **2000**, *154* (1–2), 217-224.

18. Esteghlalian, A.; Hashimoto, A. G.; Fenske, J. J.; Penner, M. H., Modeling and optimization of the dilute-sulfuric-acid pretreatment of corn stover, poplar and switchgrass. *Bioresource Technology* **1997**, *59* (2–3), 129-136.
19. Sun, Y.; Cheng, J., Hydrolysis of lignocellulosic materials for ethanol production: a review. *Bioresource Technology* **2002**, *83* (1), 1-11.
20. Sigoillot, J.-C.; Berrin, J.-G.; Bey, M.; Lesage-Meessen, L.; Levasseur, A.; Lomascolo, A.; Record, E.; Uzan-Boukhris, E., Chapter 8 - Fungal Strategies for Lignin Degradation. In *Advances in Botanical Research*, Lise, J.; Catherine, L., Eds. Academic Press: 2012; Vol. Volume 61, pp 263-308.
21. Cui, F.; Wijesekera, T.; Dolphin, D.; Farrell, R.; Skerker, P., Biomimetic degradation of lignin. *Journal of Biotechnology* **1993**, *30* (1), 15-26.
22. Bertini, I.; Gray, B. H.; Lippard, J. S.; Valentine, S. J., *Bioinorganic Chemistry*. University Science Books: Mill Valley, 1994.
23. Enguita, F. J.; Martins, L. O.; Henriques, A. O.; Carrondo, M. A., Crystal Structure of a Bacterial Endospore Coat Component: A LACCASE WITH ENHANCED THERMOSTABILITY PROPERTIES. *Journal of Biological Chemistry* **2003**, *278* (21), 19416-19425.
24. Cai, D.; Tien, M., Characterization of the oxycomplex of lignin peroxidases from *Phanerochaete chrysosporium*: equilibrium and kinetics studies. *Biochemistry* **1990**, *29* (8), 2085-2091.
25. TIEN, M.; KIRK, T. K., Lignin-Degrading Enzyme from the Hymenomycete *Phanerochaete chrysosporium* Burds. *Science* **1983**, *221* (4611), 661-663.
26. Sutherland, G. R. J.; Khindaria, A.; Chung, N.; Aust, S. D., The Effect of Manganese on the Oxidation of Chemicals by Lignin Peroxidase. *Biochemistry* **1995**, *34* (39), 12624-12629.
27. Kent Kirk, T.; Tien, M.; Kersten, P. J.; Kalyanaraman, B.; Hammel, K. E.; Farrell, R. L., [27] Lignin peroxidase from fungi: *Phanerochaete chrysosporium*. In *Methods in Enzymology*, Mary, E. L., Ed. Academic Press: 1990; Vol. Volume 188, pp 159-171.



28. Hallett, J. P.; Welton, T., Room-Temperature Ionic Liquids: Solvents for Synthesis and Catalysis. 2. *Chemical Reviews* **2011**, *111* (5), 3508-3576.
29. Tsuda, T.; Hussey, C. L., Electrochemical Applications of Room-Temperature Ionic Liquids. *Interface* **2007**, *16* (1), 42-49.
30. Olivier-Bourbigou, H.; Magna, L.; Morvan, D., Ionic liquids and catalysis: Recent progress from knowledge to applications. *Applied Catalysis A: General* **2010**, *373* (1–2), 1-56.
31. Holbrey, J. D.; Seddon, K. R.; Wareing, R., A simple colorimetric method for the quality control of 1-alkyl-3-methylimidazolium ionic liquid precursors. *Green Chemistry* **2001**, *3* (1), 33-36.
32. Xiao, Y.; Malhotra, S. V., Friedel–Crafts alkylation reactions in pyridinium-based ionic liquids. *Journal of Molecular Catalysis A: Chemical* **2005**, *230* (1–2), 129-133.
33. Jia, S.; Cox, B. J.; Guo, X.; Zhang, Z. C.; Ekerdt, J. G., Hydrolytic Cleavage of  $\beta$ -O-4 Ether Bonds of Lignin Model Compounds in an Ionic Liquid with Metal Chlorides. *Industrial & Engineering Chemistry Research* **2010**, *50* (2), 849-855.
34. Patterson, R. F.; West, K. A.; Lovell, E. L.; Hawkins, W. L.; Hibbert, H., Studies on Lignin and Related Compounds. LI. The Solvent Fractionation of Maple Ethanol Lignin. *Journal of the American Chemical Society* **1941**, *63* (8), 2065-2070.
35. El Hage, R.; Brosse, N.; Sannigrahi, P.; Ragauskas, A., Effects of process severity on the chemical structure of Miscanthus ethanol organosolv lignin. *Polymer Degradation and Stability* **2010**, *95* (6), 997-1003.
36. With, T. K., A short history of porphyrins and the porphyrias. *International Journal of Biochemistry* **1980**, *11* (3–4), 189-200.
37. Brand, H.; Arnold, J., Recent developments in the chemistry of early transition metal porphyrin compounds. *Coordination Chemistry Reviews* **1995**, *140* (0), 137-168.

38. Lindsey, J. S.; Schreiman, I. C.; Hsu, H. C.; Kearney, P. C.; Marguerettaz, A. M., Rothmund and Adler-Longo reactions revisited: synthesis of tetraphenylporphyrins under equilibrium conditions. *The Journal of Organic Chemistry* **1987**, *52* (5), 827-836.
39. Rothmund, P., A New Porphyrin Synthesis. The Synthesis of Porphin1. *Journal of the American Chemical Society* **1936**, *58* (4), 625-627.
40. Adler, A. D.; Longo, F. R.; Finarelli, J. D.; Goldmacher, J.; Assour, J.; Korsakoff, L., A simplified synthesis for meso-tetraphenylporphine. *The Journal of Organic Chemistry* **1967**, *32* (2), 476-476.
41. Syed, S. Q.; Syed, S. A., A Novel Method for the Synthesis of Meso Substituted Dipyrrromethanes. *International Journal of Applied Biology and Pharmaceutical Technology* **2011**, *2* (1), 301-306.
42. Shimada, M.; Habe, T.; Umezawa, T.; Higuchi, T.; Okamoto, T., The C=C bond cleavage of a lignin model compound, 1,2-diarylpropane-1,3-diol, with a heme-enzyme model catalyst tetraphenylporphyrinatoiron (III) chloride in the presence of tert-butylhydroperoxide. *Biochemical and Biophysical Research Communications* **1984**, *122* (3), 1247-1252.
43. Pan, Z.; Newcomb, M., Kinetics and Mechanism of Oxidation Reactions of Porphyrin-Iron(IV)-Oxo Intermediates. *Inorganic Chemistry* **2007**, *46* (16), 6767-6774.
44. Traylor, T. G.; Fann, W. P.; Bandyopadhyay, D., A common heterolytic mechanism for reactions of iodosobenzenes, peracids, hydroperoxides, and hydrogen peroxide with iron(III) porphyrins. *Journal of the American Chemical Society* **1989**, *111* (20), 8009-8010.
45. Traylor, T. G.; Xu, F., A biomimetic model for catalase: the mechanisms of reaction of hydrogen peroxide and hydroperoxides with iron(III) porphyrins. *Journal of the American Chemical Society* **1987**, *109* (20), 6201-6202.
46. Traylor, T. G.; Tsuchiya, S.; Byun, Y. S.; Kim, C., High-yield epoxidations with hydrogen peroxide and tert-butyl hydroperoxide catalyzed by iron(III) porphyrins: heterolytic cleavage of hydroperoxides. *Journal of the American Chemical Society* **1993**, *115* (7), 2775-2781.

47. Traylor, T. G.; Kim, C.; Richards, J. L.; Xu, F.; Perrin, C. L., Reactions of Iron(III) Porphyrins with Oxidants. Structure-Reactivity Studies. *Journal of the American Chemical Society* **1995**, *117* (12), 3468-3474.
48. Groves, J. T.; Gross, Z.; Stern, M. K., Preparation and Reactivity of Oxoiron(IV) Porphyrins. *Inorganic Chemistry* **1994**, *33* (22), 5065-5072.
49. Stephenson, N. A.; Bell, A. T., A Study of the Mechanism and Kinetics of Cyclooctene Epoxidation Catalyzed by Iron(III) Tetrakis(pentafluorophenyl) Porphyrin. *Journal of the American Chemical Society* **2005**, *127* (24), 8635-8643.
50. Stephenson, N. A.; Bell, A. T., Influence of Solvent Composition on the Kinetics of Cyclooctene Epoxidation by Hydrogen Peroxide Catalyzed by Iron(III) [tetrakis(pentafluorophenyl)] Porphyrin Chloride [(F<sub>20</sub>TPP)FeCl]. *Inorganic Chemistry* **2006**, *45* (6), 2758-2766.
51. Stephenson, N. A.; Bell, A. T., Effects of Methanol on the Thermodynamics of Iron(III) [Tetrakis(pentafluorophenyl)]porphyrin Chloride Dissociation and the Creation of Catalytically Active Species for the Epoxidation of Cyclooctene. *Inorganic Chemistry* **2006**, *45* (14), 5591-5599.
52. Khavasi, H. R.; Hosseiny Davarani, S. S.; Safari, N., Remarkable solvent effect on the yield and specificity of oxidation of naphthalene catalyzed by iron(III)porphyrins. *Journal of Molecular Catalysis A: Chemical* **2002**, *188* (1-2), 115-122.
53. Qing-Xia, W.; Ye, L., The Ionic Palladium Porphyrin as a Highly Efficient and Recyclable Catalyst for Heck Reaction in Ionic Liquid Solution Under Aerobic Conditions. *Catalysis Letters* **2009**, *128* (3/4), 487-492.
54. Cui, F.; Dolphin, D., The biomimetic oxidation of  $\beta$ -1,  $\beta$ -0-4,  $\beta$ -5, and biphenyl lignin model compounds by synthetic iron porphyrins. *Bioorganic & Medicinal Chemistry* **1994**, *2* (7), 735-742.
55. Wen, L.; Li, M.; Schlenoff, J. B., Polyporphyrin Thin Films from the Interfacial Polymerization of Mercaptoporphyrins. *Journal of the American Chemical Society* **1997**, *119* (33), 7726-7733.

56. Artaud, I.; Ben-Aziza, K.; Mansuy, D., Iron porphyrin-catalyzed oxidation of 1,2-dimethoxyarenes: a discussion of the different reactions involved and the competition between the formation of methoxyquinones or muconic dimethyl esters. *The Journal of Organic Chemistry* **1993**, *58* (12), 3373-3380.
57. Wang, J.-W.; Meng, F.-H.; Zhang, L.-F., Suzuki Coupling Reaction of Aryl Halides Catalyzed by an N-Heterocyclic Carbene–PdCl<sub>2</sub> Species Based on a Porphyrin at Room Temperature. *Organometallics* **2009**, *28* (7), 2334-2337.
58. Patra, R.; Chaudhary, A.; Ghosh, S. K.; Rath, S. P., Axial Ligand Orientations in a Distorted Porphyrin Macrocyclic: Synthesis, Structure, and Properties of Low-Spin Bis(imidazole)iron(III) and Iron(II) Porphyrinates<sup>††</sup> Dedicated to Prof. Animesh Chakravorty on the occasion of his 75th birthday. *Inorganic Chemistry* **2010**, *49* (5), 2057-2067.
59. Liu, Y.; Zhang, H.-J.; Lu, Y.; Cai, Y.-Q.; Liu, X.-L., Mild oxidation of styrene and its derivatives catalyzed by ionic manganese porphyrin embedded in a similar structured ionic liquid. *Green Chemistry* **2007**, *9* (10), 1114-1119.
60. DiMaggio, S. G.; Wertsching, A. K.; Ross, C. R., Electronic Consequences of Nonplanar Core Conformations in Electron-Deficient Porphyrins: The Structure and Spectroscopic Properties of [5,10,15,20-Tetrakis(heptafluoropropyl)porphinato]cobalt(II). *Journal of the American Chemical Society* **1995**, *117* (31), 8279-8280.
61. Mayer, I.; Formiga, A. L. B.; Engelmann, F. M.; Winnischofer, H.; Oliveira, P. V.; Tomazela, D. M.; Eberlin, M. N.; Toma, H. E.; Araki, K., Study of the spectroscopic and electrochemical properties of tetra-ruthenated porphyrins by theoretical–experimental approach. *Inorganica Chimica Acta* **2005**, *358* (9), 2629-2642.
62. Zakavi, S.; Omidyan, R.; Ebrahimi, L.; Heidarizadi, F., Substitution effects on the UV–vis and <sup>1</sup>H NMR spectra of the dications of meso and/or β substituted porphyrins with trifluoroacetic acid: Electron-deficient porphyrins compared to the electron-rich ones. *Inorganic Chemistry Communications* **2011**, *14* (11), 1827-1832.
63. Zhang, H.-J.; Liu, Y.; Lu, Y.; He, X.-S.; Wang, X.; Ding, X., Epoxidations catalyzed by an ionic manganese(III) porphyrin and characterization of manganese(V, IV)-oxo

porphyrin complexes by UV–vis spectrophotometer in ionic liquid solution. *Journal of Molecular Catalysis A: Chemical* **2008**, *287* (1–2), 80-86.

64. Anil, K., Biomimetic Oxidation of Veratryl Alcohol with H<sub>2</sub>O<sub>2</sub> Catalyzed by Iron(III) Porphyrins and Horseradish Peroxidase in Ionic Liquid<sup>1</sup>. *Synlett* **2007**, *2007* (3), 0411-0414.

65. Baciocchi, E.; Bietti, M.; Francesca Gerini, M.; Lanzalunga, O., The mediation of veratryl alcohol in oxidations promoted by lignin peroxidase: the lifetime of veratryl alcohol radical cation. *Biochemical and Biophysical Research Communications* **2002**, *293* (2), 832-835.

66. Schoemaker, H. E.; Lundell, T. K.; Hatakka, A. I.; Piontek, K., The oxidation of veratryl alcohol, dimeric lignin models and lignin by lignin peroxidase: The redox cycle revisited. *FEMS Microbiology Reviews* **1994**, *13* (2–3), 321-331.

67. Bietti, M.; Baciocchi, E.; Steenken, S., Lifetime, Reduction Potential and Base-Induced Fragmentation of the Veratryl Alcohol Radical Cation in Aqueous Solution. Pulse Radiolysis Studies on a Ligninase “Mediator”. *The Journal of Physical Chemistry A* **1998**, *102* (38), 7337-7342.

68. Gottlieb, H. E.; Kotlyar, V.; Nudelman, A., NMR Chemical Shifts of Common Laboratory Solvents as Trace Impurities. *The Journal of Organic Chemistry* **1997**, *62* (21), 7512-7515.

69. Jahan, M.; Bao, Q.; Loh, K. P., Electrocatalytically Active Graphene–Porphyrin MOF Composite for Oxygen Reduction Reaction. *Journal of the American Chemical Society* **2012**, *134* (15), 6707-6713.

70. Wang, M.; Zong, H., POLYMER-SUPPORTED GRIGNARD REAGENT AND ITS USE IN THE FUNCTIONALIZATION OF POLYMER. *Chinese Journal of Polymer Science* **1995**, *13* (1), 84-90.

## **APPENDIX**

**Table A.1: <sup>1</sup>H-NMR DATA.**

<b>Compound</b>	<b><sup>1</sup>H-NMR Signals</b>
<b>Cp1</b>	Solvent CDCl <sub>3</sub> - 9.93(s, 1H, alde), 7.79(d, 2H, CH phenyl), 7.49(d, 2H, CH phenyl), 4.43(s, 2H, CH <sub>2</sub> methyl) ppm  Literature CDCl <sub>3</sub> - 10.04(s, 1H, alde), 7.85(d, 2H, phenyl), 7.55(d, 2H, phenyl), 4.50 (s, 2H, methyl) ppm
<b>Cp2</b>	Solvent CDCl <sub>3</sub> - 8.91(s, 8H, CH pyr), 8.24(d, 8H, CH phenyl), 7.74(d, 8H, CH phenyl), 4.92(s, 8H, CH methyl), -2.91(s, 2H, NH ring) ppm  Literature CDCl <sub>3</sub> 8.85(s, 8H, CH pyr), 8.19(d, 8H, CH phenyl), 7.82(d, 8H, CH phenyl), 4.84(s, 8H, CH methyl), 2.8(s, 2H, NH ring) ppm <sup>55</sup>
<b>Cp3</b>	Solvent Methanol <sub>d4</sub> - 9.54(s, 4H, CH imid), 8.79(s, 8H, CH pyr), 8.26(d, 8H, CH phenyl), 8.08(d, 4H, CH imid), 7.88(d, 8H, CH phenyl) 7.85(d, 4H, CH imid), 5.81(s, 8H, CH <sub>2</sub> alpha), 3.97(s, 12H, CH <sub>3</sub> imid), -2.97(s, 2H, NH ring) ppm
<b>Cp4</b>	Solvent DMSO <sub>d6</sub> - 8.79(s, 8H, CH pyr), 8.05(d, 24H, CH phos), 8.02(d, 8H, CH phenyl), 7.99(m, 24H, CH phos), 7.96(m, 12H, CH phos), 7.48(d, 8H, CH phenyl), 5.66(d, 8H, CH <sub>2</sub> methyl) ppm
<b>Cp7</b>	Solvent CDCl <sub>3</sub> - 9.00(d, 8H, CH pyridyl), 8.80(s, 8H, CH pyr), 8.10(d, 8H, CH pyridyl), -2.99(s, 2H, NH ring) ppm  Literature CDCl <sub>3</sub> - 9.1(d, 8H, CH pyridyl), 8.9(s, 8H, CH pyr), 8.2(d, 8H, CH pyridyl), -2.9(s, 2H, NH ring) ppm <sup>59</sup>

**Table A.1 Continued**

<b>Cp8</b>	Solvent DMSO <sub>d6</sub> - 9.50(d, 8H, CH phenyl), 9.21(d, 8H, CH pyr), 8.98(d, 8H, CH phenyl), 5.06(t, 8H, CH), 2.85(m, 8H, CH allyl), 2.51(t, 4H, CH <sub>2</sub> alkyl), - 3.13(s, 2H, NH) ppm
<b>Cp9</b>	Solvent DMSO <sub>d6</sub> - 9.57(d, 8H, CH phenyl), 9.28(d, 8H, CH pyr), 9.08(d, 8H, CH phenyl), 6.51(m, 4H, CH allyl), 5.87(d, 4H, CH allyl), 5.66(s, 4H, CH allyl), 5.63(d, 8H, CH <sub>2</sub> alkyl) ppm
<b>Cp10</b>	Solvent Methanol <sub>d4</sub> - 9.52(d, 8H, CH phenyl), 9.37(s, 8H, CH pyr), 9.01(d, 8H, CH phenyl), 5.04(t, 8H, CH <sub>2</sub> alkyl), 2.39(m, 8H, CH <sub>2</sub> alkyl), 1.72(m, 8H, CH <sub>2</sub> alkyl), 1.19(t, 12H, CH <sub>3</sub> alkyl) ppm
<b>Cp13</b>	Solvent CDCl <sub>3</sub> - 8.86(s, 8H, CH pyr), 8.14(d, 8H, CH phenyl), 7.30(d, 8H, CH phenyl), 4.40(t, 8H, OCH <sub>2</sub> propyl), 3.79(t, 8H, CH <sub>2</sub> Br propyl), 2.52(m, 8H, CH <sub>2</sub> propyl), -2.75 (s, 2H, NH ring) ppm  Literature CDCl <sub>3</sub> - 8.98 (s, 8H, CH pyr), 8.12-8.14 (d, 8H, CH phenyl), 7.32-7.34 (d, 8H, phenyl), 4.35 (t, 2H, OCH <sub>2</sub> propyl), 3.57 (t, 2H, CH <sub>2</sub> Br propyl), 2.3 (m, 2H, CH <sub>2</sub> propyl), -2.79 (s, 2H, NH ring) ppm <sup>57</sup>



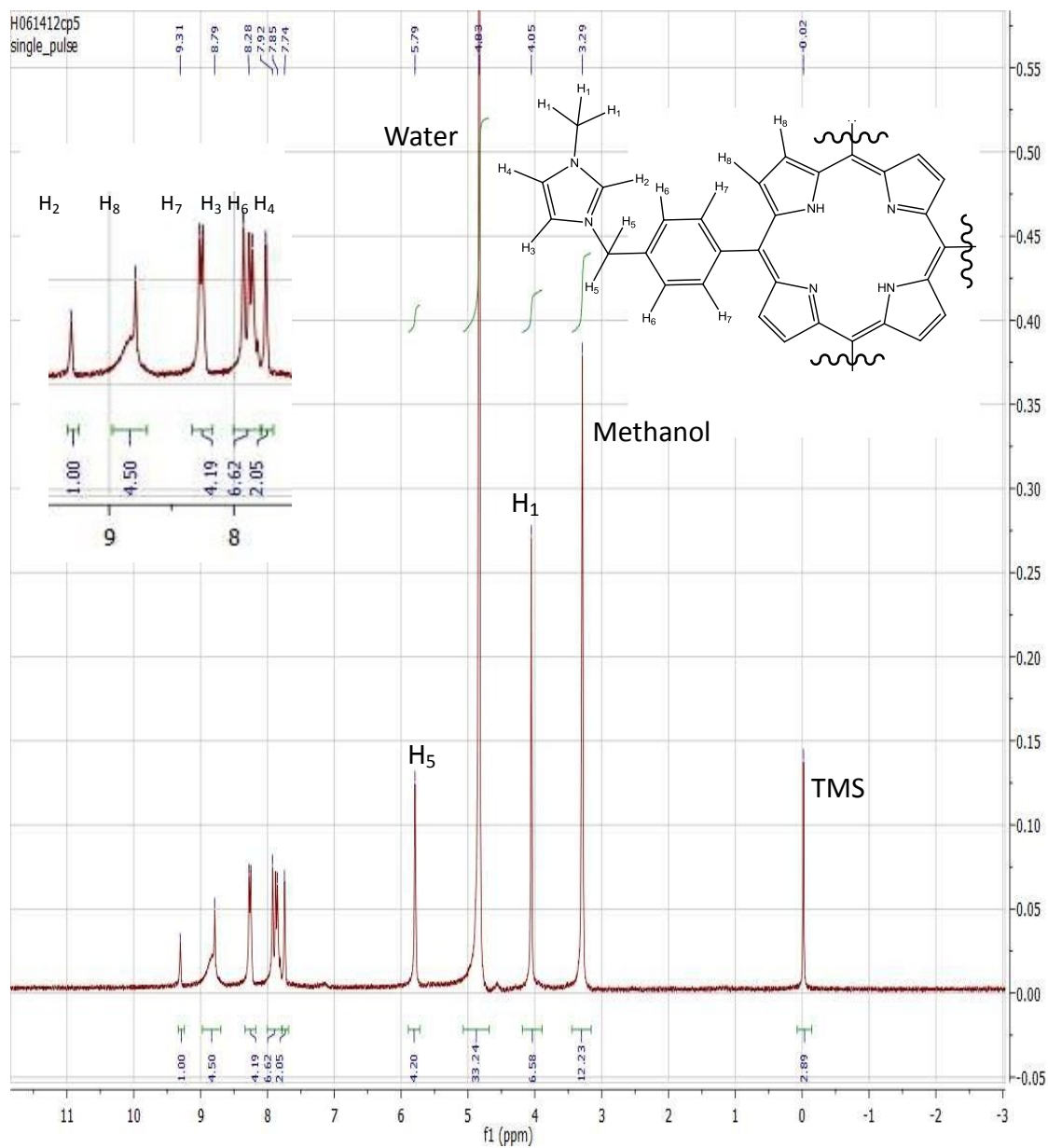


Figure A.1:  $^1\text{H-NMR}$  of  $\text{Cp}_3$  in  $\text{Methanol-d}_4$ .<sup>68</sup>

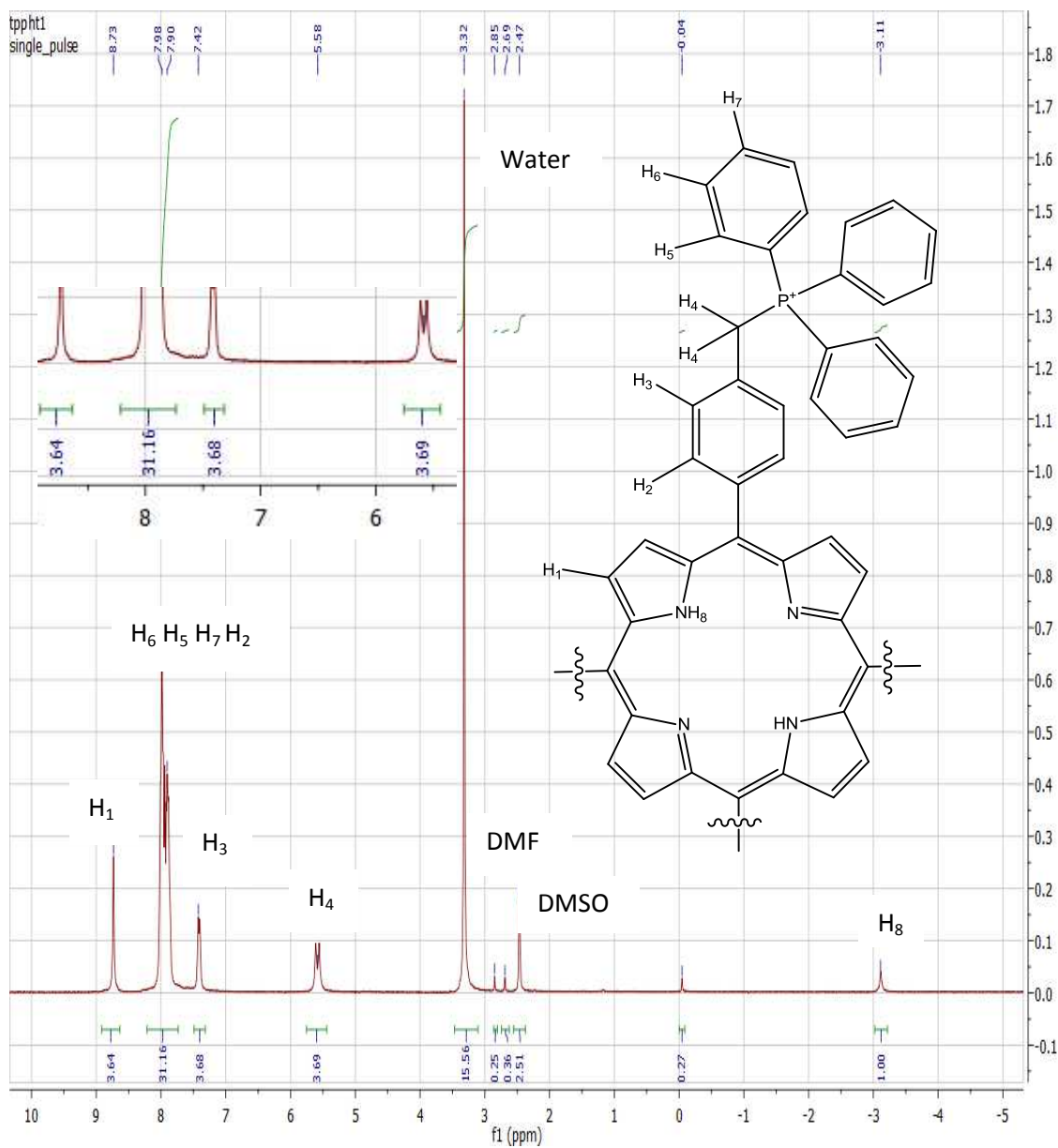


Figure A.2:  $^1\text{H-NMR}$  of Cp4 in  $\text{DMSO-d}_6$ .

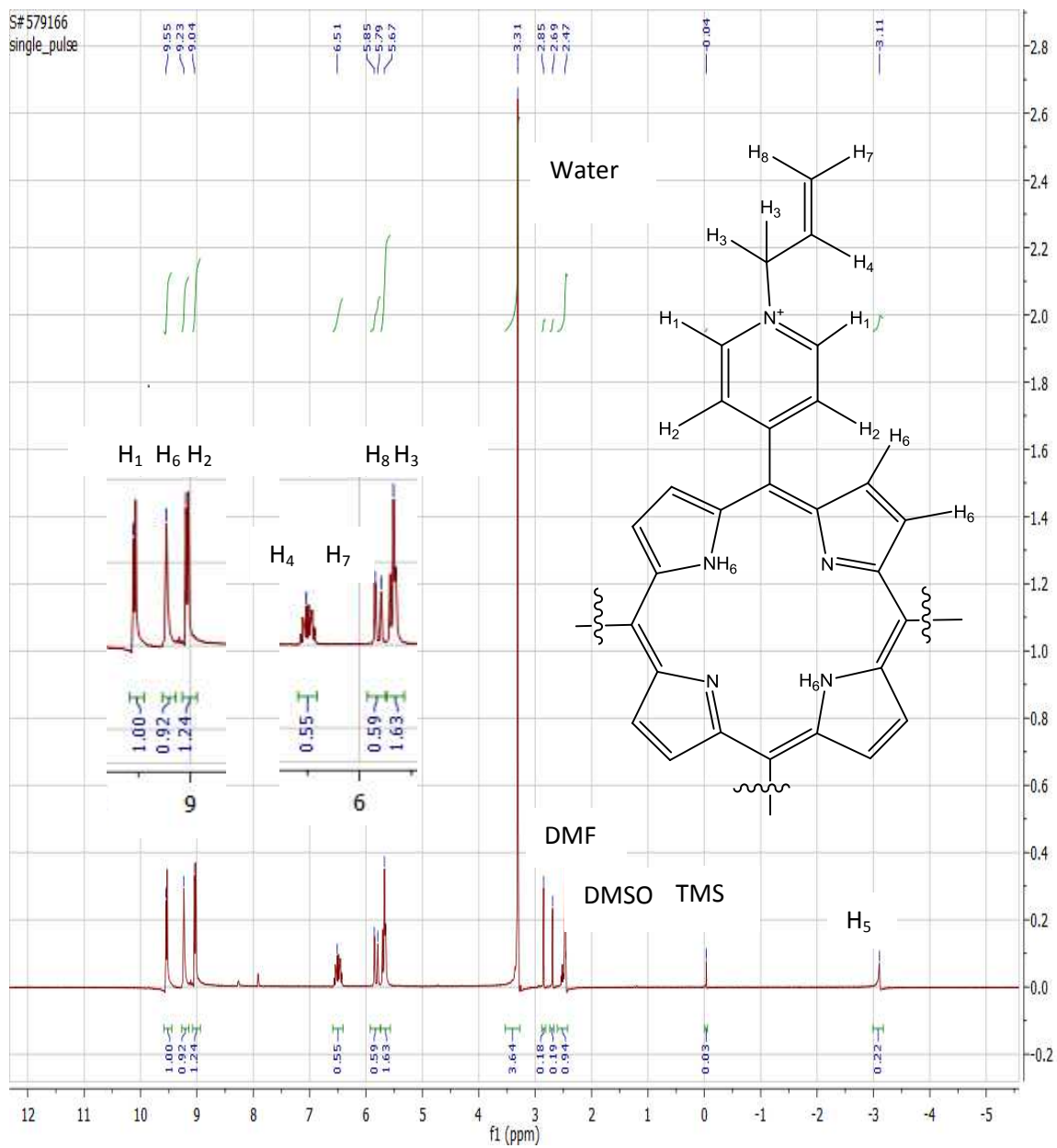


Figure A.3: <sup>1</sup>H-NMR of Cp9 in DMSO<sub>d6</sub>.

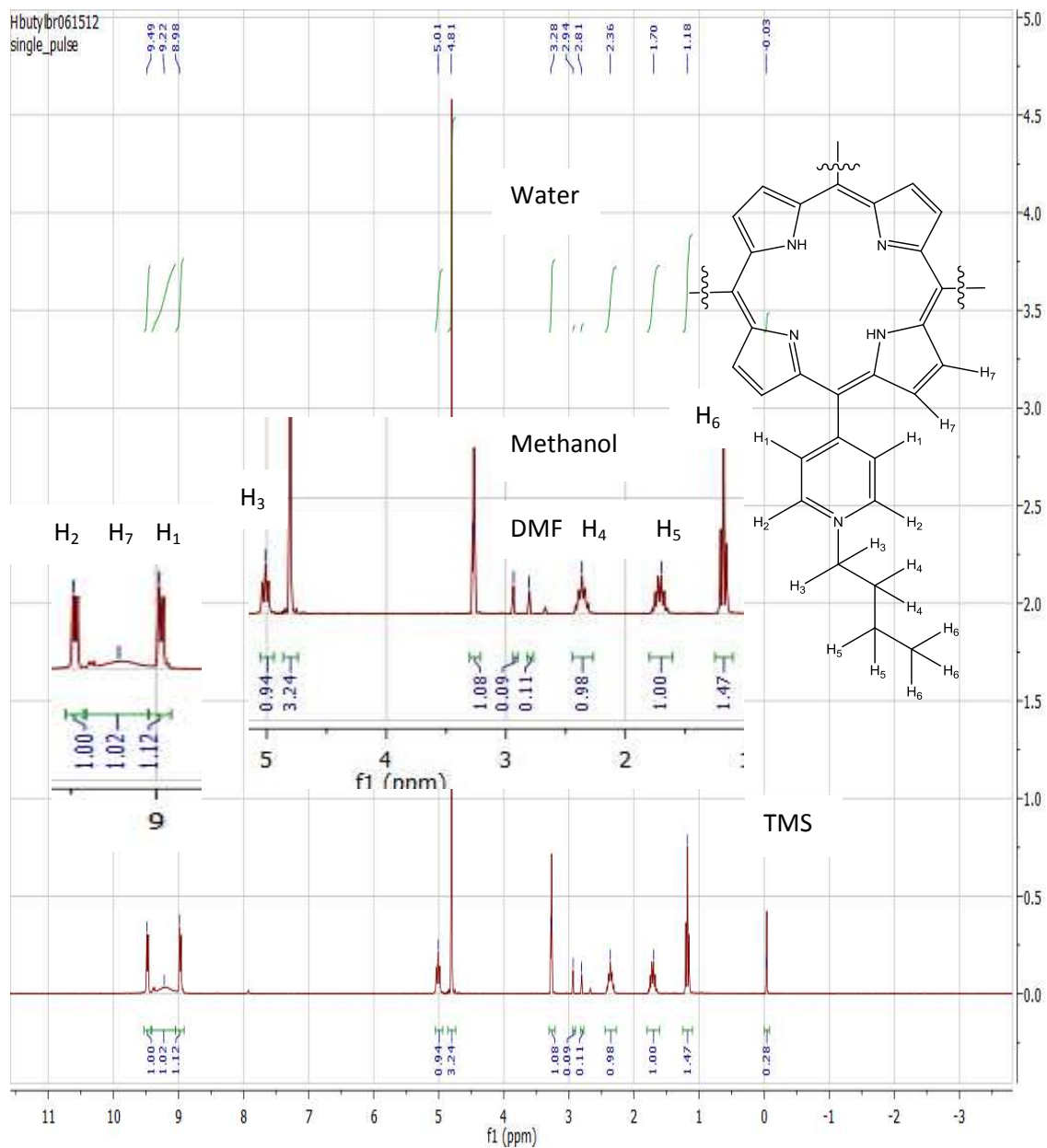


Figure A.4: <sup>1</sup>H-NMR of Cp10 in Methanol<sub>d4</sub>.

**Table A.2: IR DATA.**

<b>Compound</b>	<b>IR Signals</b>
<b>Cp2</b>	Experimental – 3326 and 3307 (m, N-H), 3028 (m, C-H), 1608, 1555, and 1502 (m, C=C), 1259 (s, CH <sub>2</sub> Br) cm <sup>-1</sup>  Literature – 3325 and 3308 (m, N-H), 3027 (m, C-H), 1614, 1575, 1540 (m, C=C), 1221 (s, CH <sub>2</sub> Br), 595 (s, C-Br) <sup>55</sup> cm <sup>-1</sup>
<b>Cp3</b>	Experimental – 3142 and 3106 (m, C-H), 1611, 1571, and 1559 (m, C=C), 1157 (s, C-N) cm <sup>-1</sup>
<b>Cp5</b>	Experimental – 3141 and 3105 (m, C-H), 1613, 1572, and 1560 (m, C=C), 1158 (s, C-N), 998 (s, N-Fe) <sup>69</sup> cm <sup>-1</sup>
<b>Cp6</b>	Experimental – 3056(m, C-H), 1615, 1586, and 1553 (m, C=C), 1436 and 1110 (s, C-P) <sup>70</sup> , 996 (s, N-Fe) cm <sup>-1</sup>
<b>Cp7</b>	Experimental – 3312(m, N-H), 3089(m, C-H), 1594(s, C=C) cm <sup>-1</sup>
<b>Cp9</b>	Experimental – 3088 and 3030 (m, C-H), 1630, 1592, 1559, and 1507 (m, C=C) cm <sup>-1</sup>
<b>Cp10</b>	Experimental – 3309 (m, N-H), 3092, 3058, and 3022 (m, C-H), 1592, and 1542 (m, C=C), 1350 (s, C-N) cm <sup>-1</sup>
<b>Cp11</b>	Experimental – 3112, 3085, and 3051 (m C-H), 1631, 1610 and 1596 (m, C=C), 1000 (s, N-Fe) cm <sup>-1</sup>
<b>Cp12</b>	Experimental –3122, 3083, and 3054 (m, C-H), 1596, 1538, and 1494 (m, C=C), 991 (s, N-Fe) cm <sup>-1</sup>

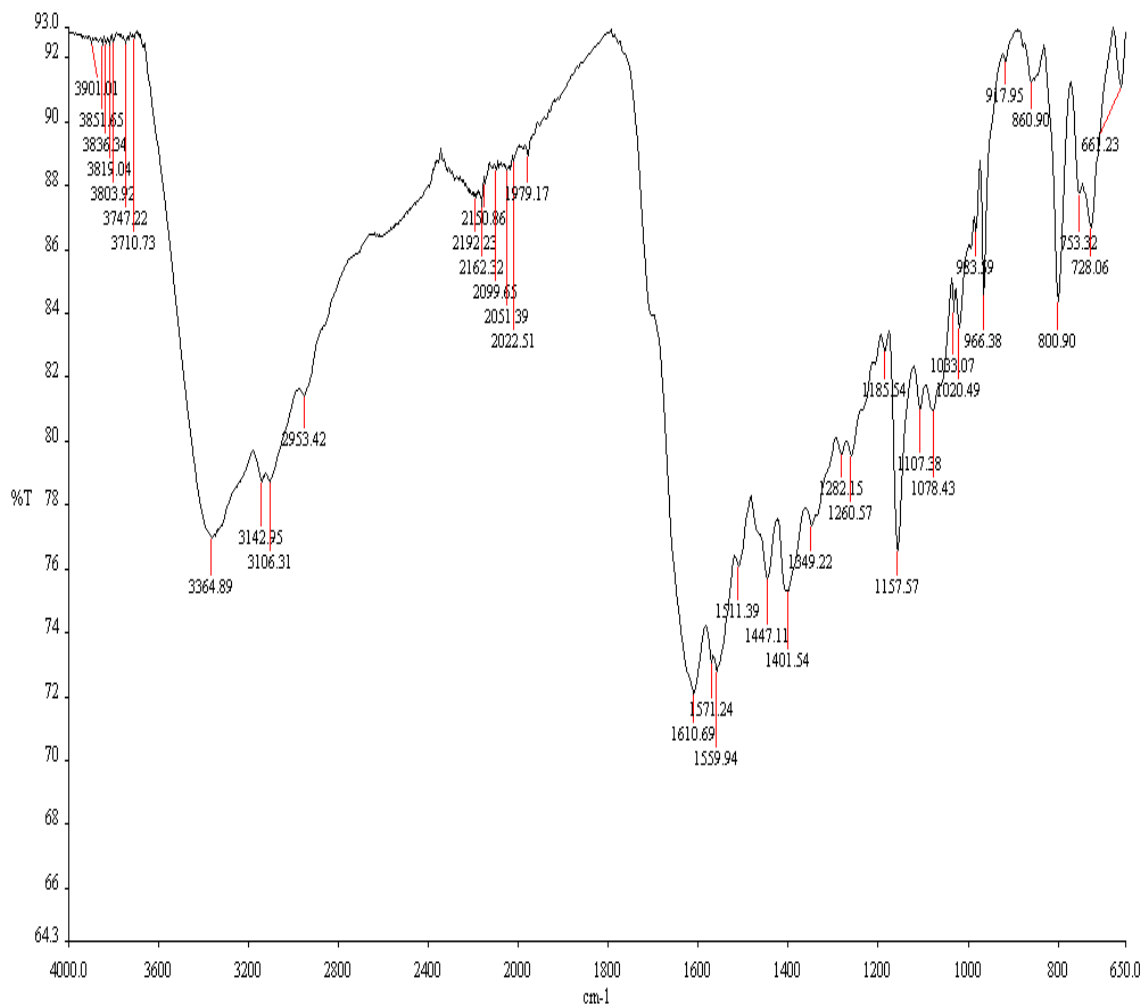


Figure A.5: IR of Cp3.

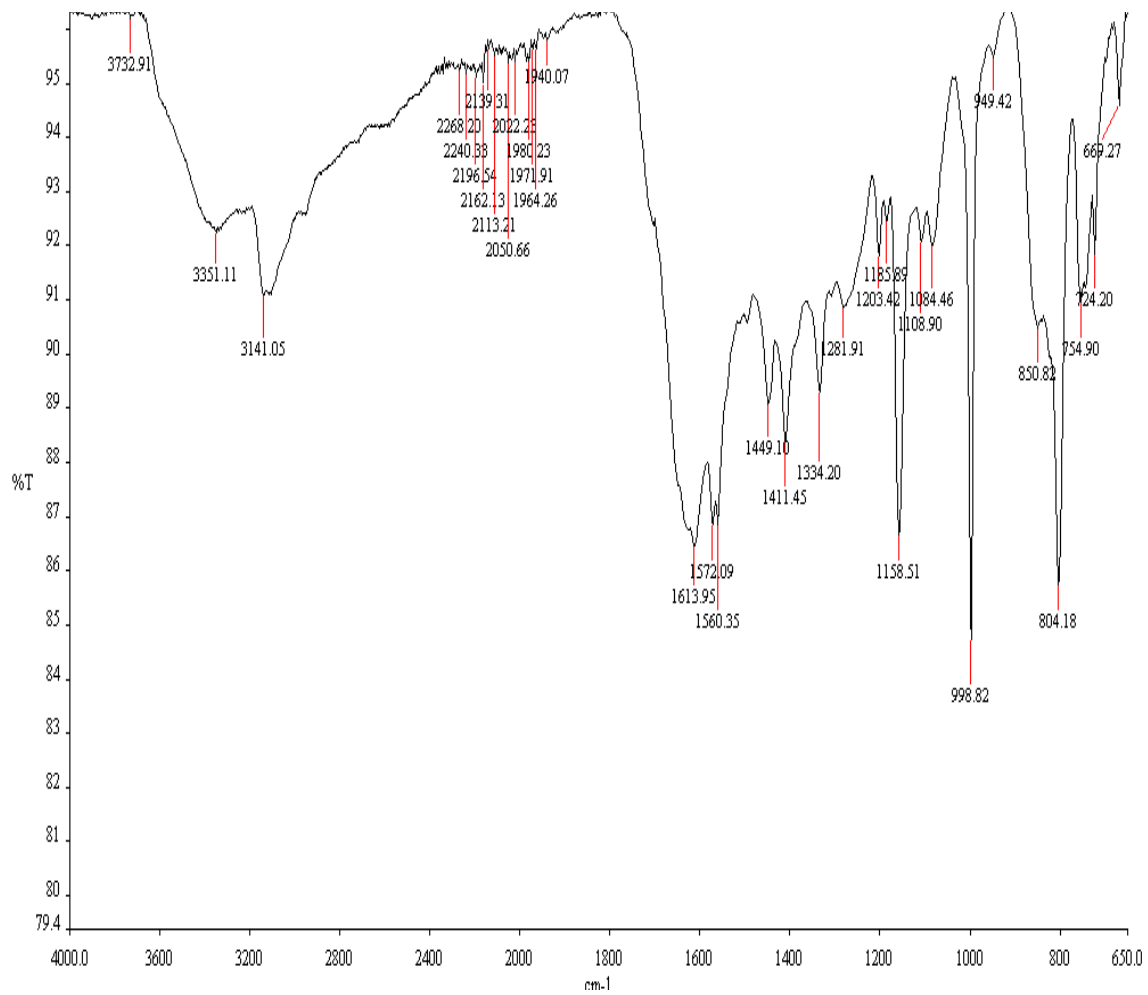


Figure A.6: IR of Cp5.

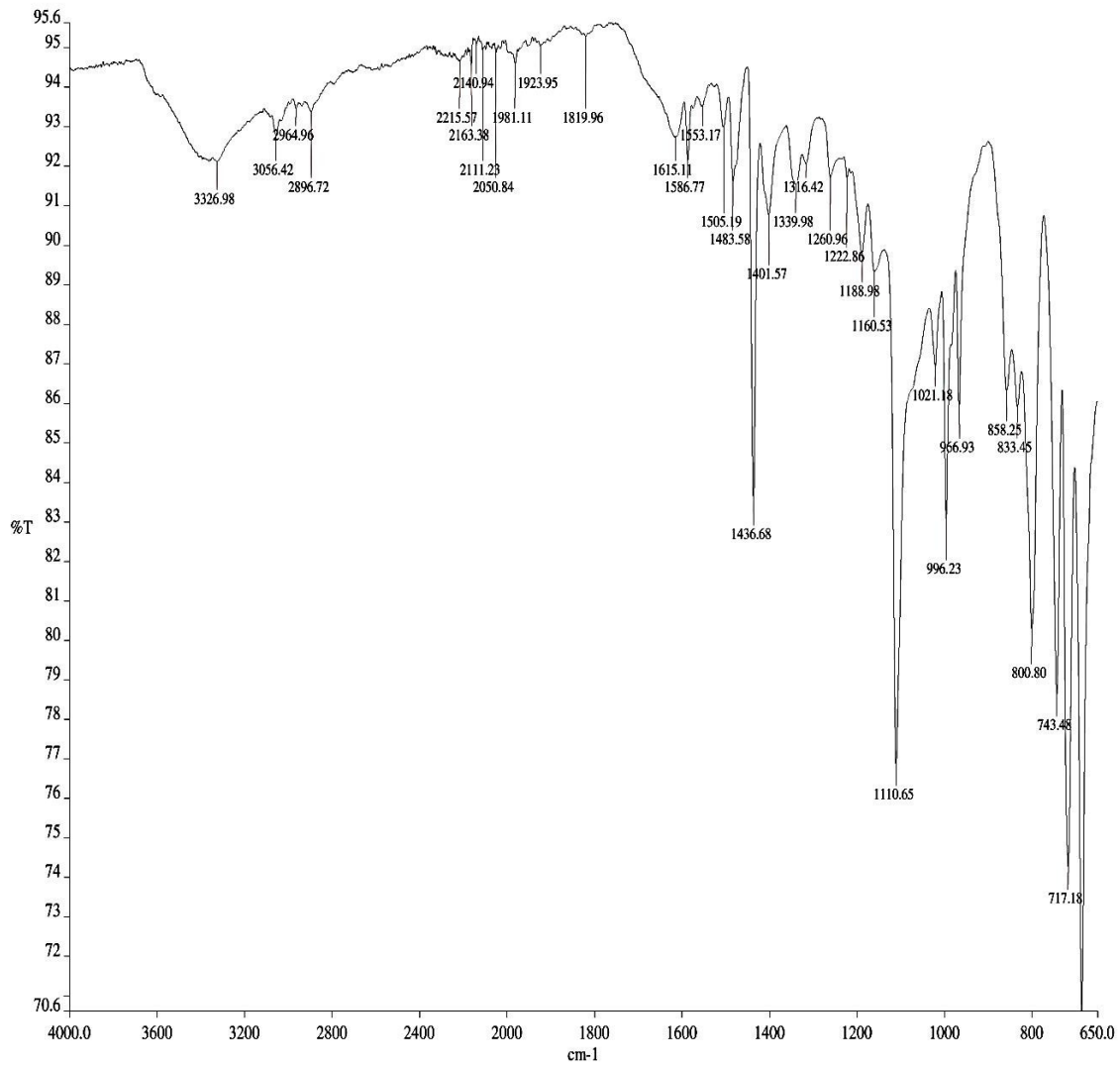
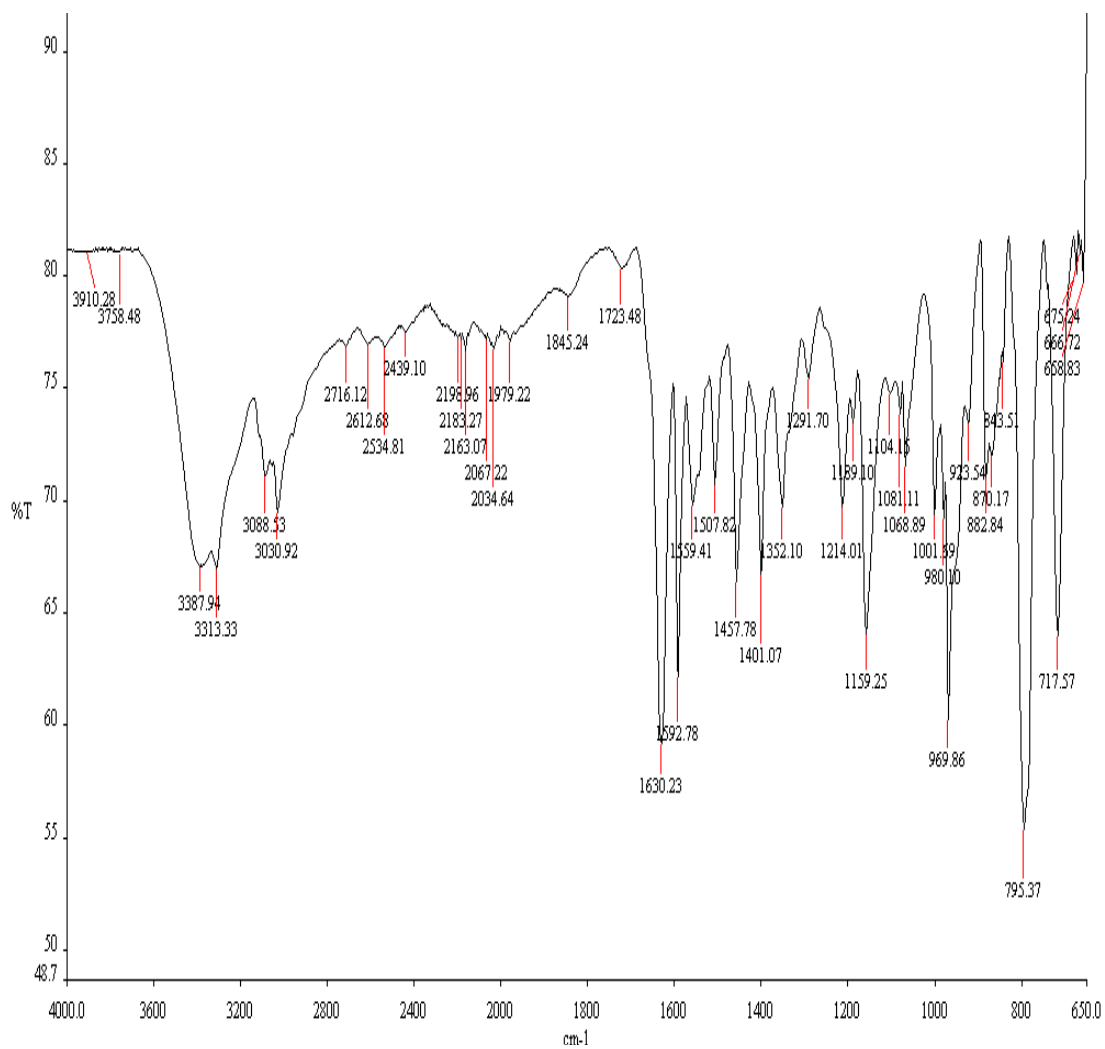


Figure A.7: IR of Cp6.





**Figure A.8: IR of Cp9.**

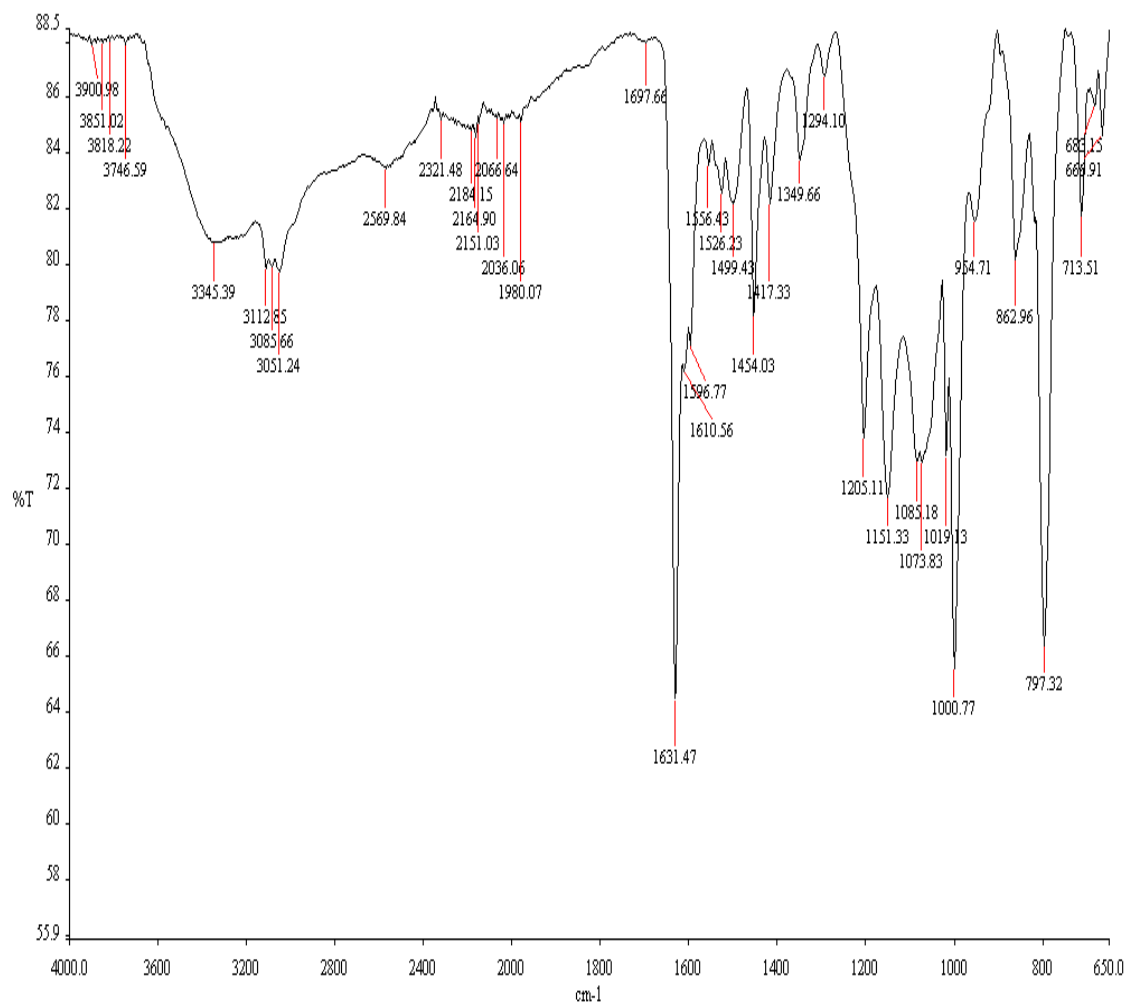
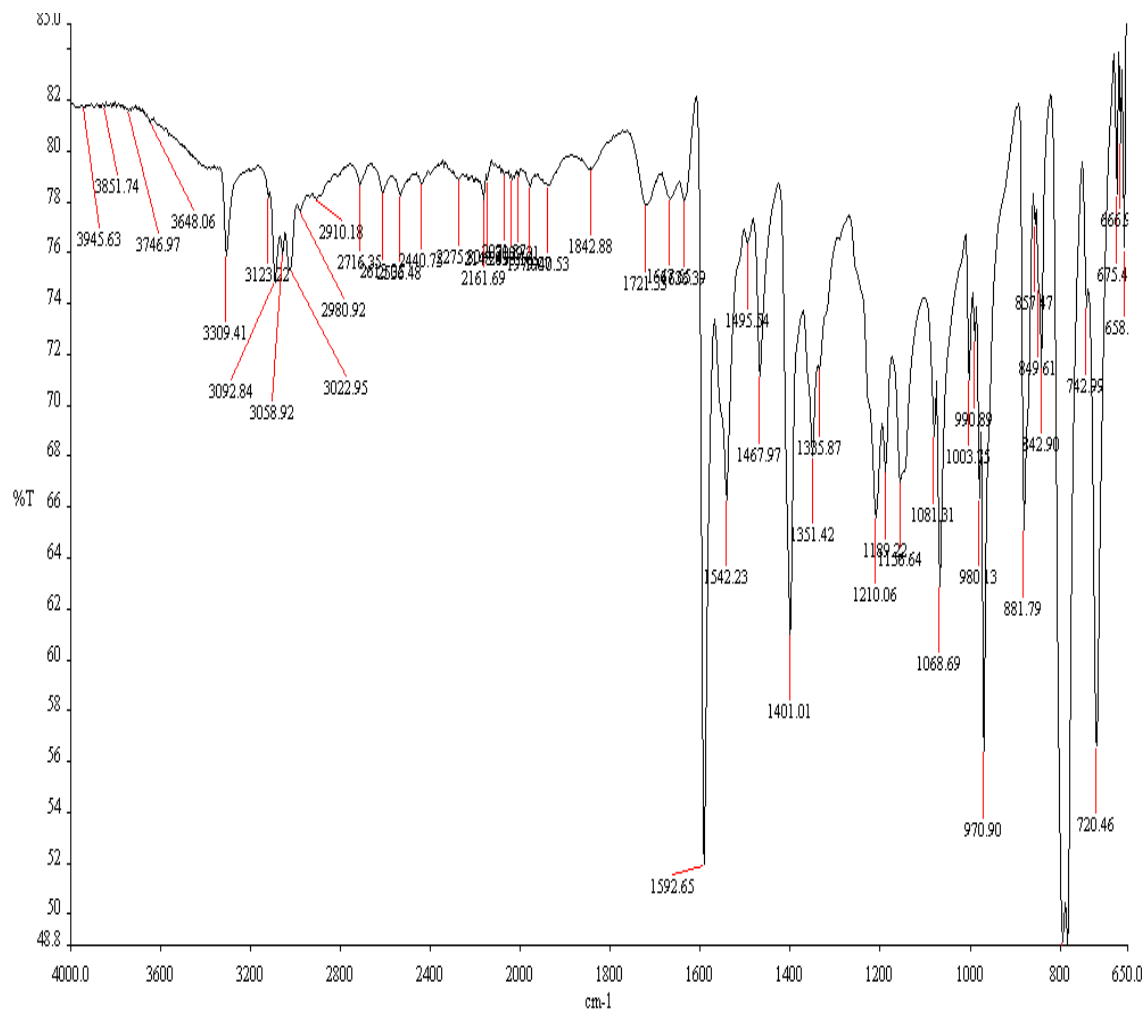


Figure A.9: IR of Cp11.



**Figure A.10: IR of Cp10.**

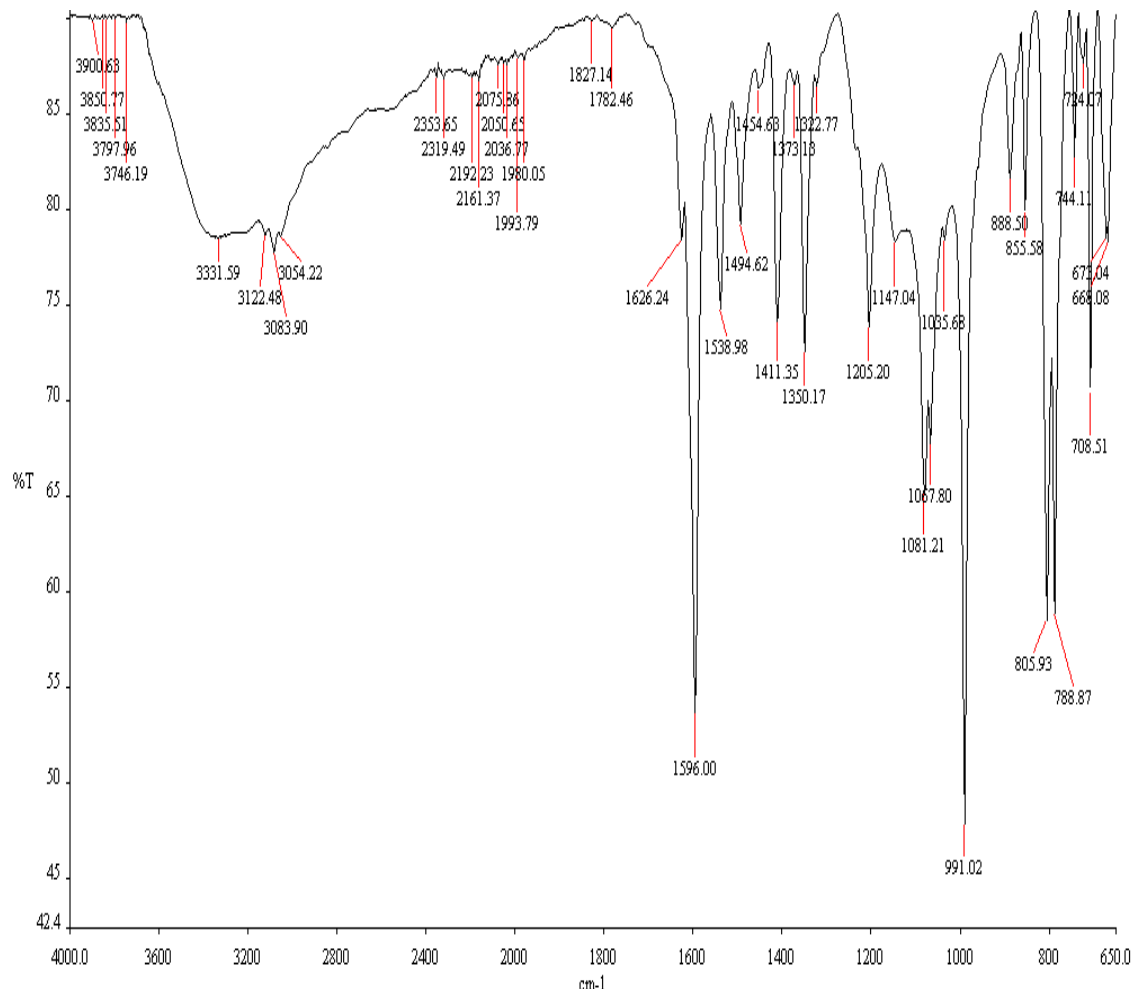


Figure A.11: IR of Cp12.

**Table A.3: UV-VIS DATA.**

<b>Compound</b>	<b>Signals</b>
<b>Cp2</b>	Experimental in CHCl <sub>3</sub> – 420max, 517, 551, 589, 646 nm Literature in CHCl <sub>3</sub> – 420max, 516, 551, 589, 646 nm
<b>Cp3</b>	Experimental in H <sub>2</sub> O- 415max, 516, 558 nm
<b>Cp5</b>	Experimental in H <sub>2</sub> O – 394max, 524 nm
<b>Cp6</b>	Experimental in H <sub>2</sub> O – 419max, 520 nm
<b>Cp7</b>	Experimental in CHCl <sub>3</sub> – 419max, 513, 543, 587, 643 nm Literature – 417max, 513, 547, 588, 644 nm
<b>Cp9</b>	Experimental in H <sub>2</sub> O - 423max, 519, 585 nm
<b>Cp10</b>	Experimental in H <sub>2</sub> O – 422max, 529, 565, 598 nm
<b>Cp11</b>	Experimental in H <sub>2</sub> O – 402max, 414, 523 nm
<b>Cp12</b>	Experimental in H <sub>2</sub> O – 418, 452max, 544 nm
<b>Cp13</b>	Experimental in CHCl <sub>3</sub> – 420max, 518, 555, 593, 650 nm

## CATALYTIC DATA TABLES

**Table A.4:** Average Mass of Veratryl Alcohol in AMIMXS Mixture Based on HPLC.

Time (h)	FeT1239 Veratryl (mg)	Time (h)	Cp5 Veratryl (mg)	Cp11 Veratryl (mg)
0	23.49	0	25.56	27.59
3.32	21.25	2	19.98	21.51
6.64	19.82	4	20.04	21.60
9.96	19.54	6	20.14	21.53
13.28	19.45	8	20.10	21.35

**Table A.5:** Average Mass of Veratraldehyde in AMIMXS Mixture Based on HPLC

Time (h)	FeT1239 Aldehyde (mg)	Time (h)	Cp5 aldehyde (mg)	Cp11 aldehyde (mg)
0	0	0	0	0
3.32	1.28	2	3.50	3.76
6.64	1.86	4	3.50	3.82
9.96	1.94	6	3.51	3.87
13.28	1.97	8	3.51	3.87

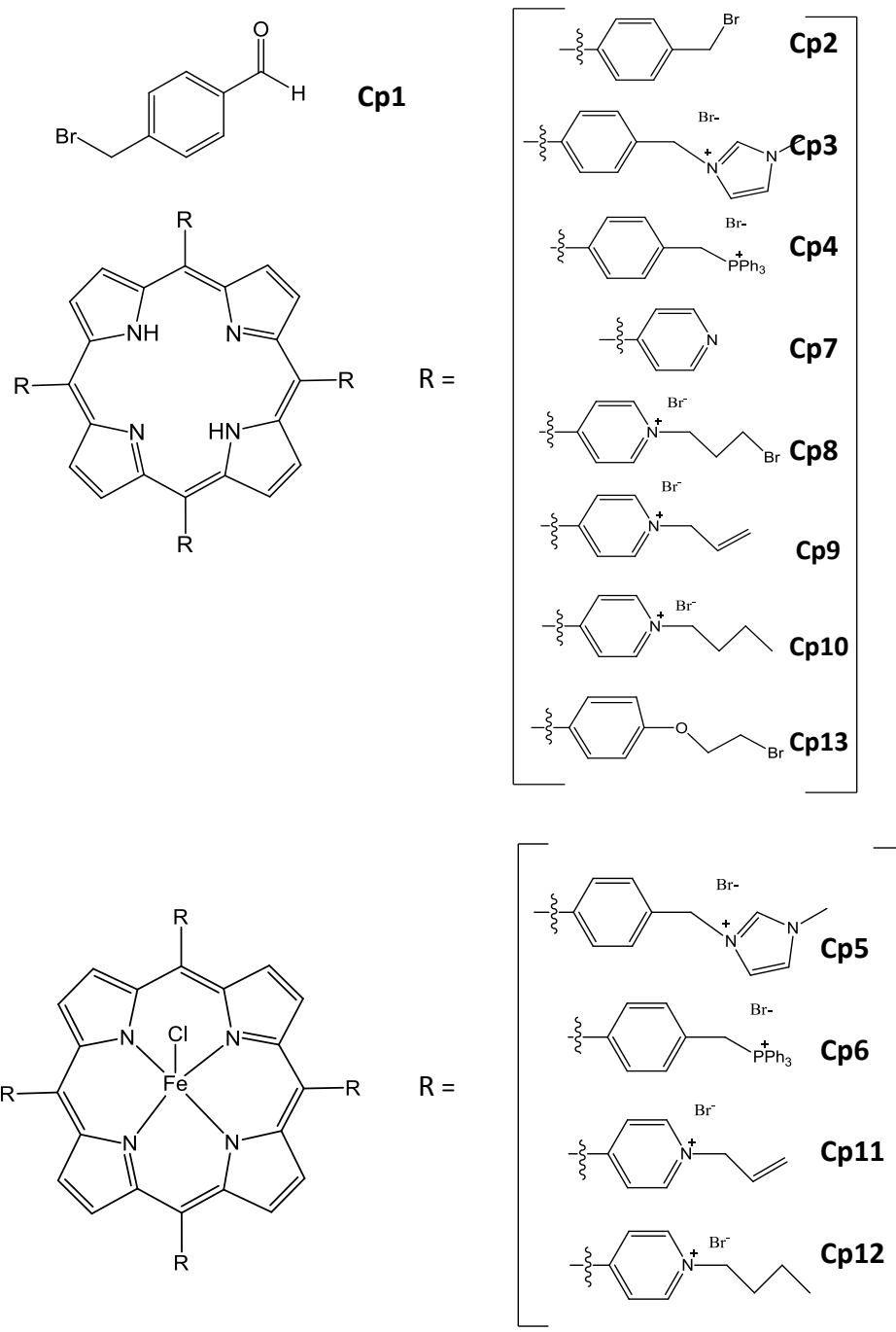


**Figure A.12:** Synthesized Chemical Structures.